Ancient food and water supply in drylands. Geoarchaeological perspectives on the water harvesting systems of the two ancient cities Resafa, Syria and Petra, Jordan.

Dissertation

zur Erlangung des Doktorgrades
der Naturwissenschaften (Dr. rer. nat.)

am Fachbereich Geowissenschaften
der Freien Universität Berlin

vorgelegt von Brian Beckers

Berlin 2012

Erstgutachterin:

Prof. Dr. Brigitta Schütt
Institut für Geographische Wissenschaften
Fachbereich Geowissenschaften
Freie Universität Berlin

Zweitgutachter:

Prof. Dr. Manfred Frechen
Abteilung: S 3 – Geochronologie und Isotopenhydrologie
Leibnitz Institut für Angewandte Geophysik Hannover

Tag der Disputation: 28.01.2013

Erklärung

Hiermit erkläre ich, dass ich die Dissertation *Ancient food and water supply in drylands. Geoarchaeological perspectives on the water harvesting systems of the two ancient cities Resafa, Syria and Petra, Jordan* selbständig angefertigt und keine anderen als die von mir angegebenen Quellen und Hilfsmittel verwendet habe.

Ich erkläre weiterhin, dass die Dissertation bisher nicht in dieser oder in anderer Form in einem anderen Prüfungsverfahren vorgelegen hat.

Berlin, 15. November 2012

Brian Beckers

Acknowledgements

This Thesis was supported by the DFG (Deutsche Forschungsgemeinschaft) funded Cluster of Excellence TOPOI Exc 264. First of all I want to thank my first supervisor Prof. Dr. Brigitta Schütt, FU Berlin for her constant and generous support during years of work. The work in and on Resafa would not have been possible without the help of Prof. Dr.-Ing. Dorothée Sack, TU Berlin and I want to thank her for that. Many others in her working team contributed to my studies in Resafa. Among those are Christoph Konrad and Martin Gussone and all the others of the team which offered help and fruitful discussions. Furthermore I want to thank Prof. Dr. Stephan G. Schmid HU Berlin, who introduced me to Petra and was a great help in setting up and accomplish the field work in Petra. Thanks also to Dr. Michel Mouton, CNRS Paris for his help and the possibility to work with his team in Petra. Special thanks to Prof. Dr. Manfred Frechen of the Leibnitz Institute for Applied Geophysics (LIAG) who offered me to work with him on the OSL samples and was of great help. In this regard the staff of the LIAG is to be thanked, most notably Dr. Sumiko Tsukamoto for her help in preparing, measuring and analysis the OSL samples and the laboratory staff Sabine Mogwitz, Astrid Techmer and Sonja Riemenschneider.

Furthermore, thanks go to the other members of the Department of Physical Geography at the FU Berlin who contributed to the thesis in one way or another: Dr. Jonas Berking for his contributions to the publications and countless hours of discussion and help, Jan Krause without whom logistics and administrative issues would have broken my neck, Jun. – Prof. Dr. Wiebke Bebermeier for giving helpful suggestions, Dr. Philip Hoelzmann and Manuela Scholz for support in the Geomorphological Laboratory, Prof. Dr. Tilman Rost for helpful comments on my work, Daniel Knitter for theoretical input, Nils Rhensius who supported me in my field work in Petra, Anne Beck for proofreading the papers which are all too often full of errors, and all the others in the department.

Last but not least I want to thank my friends and parents for help and everything else.

Summary

Two ancient cities in the dryland of West Asia are investigated in this thesis with a focus on different aspects of their water and food supply systems.

Resafa initially a fortified Roman military post located in the Syrian desert steppe, has been a Christian pilgrimage site and was the residence of the Ummayyad Caliph Hisham ibn ‘abd al-Malik. The city was finally abandoned in the 13th century AD after the Mongol invasion. Nowadays, the well-preserved city walls, ruined churches and large cisterns attest to Resafa´s former religious, political and economic importance that lasted from the 1st to the 13th century AD. The city is located ~ 25km to the south of the Euphrates at the confluence of various wadi systems that drain the surrounding undulating desert steppe. The drinking water supply of the city relied predominantly on an elaborated floodwater harvesting system. The major research question in Resafa was how reliable this floodwater harvesting system was. The reliability is assessed by applying a rainfall runoff model. Moreover constructional details of the floodwater harvesting system are investigated by applying a hydraulic model. The main findings of this study were that the floodwater harvesting system was reliable. In general the floodwater harvesting system could have harvested a sufficient amount of water at least every 13 – 14 months. Furthermore, it could be shown that the floodwater harvesting system consisted in addition to a previously excavated dam and large cisterns, of a several hundred meter long embankment system that channeled the floods to the dam.

Ancient Petra was the capital of the Nabataean kingdom and was founded around the beginning of the Common Era in the arid Eastern Highlands of Jordan. The city was annexed by the Romans at the beginning of the 2nd century and finally abandoned in the 4th century AD when. The unfavorable environs of Petra were reclaimed by installing numerous agricultural terraces, dams and channels. Little is known about the chronology, development and dynamics of this cultural landscape. The main research questions include: When did the reclamation of the environs around Petra began and what where the effects of this development on the environment? The chronological methods applied were Optical Stimulated Luminescence (OSL) Dating and radiocarbon dating. The chronological study is supplemented with geomorphological field and laboratory work. The focus lies on the terraced wadi systems of the region. The major results are that the agricultural terraces were most likely built around the beginning of the Common Era and used, maintained and extended at least until the 8th century AD. The terraces converted the formerly gravel-bedded wadis and floodplains of the region to arable land.

Zusammenfassung

Zwei antike Städte in den Trockengebieten West Asien werden hinsichtlich verschiedener Aspekte ihrer Wasser- und Essensversorgungssysteme in dieser Dissertation untersucht.

Resafa wurde ursprünglich als einer von vielen römischen Limesposten in der syrischen Wüstensteppe gegründet. Im 6. Jahrhundert wurde Resafa ein christlicher Pilgerort und im 7. Jahrhundert von dem Ummayaden Kalifen Hisham ibn ‘abd al-Malik als Residenz erwählt. Heutzutage zeugen eine gut erhaltene Stadtmauer, verfallene Kirchen und riesige Zisternen von der einstigen wirtschaftlichen, religiösen und ökonomischen Bedeutung der Stadt. Die Stadt liegt ungefähr 30 km südlich des Euphrats an dem Zusammenfluss verschiedener Wadiläufe. Die Trinkwasserversorgung Resafas basierte hauptsächlich auf einem System das es ermöglichte die regelmäßigen Fluten der Wadis abzuleiten und in großen Zisternen zu speichern. Die Hauptforschungsfrage im Falle Resafa war wie verlässlich dieses System funktionierte. Dieser Frage wurde durch die Anwendung eines Niederschlags-Abfluss-Modells nachgegangen. Des Weiteren wurden bautechnische Details dieses Wasserversorgungssystems mit Hilfe eines hydraulischen Modells erforscht.

Die Haupterkenntnisse dieser Studie sind, dass das Versorgungssystem verlässlich funktioniert hat. Es konnte normalerweise mindestens alle 13 – 14 Monate eine ausreichende Menge an Wasser gewonnen werde. Des Weiteren konnte mit Hilfe der hydraulischen Simulation die bautechnischen Kenntnisse über das Flutwassersystem erweitert werde. Neben einem in vorherigen Studien ausgegrabenen Damm der über ein Kanalsystem mit verschiedenen Zisternen verbunden war konnte gezeigt werden, dass ein mehrere hundert Meter langes Deichsystem die Fluten zu diesem Damm geleitet hat. Ferner dienten die Deiche höchstwahrscheinlich zum Hochwasserschutz.

Das antike Petra war die Hauptstadt des nabatäischen Königreiches. Sie wurde ungefähr um die Zeitenwende in den trockenen östlichen Gebirgen Jordaniens gegründet. Anfang des 2. Jh. n. Chr. wurde Petra von den Römern annektiert und im 4. Jh. n. Chr. verlassen. Die Umgebung Petras wurde durch die Anwendung eines ausgeklügelten Systems landwirtschaftlicher Terrasse urbar gemacht. Es ist wenig bekannt über die Chronologie der Kulturlandschaft die Petra umgibt. Die Hauptfragen dieser Fallstudie waren: Wann begann der Bau landwirtschaftlicher Terrassen und welchen Einfluss hatten diese auf den natürlichen Landschaftshaushalt? Zur Beantwortung dieser Fragen wurden neben geomorphologische Feld- und Laboruntersuchungen, Optisch Stimulierte Lumineszenz - und Radiokarbon - Datierungen vorgenommen. Die wichtigsten Ergebnisse dieser Studie sind, dass die landwirtschaftlichen Terrassen Anfang des 1. Jh. n. Chr. gebaut wurden und bis in 8 Jh. n. Chr. genutzt, gepflegt und ausgebaut wurden. Die Terrassen hatten ferner einen starken Einfluss auf die Ablagerungsverhältnisse. In den untersuchten Sedimentprofilen der landwirtschaftlichen Terrassen zeigt sich ein plötzlicher Wechsel von Schotterablagerungen zu Sandablagerungen. Diese Wechsel fallen stratigraphisch nahezu immer mit dem Bau von Terrassenmauern zusammen.

Table of Contents

List of figures

List of tables

1. Introduction

The causes of the decline of ancient civilizations have been a much debated question among scholars since the 18th century (Butzer and Endfield, 2012). Following common intellectual discourses, the sometimes simplistic explanations have been oscillating between those influenced by environmental determinism and those which emphasis political and socio-economic reasons (Butzer and Endfield, 2012). Similar debates are held regarding the causes of the shrinkage and abandonment of ancient settlements (Barker and Gilbertson, 2000). This controversy has recently regained attention among urban researchers and practitioners as many cities worldwide, and especially in the "first" world have increasingly been challenged inter alia with depopulation, deindustrialization and changing environmental conditions during the past few decades (Oswalt and Rieniets, 2006). In this regard often asked questions are: Did climate change or environmental catastrophes trigger the decline and abandonment of settlements? Have the dwellers overexploited their environment and destroyed the basis of their livelihood? Can political or economic reasons to be held responsible such as economic decline, shifting trade routes or war? It is often emphasized that a major problem to properly answer those questions is the limited availability of reliable data especially in archaeological studies and where written sources are limited or not existent (Barker and Gilbertson, 2000; Butzer, 2012). This thesis presents two geoarchaeological case studies which can provide valuable information to address these questions.

The research focus is on the food and water supply of two once prosperous ancient cities located in the drylands of West Asia - the Roman/Early Islamic city of Resafa in Syria and the Nabataean/Roman city of Petra in Jordan (Fig. 1 A). Resafa was founded in the 1st century AD as one of various Roman military posts of the eastern Limes in the largely unsettled Syrian desert steppe. The city was located about 30 km south of the Euphrates and the next settlements were in 10 to 20 km distance. It became a Christian pilgrimage site and after the Islamic conquest in the 8th century AD the Umayyad Caliph Hisham took residence in Resafa. The city was finally abandoned in the 13th century AD (Fig. 1 A) (Mackensen, 1984). Petra was the capital of the Nabataean Kingdom and most likely founded around the beginning of the Common Era. It was built in the rugged mountains of the Eastern Highlands in Jordan and surrounded by an extensive cultural landscape with smaller farmsteads and villages . The Romans annexed Petra at the beginning of the 2nd century AD and the city was abandoned in the 4th century AD (Schmid, 2008) .

One significant similarity of both cities is that they were located at places which can be regarded marginal in terms of food and water supply. The annual rainfall at both sites is nowadays below 200 mm (Fig. 1 B) and most studies show that the climate during the settlement of the cities was similar to the present. Moreover, sufficient perennial water sources were lacking. In consequence a complex water supply system was necessary to allow their existence.

In Resafa the drinking water supply was conducted mainly by an elaborated system that allowed the capturing and storage of periodically floods that occurred during or shortly after sufficient rainfall events (Brinker, 1991). Yet, it is largely unknown how reliable this system was and how it functioned in detail. In the case of Resafa, the major aim of the case study is to estimate the reliability of its water supply system and to reveal how the system worked in detail. The major tool applied to address these questions was rainfall-runoff modeling.

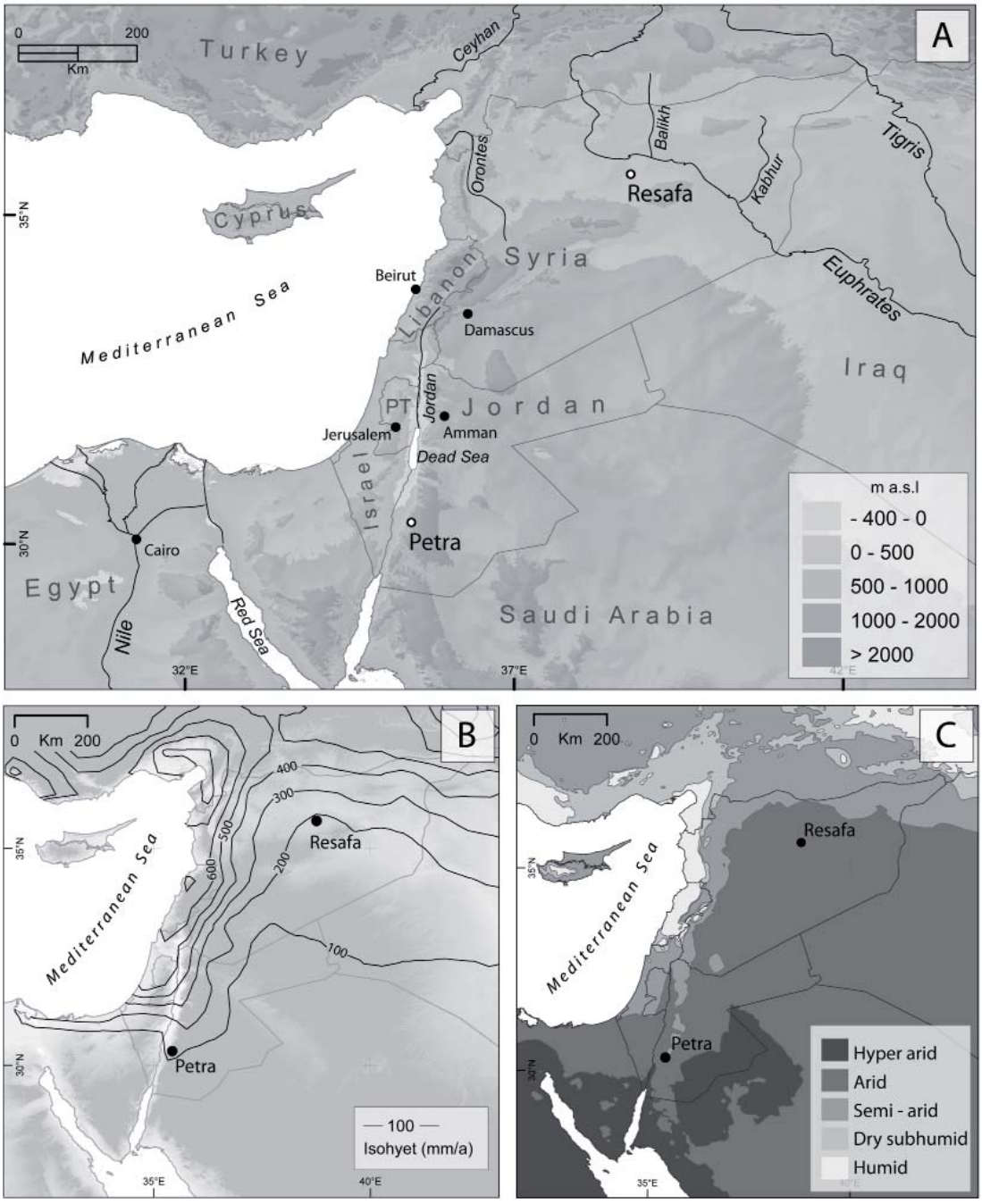

Fig. 1 A: Regional overview and location of the case studies Resafa, Syria and Petra, Jordan, B: Mean annual rainfall, C: Aridity index according to UNEP (1997). (Data base: Topography: SRTM, rainfall data: CRU (Mitchell and Jones, 2005).)

The city center of Petra was supplied with water by aqueducts that channeled the little spring water to the city, reservoirs that stored local rainfall and runoff and dams and tunnels that diverted and channeled floods from large ephemeral streams (Ortloff, 2005). The agricultural fields and terraces surrounding Petra were irrigated with indigenous systems that captured and stored rainfall and runoff (Tholbecq, 2001). Whereas the chronology of the water supply system of the city center is reasonably well known, the time of construction and usage of the agricultural terraces is still debated. The major aim of the case study in Petra was to establish a chronology of these terraces by applying OSL – dating supplemented with results from radiocarbon dating.

It is largely accepted among scholars that the major factors responsible for the abandonment of Petra and Resafa were of political respectively economical nature (Fowden,

1999; Schmid, 2008). Resafa owed much of its wealth to pilgrimage and its location at a nodal point for caravan routes that crossed the Syrian desert steppe. After the Mongol invasion in the 13th century AD these caravan routes have ceased and the pilgrimage declined. In Petra a similar reason is quoted. Petra became powerful by controlling an area of intersecting trade route networks (e.g. the incense road) in the southern Levant. As these trading routes shifted to outside the territory the city lost its importance and was finally abandoned.

As the major cause of the abandonment of the cities is apparently known what is the significance of the two studies to the aforementioned debate?

Remarkable is that the cities not only shrunk but were almost completely abandoned while at the same time smaller farmsteads and villages remained inhabited in the wider regions of Petra and Resafa (Konrad, 2001; Kouki, 2009). Moreover, the cities offered an established water supply system in an arid region in which the water and food supply is challenging and expensive (Musil, 1928; Brinker, 1991; Ortloff, 2005). It is a common notion that the more complex water and food supply strategies of settlements are the more susceptible they are to external and internal socio-economic changes (Oweis et al., 2012). In this thesis it is argued that the high maintenance expenses and the complexity of the supply systems accelerated the shrinking process after the fundamental source of income or importance ceased. It is not the aim of this thesis to conclusively verify or falsify this hypothesis but it will be discussed whether the results of the case studies support this assumption.

Structure of the Thesis

The thesis is structured into 6 chapters. The introduction chapter 1 gives an overview to the general research background of this work and a brief introduction to the study sites. Chapter 2 introduces to the main methods applied in this thesis and gives background information to sediment analysis, rainfall-runoff modeling and Optical Stimulated Luminescence (OSL) Dating and the methods are specified in the respective case studies. Chapter 3 gives an overview over ancient water harvesting techniques that were applied in the Mediterranean region and West Asia (Beckers et al., 2013 B). Chapters 4 to 5 present the results of the two case studies and consist of four self-contained and published research papers: Chapter 4 deals with the water supply system of Resafa and consists of two papers (Berking et al. 2010; Beckers et al., 2013 C). The first paper compares the water supply systems and their environmental boundary conditions of Resafa to the one of the ancient city of Naga in Sudan. It gives a brief introduction to the study area of Resafa and focuses on the approaches which were applied to set up a hydrological model. The paper was written in cooperation with the TOPOI project Egypt lies in Africa. The second paper presents the study area and the water supply system of Resafa in more detail, assesses the reliability of the system and reveals previously unrecorded construction details of the floodwater harvesting system. Chapter 5 deals with the agricultural terraces of Petra and their age determination (Beckers and Schütt, 2013; Beckers et al. 2013 A). The first section introduces the study area and summarizes the results of the case study. The second section consists of the original research paper on the age determination of the agricultural terraces. The work in Petra was conducted in cooperation with the Leibniz Institute for Applied Geophysics (LIAG). The final chapter 6 synthesizes the results from the case studies and integrates them into the geoarchaeological framework of this study. This thesis was conducted within the framework of the research cluster TOPOI and is integrated in the research group Central Places and their Environment.

References

Barker, G., Gilbertson, D., 2000. Living at the margin: themes in the archaeology of drylands, in: Barker, G., Gilbertson, D.D. (Eds.), The Archaeology of Drylands: Living at the Margin, One World Archaeology. Routledge, London ; New York.

Beckers, B., Schütt, B., 2012. On the chronology of Petra's Engineered Landscape. Optical Luminescence and Radiocarbon Dates from the Terraced Wadis of the Petra Region, in Mouton, M. and Schmid, S. (eds.), 2012. Early Petra. Logos Verlag.

Beckers, B., Schütt, B., Tsukamoto, S., Frechen, M., 2013 A. Age determination of Petra's engineered landscape - optically stimulated luminescence (OSL) and radiocarbon ages of runoff terrace systems in the Eastern Highlands of Jordan. Journal of Archaeological Science, 40-1, 333-348.

Beckers, B., Berking, J., Schütt, B., 2013 B. Ancient water harvesting methods in the drylands of the Mediterranean and Western Asia, in eTopoi, Vol. 2, Journal for Ancient Studies, 145-164.

Beckers, B., Schütt, B., 2013 C. The elaborate floodwater system of ancient Resafa in Syria - Construction and reliability. Journal of Arid Environments, 96, 32-47.

Berking, J., Beckers, B., Schütt, B., 2010. Runoff in two semi-arid watersheds in a geoarchaeological context: A case study of Naga, Sudan, and Resafa, Syria. Geoarchaeology, 25, 815-836.

Brinker, W., 1991. (in German) Zur Wasserversorgung von Resafa-Sergiupolis. Damaszener Mitteilungen 5, 119 – 146.

Butzer, K.W., 2012. Collapse, environment, and society. PNAS 109, 3632–3639.

Butzer, K.W., Endfield, G.H., 2012. Critical perspectives on historical collapse. PNAS 109, 3628–3631.

Fowden, E.K., 1999. The barbarian plain: Saint Sergius between Rome and Iran, The transformation of the classical heritage. University of California Press, Berkeley.

Konrad, M., 2001. Der spätrömische Limes in Syrien. Zabern.

Kouki, P., 2009. Archaeological Evidence of Land Tenure in the Petra Region, Jordan: Nabataean-Early Roman to Late Byzantine. Journal of Mediterranean Archaeology 22, 29–56.

Mackensen, M., 1984. (in German) Resafa: Eine befestigte spätantike Anlage vor den Stadt-mauern von Resafa. Zabern.

Mitchell, T.D., Jones, P.D., 2005. An improved method of constructing a database of monthly climate observations and associated high-resolution grids. International Journal of Climatology 25, 693–712.

Musil, A., 1928. Palmyrena, a topographical itinerary. American Geographical Society of Oriental Explorations and Studies No. 4, Ed. J.K. Wright, Czech Academy of Sciences and Arts, New York.

Ortloff, C.R., 2005. The Water Supply and Distribution System of the Nabataean City of Petra (Jordan), 300 BC– AD 300. Cambridge Archaeological Journal 15, 93–109.

Oswalt, P., Rieniets, T., 2006. Atlas of Shrinking Cities: Atlas Der Schrumpfenden Städte. Hatje Cantz Verlag GmbH & Company KG.

Oweis, T.Y., Prinz, D., Hachum, A.Y., 2012. Rainwater Harvesting for Agriculture in the Dry Areas. Crc Pr Inc.

Schmid, S.G., 2008. The Hellenistic Period and the Nabataeans, in: Adams, R. (Ed.), Jordan: An Archaeological Reader. Equinox Pub, Oakville, CT.

Tholbecq, L., 2001. The hinterland of Petra from Edomite to the Islamic periods: The Jabal ash-Sharah Survey (1996 - 1997). SHAJ 399–405.

UNEP, 1997. World Atlas of Desertification. UNEP, London.

2. Methods

2.1 Sediment analyses

In geoarchaeological research sedimentary deposits are a major archive to study the environmental history. Sediments have the potential to bear information on their origin, their agent of transportation and their depositional environment. Chemical and physical alterations of the deposits can give indications on the environmental conditions prevailing since its deposition (Goldberg and Macphail, 2006).
In Petra and Resafa sediments were analyzed to reveal significant shifts in the depositional environment of key sites (e.g. from high - to low energetic fluvial deposition regimes) and to investigate changes in the carbonate content. The former was investigated by means of grain size distribution and the latter with Loss On Ignition (LOI) and with a carmhograph. The three methods will be described briefly in the following.

Sediment sampling

While in Petra sediments were sampled and described on readily available sediment profiles, in Resafa additionally sediment cores were obtained with a hand-operated vibracorer. In the field the sediments were macroscopically described particularly according to their bedding, grain size distribution, and color following the guidelines of the Bodenkundliche Kartieranleitung (Ad Hoc Boden, 2005). Samples were taken in 10 – 20 cm intervals for later analysis in the laboratory. The LOI and the carmhograph analysis was conducted in the geomorphological laboratory at the Department of Earth Sciences of Freie Universität Berlin and grain size analysis were performed at the Leibniz Institute for Applied Geophysics in Hannover.

Loss On Ignition

LOI is a widely applied method to estimate the organic and carbonate content of sediments (Heiri et al., 2001). The procedure, initially described by Dean (1974), is based on the combustion of carbonates at different temperatures. Organic matter is oxidized at 500 - 550 °C to carbon dioxide and ash, and carbon dioxide evolves from carbonate at 850 - 1000 °C, leaving oxide (Heiri et al., 2001). Weighing of the samples before and after exposing it to the respective temperatures gives a mass difference which can then be expressed in relative carbonate content (mass-%).
The procedure applied in this study follows the norms of the DIN 19684 (1977). Prior to analysis the samples were dried at 105 °C and sieved for material < 2 mm and homogenized in an agate oscillating disk mill. The preprocessed samples (< 2 mm - fraction) were sequentially heated in a muffle furnace, i.e. to 550 °C and 880 °C for five hours respectively. After heating the samples were cooled to 200 °C and subsequently cooled to room temperature in a desiccator and weighed.
The LOI_{550} is then calculated by:

$$LOI_{550} = ((DW_{105} - DW_{550}) / DW_{105}) * 100$$

Where LOI_{550} is the LOI at 550 °C in mass-%, DW_{105} is the dry weight of the sample after drying at 105 °C and DW_{550} is the dry weight of the sample after combustion, all weights given in gram (Heiri et al., 2001).
The LOI_{880} is calculated by:

$$LOI_{880} = ((DW_{550} - DW_{880}) / DW_{105}) * 100$$

Where LOI_{880} is the LOI at 880 °C in mass-%, DW_{550} the dry weight of the sample after LOI_{550} and DW_{880} is the dry weight of the sample after heating to 880 °C (for DW_{105}, see above) (Heiri et al., 2001).
The weight loss during LOI has shown to be a proxy for soil organic content and carbonate content (Dean, 1974). However, several authors state that clay might lose structural water during LOI (Heiri et al., 2001, and references cited). Additionally, structural water may be lost by metal oxides and volatile salts might contribute to a weight loss during LOI, possibly leading to a overestimation of the carbonate content . Careful investigation of the mineralogical composition prior to LOI and comparison to independent methods to estimate carbon content (see below) are therefore mandatory.

Determination of carbon content by means of a carmhograph

Another widely applied method to determine the carbon content of sediment samples is applying a carmhograph (Dean, 1974). Here, the Woesthoff Carmhograph C-16 was applied. To determine the total carbon content (TC) of sediments the samples were dry combusted in an oxygen atmosphere at 1000 °C. The evolved CO2 is subsequently quantified in 20 ml 0.05 N NaOH solution by measuring the conductivity of the solution (Schütt et al., 2010). To determine the total inorganic carbon (TIC) content of the sample it was treated with H3PO4 - acid and heated to 80 °C to release CO2 which was then quantified similar to the procedure described for determining the TC. The total organic content (TOC) was calculated by subtracting the TIC from the TC. The detection limit for this method is ca. 0.02 mass-%.

Particle size analysis of sediments

The grain size of sediments has major influence on their entrainment, their mode of transportation and their deposition. In turn the character of those components of the sediment cycle might be estimated from the grain size distribution of the deposits (Pye and Blott, 2004).
In the field the investigated sediment profiles were macroscopically divided to stratigraphic units according to their grain size distribution. Gravel and pebble beds were described in the field (sizes and shape of exemplary pebbles or gravels). Sediment units which largely comprised of particles < 2 mm were sampled for further analysis in the laboratory. The < 2mm fraction was analyzed by a Beckman Coulter LS13320 laser diffractometer. Laser diffractometers measure the scatter of light of particles which result from directing a laser beam on a dispersed samples. The intensity of the light scatter is highly dependent on the particle size of the sediments (see Pye and Blott, 2004, for more details on the method).
Prior to measuring the particle size the sediments were sieved for particles < 2mm. After sieving the samples were dispersed in 1 % Ammonium hydroxide solution and put in a rotator for 12 hours. The samples were subsequently treated with ultrasonic for 1 min to break up remaining aggregates and then analyzed with the laser diffractometer. The results are given in vol-%. Statistical analysis of the results were made using GRADISTAT (Blott and Pye, 2001). The results and a further discussion of the applied methods are presented in the chapters 4 and 5.

2.2 Rainfall-runoff modeling

Rainfall-runoff models have recently gained increasing attention in geoarchaeological studies as a tool to estimate the water availability of ancient settlements (Whitehead et al.,

2008; Harrower, 2010; Wade et al., 2012). A white range of different rainfall-runoff models exist and this section gives a brief overview to existing model types. Comprehensive introduction to rainfall-runoff modeling can be found in Beven (2011), Wagener et al. (2004) and Wheater (2007).

The main reason for applying a rainfall-runoff model is the limited availability and/or capability of hydrological measurements (Beven, 2011). Rainfall-runoff models offer the possibility to e.g. extrapolate available data to ungauged catchments or to make predictions on future or past catchment responses to climate or land use changes (Wagener et al., 2004). Many different types of rainfall – runoff models exist which have different spatial and temporal resolutions or a different approach to represent the hydrological system. Models in which the parameters of the hydrological system are spatially averaged over the entire modeled catchment are called lumped models. Models in which those parameters are spatially variable are called distributed models (Wheater et al., 2007). However, even those models average variables and parameters at grid or element scale (Beven, 2011). In semi-distributed models the parameters are averaged over individual subcatchments (Wheater et al., 2007). Lumped models are appropriate when e.g. the runoff volume on a catchment scale is of interest for the study. When e.g. the water level in a stream during a storm event is to be estimated the application of a distributed model has to be considered. Rainfall-runoff models can further be event based which means e.g. that the catchment response to one individual storm is modeled. Continuous models produce continuous output and are often applied in flood prediction or water resource planning (Beven, 2011). Another distinction can be made between deterministic models – the same set of inputs will produce the same results – and stochastic models which add randomness and uncertainty to its calculations (Beven, 2011). After Wheather (2007) models can further be classified into metric, conceptual and physics based models. Metric models are mainly based on measured time series of rainfall and runoff data. Based on the data the relationship between rainfall input and flow output of a catchment is determined, i.e. how much runoff is generated per unit rainfall or how much rainfall is lost due to evapotranspiration and infiltration. One example of a metric model is the widely applied unit hydrograph (Wheater et al., 2007). Conceptual models are the most developed and applied model type. They incorporate those hydrological processes which are conceived to be significant for the respective task of the model or the representation of the rainfall-runoff relationship of a catchment. These processes are parameterized and are mainly based on perceptual models such as the relationship between soil hydraulic properties and terrain unit (Wheater et al., 2007). One example is the widely applied Topmodel (Beven, 2011). Physics based models represent the hydrological processes and the catchment responses to input variables by physically based equations. Kineros (Al-Qurashi et al., 2008) for example is such a model. Physics based models are usually data and resource intensive and need extensive calibration and validation (Beven, 2011). The choice of the appropriate model is dependent on many factors such as the specific task for the model and the quality of available data on the catchment and climate variables. Important data to set up and drive a rainfall-runoff model are data on catchment physical properties, land use, climate and discharge (see Beven, 2011 for a critical review on input data). One major problem of applying rainfall-runoff models in geoarchaeological studies is the large uncertainty of the input data. The climate and catchment properties may have significantly changed and thus current measurements may be unrepresentative. How these problems are approach in Resafa is presented in detail in chapter 4. For other modeling approaches in geoarchaeological studies one is

referred to the publications of Whitehead et al. (2008), Wade et al. (2008), van Wesemael et al. (1998) and Crook (2009).

2.3 Optical Stimulated Luminescence Dating

OSL dating is a chronological method which is widely applied in archaeology and earth sciences (Duller, 2008a). In general, OSL dating estimates the time that has elapsed since mineral grains were last exposed to daylight (Preusser et al., 2008). The exposure to daylight of mineral grains from old sediments may occur during natural or anthropogenic transportation processes, e.g. when wind or water mobilizes sediments or when a trench is dug by a farmer. When the mineral grains deposit after the transportation process and are buried under sediments or other materials so as to be sealed from daylight the mineral grains start to "record" time in form of energy. This attribute is based on the property of specific minerals, e.g. quartz and feldspar to store time-dependent radiation damage within their crystal lattice (Vandenberghe, 2004). This is caused by ionizing radiation emitted by decaying, naturally occurring and ubiquitous radionuclides such as potassium, thorium and uranium and cosmogenic radiation (Preusser et al., 2008). The ionizing radiation causes the excitement of charge carriers within the crystal structure of the grain and the subsequent entrapment of these carriers in deficiencies of the crystal lattice (trapping centers) (Lüthgens, 2011; see Duller, 2008a for more information on the physical basis). This process basically stores energy within the crystal structure delivered by the radiation (Duller, 2008a). Because the energy gradually accumulates as long as the mineral is buried and trapping centers are available they act as natural dosimeter (Duller, 2008a). The SI measure of this absorbed radiation is stored energy per mass unit expressed in Gray (Gy = J/kg). When the minerals are stimulated by light or high temperatures the accumulated energy may be released in form of light (luminescence). As the intensity of the luminescence signal correlates with Gray the signal is a proxy of the stored energy (Preusser et al., 2008). Thus, age determination based on OSL basically requires two laboratory measurements: (i) the total energy accumulated during burial, referred to as the equivalent dose (De) in Gy and (ii) the energy delivered in time from radioactive decay called the dose rate usually expressed as Gy/a (Duller, 2008a). The general OSL age equation can be expressed as:

$$age\ [a] = \frac{equivalent\ dose\ [Gy]}{dose\ rate\ \left[\frac{Gy}{a}\right]}$$

The process being dated with OSL is the resetting of the OSL signal which is commonly called bleaching or zeroing. Bleaching occurs when mineral grains are sufficiently and homogenously exposed to sunlight (Fig. 1 A). In this case the mineral grains would yield the same and correct burial age. However, when the exposure to sunlight during transport is limited or varies from one grain to the other some grains might release their trapped charge while others may not or only a part of it (Fig. 1 B)(Duller, 2008b). This process is called incomplete bleaching. When incomplete bleaching occurs and mineral grains bear a residual signal the burial age may be overestimated. The degree of bleaching of a mineral grain or the uniformity of bleaching within a sample population is highly dependent on the transportation and deposition environment. Aeolian transported sediments are usually considered well bleached while e.g. fluvially transported sediments or sediments transported with a glacier are often incompletely bleached. Moreover sediments may be transported and buried at night (Rittenour, 2008; Rhodes, 2011).

The burial age determination of mineral grains usually require the following steps: (a) sampling of sediments by avoiding exposure to daylight (b) stimulating the sediment

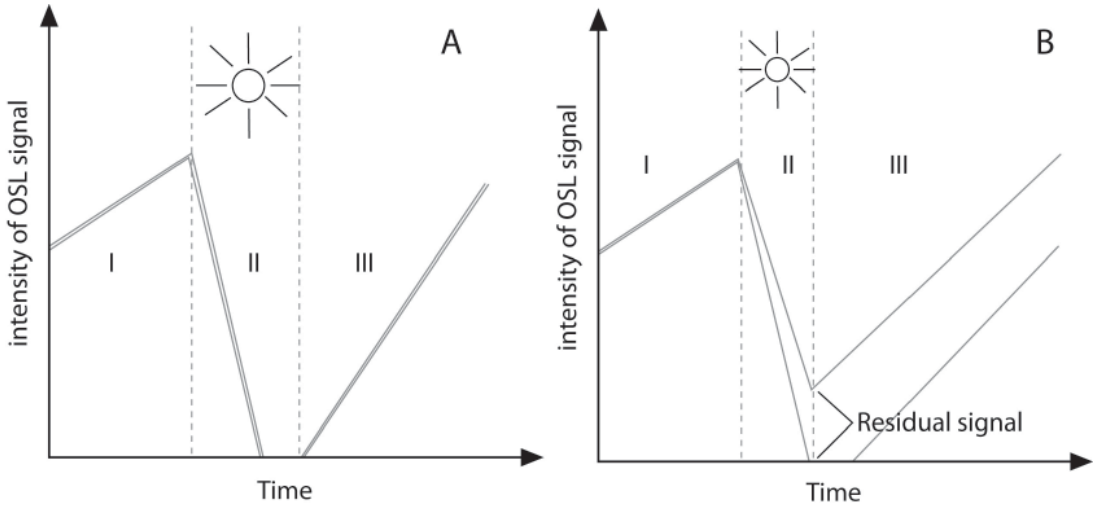

Fig. 1 Illustration of the (incomlete) bleaching process A: (I) Sediments are eroded and mobilized from old sediments. The grains bear trapped charge within their crystal lattice (II) The mineral grains are evenly and homogenously exposed to sunlight and release their trapped charge (II) the sediments are buried and accumulate charge. When the sediments are sampled and measured they yield the same and correct burial age. B: (I) Sediments are eroded and mobilized from old sediments. The grains bear trapped charge within their crystal lattice (II) The exposure to sunlight is limited or varies from one grain to the other and some grains may retain a residual signal (II) the sediments are buried and add charge to their residual signal. The burial age of the upper grain may be overestimated. Adapted from (Duller, 2008b).

sample with an artificial light source (optical stimulation) in the laboratory and subsequent measurement of the luminescence signal (c) determination of the burial dose rate and (d) calculation of the age (Rhodes, 2011). Step (a) requires extensive pre-treatments of the sediments and different measurement and analysis procedures exist that have to be adapted to the nature of the sampled sediments (e.g. well – bleached samples vs. incompletely bleached samples). An overview of common laboratory procedure for OSL dating are presented in more detail in Duller (2008a) and Rhodes (2011). In chapter 5.2 the specific laboratory procedures and analysis approaches that were applied in Petra are presented in detail.

References

Ad Hoc Boden, 2005. Bodenkundliche Kartieranleitung. Schweizerbart, Stuttgart.

Al-Qurashi, A., McIntyre, N., Wheater, H., Unkrich, C., 2008. Application of the Kineros2 rainfall–runoff model to an arid catchment in Oman. Journal of Hydrology 355, 91–105.

Beven, K., 2011. Rainfall-runoff modelling: the primer, 2nd ed. ed. Wiley, Hoboken.

Blott, S.J., Pye, K., 2001. GRADISTAT: a grain size distribution and statistics package for the analysis of unconsolidated sediments. Earth Surface Processes and Landforms 26, 1237–1248.

Crook, D., 2009. Hydrology of the combination irrigation system in the Wadi Faynan, Jordan. Journal of Archaeological Science 36, 2427–2436.

Dean, W.E., 1974. Determination of carbonate and organic matter in calcareous sediments and sedimentary rocks by loss on ignition; comparison with other methods. Journal of Sedimentary Research 44, 242–248.

Duller, G., 2008a. Luminescence Dating: guidelines on using luminescence dating in archaeology. Swindon: English Heritage.

Duller, G.A.T., 2008b. Single-grain optical dating of Quaternary sediments: why aliquot size matters in luminescence dating. Boreas 37, 589–612.

Goldberg, P., Macphail, R., 2006. Practical and theoretical geoarchaeology. Blackwell Science, Malden, Massachusetts.

Harrower, M.J., 2010. Geographic Information Systems (GIS) hydrological modeling in archaeology: an example from the origins of irrigation in Southwest Arabia (Yemen). Journal of Archaeological Science 37, 1447–1452.

Heiri, O., Lotter, A.F., Lemcke, G., 2001. Loss on ignition as a method for estimating organic and carbonate content in sediments: reproducibility and comparability of results. Journal of Paleolimnology 25, 101–110.

Lüthgens, C., 2011. The age of Weichselian main ice marginal positions in north-eastern Germany inferred from Optically Stimulated Luminescence (OSL) dating (Dissertation).

Preusser, F., Degering, D., Fuchs, M., Hilgers, A., Kadereit, A., Klasen, N., Krbetschek, M., Richter, D., Spencer, J., 2008. Luminescence dating: basics, methods and applications. E&G – Quaternary Science Journal Vol. 57 No 1-2, 95–149.

Pye, K., Blott, S.J., 2004. Particle size analysis of sediments, soils and related particulate materials for forensic purposes using laser granulometry. Forensic Science International 144, 19–27.

Rhodes, E.J., 2011. Optically Stimulated Luminescence Dating of Sediments over the Past 200,000 Years. Annual Review of Earth and Planetary Sciences 39, 461–488.

Rittenour, T.M., 2008. Luminescence dating of fluvial deposits: applications to geomorphic, palaeoseismic and archaeological research. Boreas 37, 613–635.

Schütt, B., Berking, J., Frechen, M., Frenzel, P., Schwalb, A., Wrozyna, C., 2010. Late Quaternary transition from lacustrine to a fluvio-lacustrine environment in the northwestern Nam Co, Tibetan Plateau, China. Quaternary International 218, 104–117.

van Wesemael, B., Poesen, J., Solé Benet, A., Cara Barrionuevo, L., Puigdefábregas, J., 1998. Collection and storage of runoff from hillslopes in a semi-arid environment: geomorphic and hydrologic aspects of the aljibe system in Almeria Province, Spain. Journal of Arid Environments 40, 1–14.

Vandenberghe, D., 2004. Investigation of the optically stimulated luminescence dating method for application to young geological sediments.

Wade, A.J., Smith, S.J., Black, E.C.L., Brayshaw, D.J., Holmes, P.A.C., El-Bastawesy, M., Rambeau, C.M.C., Mithen, S.J., 2012. A new method for the determination of Holocene palaeohydrology. Journal of Hydrology 420–421, 1–16.

Wagener, T., Wheater, howard S., Gupta, H.V., 2004. Rainfall-Runoff Modelling In Gauged And Ungauged Catchments. World Scientific Publishing Company.

Wheater, H., Sorooshian, S., Sharma, K.D., 2007. Hydrological Modelling in Arid and Semi-Arid Areas, 1st ed. Cambridge University Press.

Whitehead, P.G., Smith, S.J., Wade, A.J., Mithen, S.J., Finlayson, B.L., Sellwood, B., Valdes, P.J., 2008. Modelling of hydrology and potential population levels at Bronze Age Jawa, Northern Jordan: a Monte Carlo approach to cope with uncertainty. Journal of Archaeological Science 35, 517–529.

3. Ancient water harvesting methods in the drylands of the Mediterranean and Western Asia

Brian Beckers, Jonas Berking and Brigitta Schütt, 2013. eTOPOI, Journal for Ancient Studies, 2, 145-164.

3.1 Introduction

Archaeological remains are abundant in the drylands1 of the Mediterranean region and West – Asia. Many of those show evidence of more or less elaborated water supply structures that allowed the existence of (semi -) permanent settlements at locations of which nowadays many are abandoned (Barker and Gilbertson, 2000). A great variety of ancient water supply techniques have been documented for the region, reflecting the historical evolution of these techniques and the specific hydrological conditions to which they had been adapted to (Wikander, 1999). The natural water sources in drylands can broadly be classified into those which are generated in humid regions or inherited from wetter climate periods (allogenic) and those which are locally generated (autogenic) (Roberts, 1977 citing; Goudie and Wilkinson, 1977). Allogenic or perennial sources are predominantly fossil groundwater and major rivers such as the Nile and the Euphrates which have their origin in humid areas and pass through drylands (see e.g. Woodward, 2009). Autogenic or intermittent sources are in general rainfall, local runoff and floods in intermittent streams (wadis) or shallow groundwater (see Shanan, 2000; Tooth, 2000; Bull and Kirkby, 2002; Wheater and Al-Weshah, 2002, for overviews in dryland hydrology). The focus of this paper lies on water techniques that harness autogenic water sources which are commonly grouped under the term water harvesting systems. Some of these techniques have regained attention in the past several decades especially in regard to their reimplementation to mitigate current food and water supply problems in drylands (Oweis et al., 2012). For this purpose the study of ancient water harvesting technologies can not only give valuable information to engineers, planers and local initiatives on technical aspects of those systems. It can also give indications for possible short- and long-term effects of those systems on the environment and the involved people (Barker and Gilbertson, 2000).

This paper will provide a brief overview on water harvesting systems and intents to give a preliminary compendium for upcoming projects which will study the diffusion of ancient water supply technologies in the Old World and assess the viability and reliability of such systems. Water supply techniques which rely on allogenic sources will be part of an upcoming paper. Several books and papers exist on ancient water harvesting techniques (Evenari et al., 1961; Bruins et al., 1986; Critchley et al., 1994; Prinz, 1994; Wikander, 1999; Ortloff, 2009; Mays, 2010a; Oweis et al., 2012) and this paper largely draws its information out of these publication. The basic principles of the respective techniques will be explained and supplemented with references to archaeological case studies reaching from the Bronze Age to the Middle Ages.

3.2. Water Harvesting

Water harvesting is here understood as the process of harnessing water for beneficial use with any kind of device or technique that collects, stores, and/or increases the availability of intermittent surface runoff and groundwater in drylands (Bruins et al., 1986; Prinz, 1994; Oweis et al., 2012 for other definitions and reviews). Water harves-

ting is applied to irrigate crops and to supply water for animal and human consumption (Prinz, 1994). Especially regarding agricultural purposes the basic principle of water harvesting can be illustrated by a hypothetical calculation. A region receiving 100 mm rainfall per year might not offer enough moisture for a continuous vegetation cover or for crops to grow. If however, these 100 mm of rainfall are collected and concentrated in a subarea of suppositional a fourth of the total region´s size, 400 mm of water column would be available in this subarea, which in turn would be sufficient for plants to grow on this area (cf. Evenari and Tadmor, 1982). In principal this process occurs naturally when rainfall is converted to runoff and collected by the topography, e.g. in a riverbed or at the foot of a hillslope. In this sense water harvesting is the attempt to mimic and/or make use of these processes.

Commonly, water harvesting techniques are distinguished by the source of water they harvest and called Groundwater harvesting, Runoff harvesting and Floodwater harvesting.

The specific device or technique applied is the water harvesting system (Frasier and Myers, 1984). Those systems range in their complexity from simple cultivated earth pits (section 3.2.2.2) that collect local runoff to such elaborated systems as the irrigation system of Ma´rib in Yemen which relied on the floods of a large wadi (referring to a valley or an ephemeral channel) (Brunner, 2000). In general, water harvesting systems consist of three components (modified from Oweis et al., 2012):

(i) The catchment

The catchment is the area from which the water is collected. It may be the catchment of a wadi (section 3.2.3.), parts of it like a hillside (section 3.2.2.3), or even just a few square meters (section 3.2.2). Suitable catchments are ones where surface and soil characteristic are such that runoff is generated regularly, i.e. that the infiltration rates are occasionally lower than rainfall intensities (Bruins, 2012). However, catchments may be modified to induce runoff and reduce infiltration rates as was e.g. done in the Negev in Israel by clearing the surface of the catchments from vegetation and stones (Evenari et al., 1961). Moreover, catchments can be artificially constructed by installing bunds or excavating a pit or a trench. Also roofs of a house are catchments from where water can be collected after channeling it in drip moulding and drain pipe (=conveyance).

(ii) The Conveyance or deflection device

The conveyance device concentrates and channels the collected runoff from a catchment to the storage facility. Commonly they consist of bunds or canals and may be equipped with control devices such as sluice gates and distribution systems. Conveyance devices are often installed in larger catchments or on long hillslopes where runoff would otherwise be lost due to infiltration or where the storage facilities are located in great distance from the catchment. In small cultivated catchments conveyance devices are largely unnecessary as the catchments adjoin the storage device. In floodwater harvesting (section 3.2.3.) deflection devices are built in wadi streams to tab occasional floods which were generated in remote catchments.

(iii) The storage facility

Storage facilities can be of many types including natural sediment bodies, (sub-) surface cisterns and open reservoirs which are e.g. formed by a dam or retaining wall. Storage facilities function as a buffer between the short rainfall and runoff events when natural water is provided and the long dry periods when water is required. Hence, their storage capacity has to meet the water demands during dry periods. When water harvesting is

accompanied with farming the storage devices often also act as the cropping area and the water is stored in the sediment column respectively, in the root zone of crops. In areas where a sufficient sediment layer is lacking or is prone to erosion storage devices might be built to collect and conserve sediments. In those instances the storage facilities are both, water and soil conservation measures (Critchley et al., 1994).

In the evaluation and planning of water harvesting systems certain indices have been established that reflect a specific environmental regime and demands of the end user (Prinz, 1994). Among the most important is the ratio between the runoff area (the catchment) and the run-on area (retaining area). Because water harvesting is often associated to farming this index is commonly called the catchment to cropping area ratio (CCR) (Oweis et al., 2012). The runoff area is always equal to or larger than the run-on area (Oweis et al., 2012). The lesser the rainfall and runoff yield and the larger the water demand the larger the catchment has to be compared to the cropping area. The ratio varies from 1:1 in wetter regions to more than 30:1 in arid regions (Evenari and Tadmor, 1982). However, the efficiency (volume of runoff per unit area) of a catchment decreases with increasing size (Evenari et al., 1961), as does the frequency and predictability of harvestable runoff events (Shanan, 2000). This phenomenon is commonly attributed to the increasing infiltration losses of runoff in downslope or downstream direction, i.e. the farther a flood or runoff event flows on the surface the lesser is the runoff yield at a specific point (Yair and Raz-Yassif, 2004).

The size of the catchment also has several implications on technical and organizational aspects of water harvesting systems. The character of runoff generated in small catchments tends to be moderate and manageable, flowing as sheet flow or along small rills. Thus, the water harvesting facilities can be of simple construction and can be implemented and maintained by individual non-expert households. Moreover, the runoff is usually generated locally, often within the borders of a farm or other small organizational units. Hence, the water distribution has only to be internally organized. In larger catchments such as that of a high-order wadi, runoff can get the character of flash flood, being torrential and unpredictable. The harvesting facilities have to be sophisticated to be able to manage short-term appearing large water volumes attended by high maintenance costs. Moreover, the water distribution might has to be organized between different organizational units (Oweis et al., 2012).

3.1.1 Groundwater Harvesting

Water wells (artificial holes that reach the groundwatertable) were probably the first structures that allowed the settlement of drylands beyond natural perennial surface water sources (Issar, 2001). Issar (2001) assumes that the first wells were temporary scoopholes (hand dug shallow wells) dug in beds of ephemeral streams (wadis). More sophisticated water wells which are lined and equipped with some kind of human or animal powered lifting device are abandoned at archeological sites in the study region (Mays, 2010b). If the tapped groundwater aquifer is prone to strong seasonal variations water wells were sometimes combined with techniques that artificially recharged the groundwater e.g. by channeling water from mountain streams to shallow aquifers in the lowlands as was e.g. done in Granada, Spain (Pulido-Bosch and Sbih, 1995) or by building groundwater dams (section 3.2.3.1).

A most subtle way of groundwater harvesting techniques are Qanats. Qanats are subsurface conduits or tunnels tapping an upslope aquifer whose gathering ground is naturally different from that of the area of usage. A tunnel connects the aquifer with a foreland

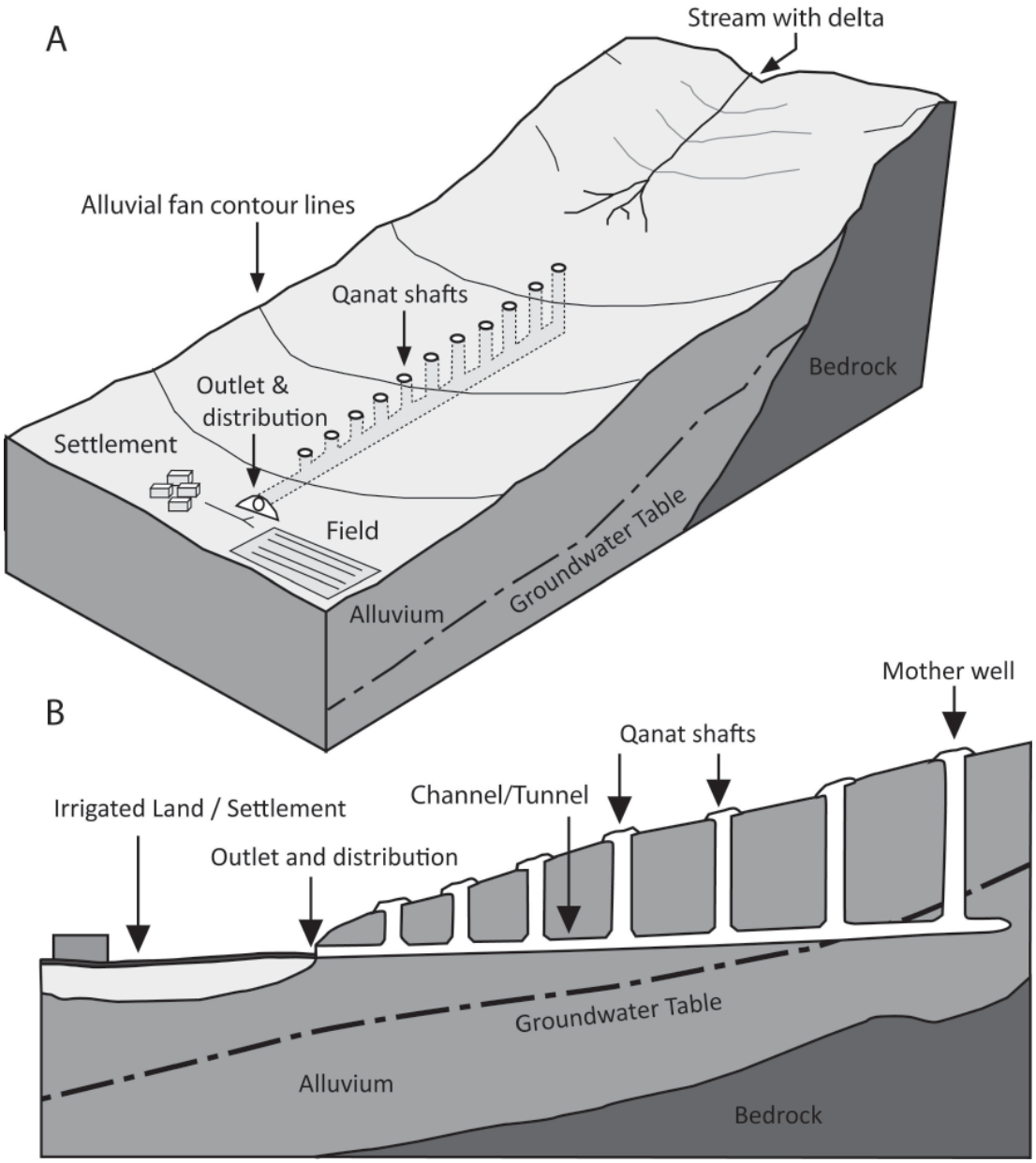

Fig. 1 Sketches of a typical qanat. For explanations see text. A: adapted from Cech (2009) B: adapted from Lightfoot (1996b).

outflow facility (Fig. 1). The tunnel is gently inclined towards the outlet. A dense series of vertical shafts, or wells, which connect the tunnel with the surface serve as construction and maintenance access shafts and regulate air pressure in the system; the uppermost of these shafts is called mother well. The tunnel usually channels the groundwater to a reservoir, frequently connected by a covered canal with the outlet of the tunnel, from the reservoir a canal system distributes the water to fields or settlements. If a tunnel fails to deliver enough water, e.g. due to a depletion of the groundwater additional tunnels may be constructed which branch of from the main tunnel until the groundwater is tabbed again (Lightfoot, 1996b). To avoid infiltration of the water frequently the tunnel beds are sealed with mortar. Qanats can often be found at the outlet of mountainous catchments, i.e. below the alluvial fans which bear reachable groundwater aquifers and workable subgrounds. Qanats are abundant in Iran (Motiee et al., 2006; Boustani, 2009) and can also be found e.g. in Syria (Lightfoot, 1996b), as well as in Morocco where they are called

khettara (Lightfoot, 1996c), in Spain where they are called galleria (Lightfoot, 2000) and in Oman, where they are called felaj (Costa, 1983).

3.2.2. Runoff (Rainwater) harvesting

The term runoff (or rainwater) harvesting comprises the collection and storage of largely unconfined locally generated runoff from modified catchments (Prinz, 1994). Runoff flowing in rills and minor channels are included in this definition (as opposed to runoff or floods flowing in larger channels and from remote catchments, section 3.2.3). The term rainwater is often used interchangeable with runoff and signify the water running off surfaces on which rain has directly fallen (Bruins et al., 1986). The collected runoff may be used for irrigation or domestic and animal consumption. Commonly two types of runoff-harvesting are distinguished by the size of the harvested catchment: Micro - and macro catchment runoff harvesting (Prinz, 2002). Runoff harvesting is often accompanied by runoff farming, the characteristic cultivation type.

3.2.2.1 Rooftop (courtyard) – harvesting

Roofs, plastered courtyards and squares (sometimes roads) are especially suitable for the collection of runoff as their surfaces are often almost impermeable and relatively clean or to be kept clean from sediments and litter. The collected runoff is usually conveyed by a gutter system to cisterns or reservoirs and used for animal and domestic consumption and the small-scale irrigation of gardens. As the catchment area of roofs and courtyards are rather limited these systems usually provided water of high cleanness suitable for individual households or administrative and religious buildings (Fig. 2). There are many examples of the application of rooftop harvesting in ancient times. For example in the Minoan settlements in Crete rooftop and courtyard harvesting was an integral part of the water supply (Mays, 2010a). In Resafa, Syria, individual houses and churches harvested the rain falling on the roofs and stored it in bottle – shaped cisterns (Brinker, 1991).

3.2.2.2 Micro catchment runoff harvesting

Micro catchment runoff farming is the collection of runoff on small ($\sim$ 1 – 1000 m^2) treated catchments to channel it to adjacent cropping areas or individual plants (Prinz, 2002). The catchments are either modified by some kind of special tillage technique, earthen embankments or masonry walls (Fig. 2). On steeper slopes the modifications might comprise the interception of those by building counter parallel individual or continuous bunds or agricultural terraces. Abundant agricultural terrace type in the region is the contour bench terrace (Fig. 2). However many other types of agricultural terraces built on hillslopes fall within this classification (compare Spencer and Hale, 1961, Treacy and Denevan, 1994, Frederick and Krahtopoulou, 2000 for reviews on agricultural terraces). In moderately steep to flat areas the systems might be constructed by building small runoff – basins either by excavation (ditches, pits) or with bunds. Widely applied construction types are Negarims (Fig. 2), semi-circular micro catchments and contour bundings (Critchley et al., 1994; Prinz, 2002). Negarims are diamond shaped earthen bunds of few m^2. They collect runoff and channel it to its lowest corner where the water is stored in the root zone of the plant. Agricultural terraces for water harvesting purposes are abundant in the Mediterranean region and West Asia (Frederick and Krahtopoulou, 2000). Micro catchment runoff harvesting was applied e.g. in the Negev, Israel alongside other techniques (Ashkenazi et al., 2012) as well as in Tunisia (Nasri et al., 2004).

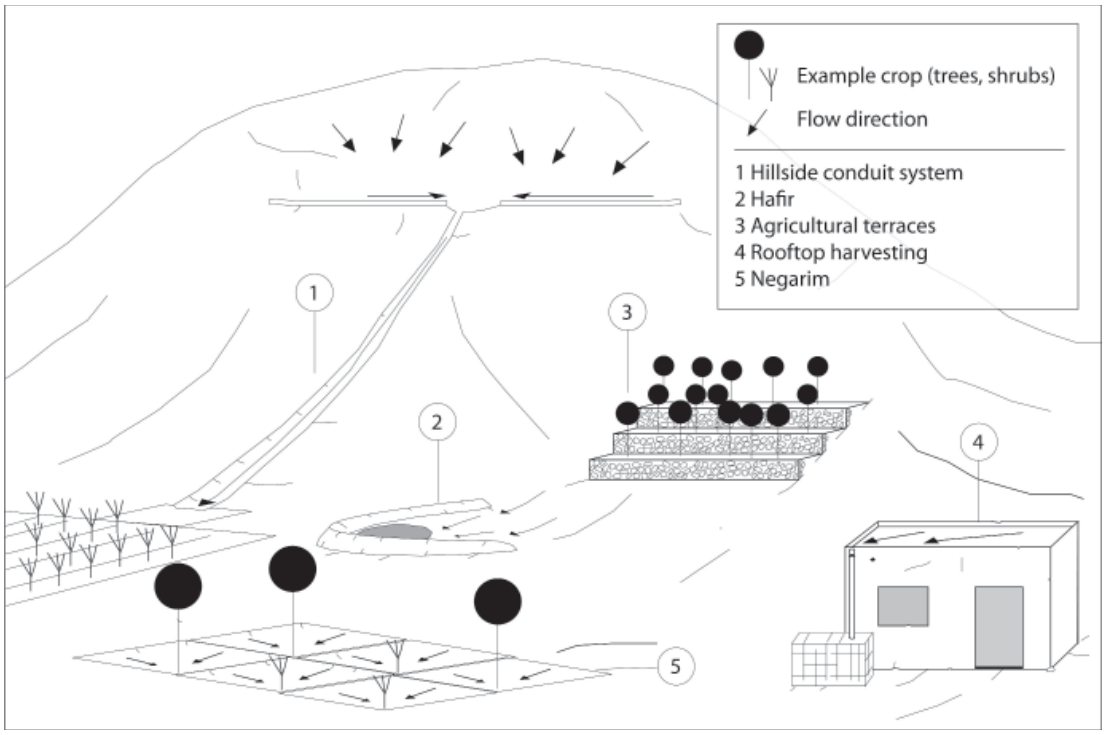

Fig. 2 Examples of micro (3-5) – and macro (1,2) runoff harvesting techniques. Slopes are exaggerated.

3.2.2.3 Macro catchment runoff harvesting

Systems which collect runoff in larger catchments such as hillsides with long slopes are commonly called Macro catchment runoff harvesting or long-slope runoff farming systems (Prinz, 2002). Often it necessitates the construction of elaborated structures and the maintenance is labor intensive (Prinz, 2002). One type is the hillside conduit system (Fig. 2) (Bruins et al., 1986). Runoff which is induced in the upper parts of a hillside might percolate or evaporate before it can reach cultivated or settled areas. By building conduits (ditches or dikes) in the upper and middle parts of the slope runoff loss can widely be reduced (Bruins et al., 1986). Hillside conduit systems usually supply agricultural fields with water. On occasions the runoff is conveyed to neighboring wadis to supplement terraced wadi systems (section 3.2.3.1). Hafirs (Fig. 2) and Tabias (also called Limans) are large open reservoirs usually built by earth embankments at the foot of plan-concave slopes. Hafirs are semicircular open water basins for animal and human consumption. Tabias are rectangular earthen bunds which store hillslope sediments and runoff. The sediment reservoirs of the Tabias are often used for cultivation (Oweis et al., 2012). Hafirs and Limans are sometimes also located in wide wadis or floodplains.

Hillside conduit systems can be found in the Negev (Shanan, 2000), Hafirs were widely applied in Sudan e.g. in Musawwarat (Näser, 2010) and Naga (Berking et al., 2010), Tabias in the Maghreb and at the Iberian Peninsula (Nasri et al., 2004). In Spain so called Aljibe systems channeled runoff from hillslope to fill cisterns (van Wesemael et al., 1998). In Petra, Jordan, the inhabitants found excellent conditions for runoff harvesting especially for drinking water purposes due to the abundance of outcropping bedrock. Here a multitude of rock carved conduit systems collected the runoff and channeled it to cisterns (Ortloff, 2005).

3.2.3. Floodwater Harvesting

Floodwater harvesting (or spate irrigation) is a technique that collects and stores water from ephemeral streams during flood events (Bruins et al., 1986). Floodwater harvesting usually requires the construction of elaborated hydraulic structures like large dams or dikes and distribution facilities (Prinz, 2002). Commonly the harvested streams are of small or medium size as the regular floods occurring are more predictable and manageable than in larger streams. Two techniques are usually distinguished: floodwater harvesting within stream (wadi) beds and off wadi harvesting or floodwater diversion (Fig. 3) (Bruins et al., 1986). The characteristic cultivation type for floodwater harvesting is called floodwater farming.

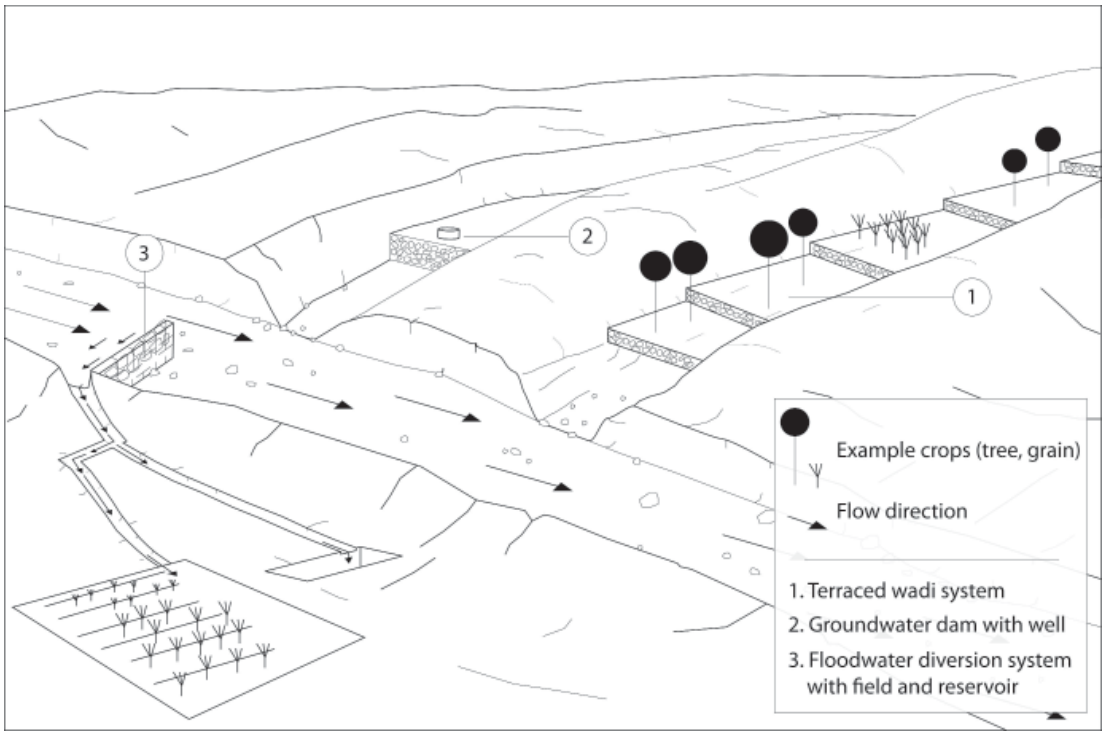

Fig. 3 Examples of floodwater harvesting techniques. Slopes are exaggerated.

3.2.3.1 Wadi-bed floodwater harvesting

Applying this method structures are built across wadi beds to partially or completely dam flood water and to store it either in surface reservoirs or in channel sediments (Fig. 3). These structures might be walls built of masonry or earthen embankments (Oweis et al., 2012). A widespread type of this technique is called terraced wadi system (Bruins et al., 1986). These systems are commonly built for agricultural purposes. Terraced wadi systems consist of a series of small dams (check dams) that intersect parts of a wadi course. The check dams lower the runoff velocity of the floods and thereby their transport capacity. In consequence the transported sediments accumulate behind the dams and gradually built a terrace or sediment reservoir upstream. Excess water flows into the subsequent component of the system where the same process proceeds. After a few years (dependent on the frequency and character of the flood events) and when the volume of the accumulated sediment body is sufficient the terraces might be cultivated (Evenari et al., 1961). The subsequently occurring floods now percolate into the terrace bodies where the water is stored and provide crops with water (Critchley et al., 1994). On occasion

the check dams may be raised, thus enlarging the cropping area and the water storage capacity of the terraces. These systems are sometimes supplemented with hillside conduit systems (section 3.2.2.3). Examples of ancient terraced wadi systems can e.g. be found in the Negev in Israel (Evenari et al., 1961), in the Petra region in Jordan (Beckers et al., 2013), in the Matmata Mountain region in Tunisia where they are called Jessour (Hill and Woodland, 2003), in Libya (Gale and Hunt, 1986; Gilbertson, 1986; Barker, 1996) and in Andalucia in Spain where the system is locally called Cultivo de cañada (Giráldez et al., 1988).

A variant of this technique are groundwater dams which predominantly collect and store flood water and intermediate flow for animal and human consumption (Hanson and Nilsson, 1986). Basically two types are distinguished: sand storage dams and subsurface dams. Sand storage dams function with the same principle as the terraced wadi system. However, the stored water in the sediment bodies is either withdrawn by water wells build in the sedimentary fill of the reservoir or by drainage devices built into the dam. Subsurface dams are built into the alluvial fill of streams by excavating a trench down to an impervious layer (e.g. bedrock, clay layer) and building a wall in the trench which is subsequently backfilled with the excavated material. Both techniques might also be combined. Groundwater dams have the advantages over systems which store water in surface reservoirs that evaporation losses and pollution risk are reduced and reservoir siltation is no problem. However, their relative water storage capacity is significantly lower (Hanson and Nilsson, 1986). Examples for ancient groundwater dams are said to be present e.g. in North Africa, Italy and Syria (Prinz, 2002).

3.2.3.2 Floodwater diversion systems

Floodwater diversion systems are built to deflect floods from a wadi channel to convey the water to adjacent storage devices or fields (Fig. 3) (Prinz, 2002). This is either accomplished by damming parts of the wadi or blocking the entire channel. The retaining structures are called diversion dams. Those systems have been used to irrigate fields or for animal and human water consumption. Blocking the channel in its entire width might be necessary if the fields or storage devices are located considerably higher than the adjacent wadi channel floor. Thereby the water level of a flood can be raised to the appropriate height (Bruins et al., 1986). An impressive example of such a system is the Great Dam in Ma´ri, Yemen (Brunner, 2000). Other examples of floodwater diversion systems are the floodwater harvesting system of Resafa in Syria (Berking et al., 2010), the Harbaqa dam in Syria (Genequand, 2006), the dam and pond system in Jawa, Jordan (Helms, 1981; Whitehead et al., 2008), diversion systems in the runoff farms of the Negev (Evenari et al., 1961), in Oman (Costa, 1983) and the Boqueras and Acequia de cañon systems in southeast Spain (Giráldez et al., 1988; Hooke and Mant, 2002).

3.3 Discussion and Conclusion

This paper gives an overview of ancient water harvesting techniques which were applied in the Mediterranean region and the Middle East; it refers to archaeological case studies for which the respective technology is documented. For most of the technologies case studies could be found throughout the study regions and for different cultural periods. However, the dating of water harvesting structures is notoriously difficult (Treacy and Denevan, 1994; Kamash, 2012) and some of the case studies lack a reliable age determination or their chronologies are controversially discussed (e.g. Rosen, 2000).

The case studies show that barely one of the techniques was used for one purpose exclusively. For example floodwater harvesting served in Mar´ib, Yemen for the irrigation of fields while in Resafa, Syria this technique was applied to supplement the drinking water supply of the city. According to the listed case studies most settlements applied at least two water harvesting techniques: One for the drinking water supply - often with water wells or rooftop harvesting - and one technique to irrigate crops – often runoff and/or floodwater harvesting.

In conclusion the study of the diffusion and reliability of ancient water supply systems will prove to be a challenging task. The age determination is often difficult and the reliability of water supply systems of settlements is affected by processes on various temporal and spatial scales. As shown by previous studies the problem of age determination can be approached by applying new dating methods (Avni et al., 2006; Guralnik et al., 2011; Beckers et al., in press) and climate and hydrological models offer the possibility to assess the reliability of the systems (Whitehead et al., 2008; Berking et al., 2010; Wade et al., 2012).

References

Ashkenazi, E., Avni, Y., Avni, G., 2012. A comprehensive characterization of ancient desert agricultural systems in the Negev Highlands of Israel. Journal of Arid Environments 86, 55–64.

Avni, Y., Porat, N., Plakht, J., Avni, G., 2006. Geomorphic changes leading to natural desertification versus anthropogenic land conservation in an arid environment, the Negev Highlands, Israel. Geomorphology 82, 177–200.

Barker, G., 1996. Farming the Desert: The UNESCO Libyan Valleys Archaeological Survey. UNESCO Publishing ; Dept. of Antiquities, Socialist People's Libyan Arab Jamahiriya ; Society for Libyan Studies, Paris : Tripoli : London.

Barker, G., Gilbertson, D., 2000. Living at the margin: themes in the archaeology of drylands, in: Barker, G., Gilbertson, D.D. (Eds.), The Archaeology of Drylands: Living at the Margin, One World Archaeology. Routledge, London ; New York.

Beckers, B., Schütt, B., Tsukamoto, S., Frechen, M., 2013. Age determination of Petra's engineered landscape – optically stimulated luminescence (OSL) and radiocarbon ages of runoff terrace systems in the Eastern Highlands of Jordan. Journal of Archaeological Science 40, 333–348.

Berking, J., Beckers, B., Schütt, B., 2010. Runoff in two semi-arid watersheds in a geoarcheological context: A case study of Naga, Sudan, and Resafa, Syria. Geoarchaeology 25, 815–836.

Beysens, D., Milimouk, I., Nikolayev, V.S., Berkowicz, S., Muselli, M., Heusinkveld, B., Jacobs, A.F.G., 2006. Comment on "The moisture from the air as water resource in arid region: Hopes, doubt and facts" by Kogan and Trahtman. Journal of Arid Environments 67, 343–352.

Boustani, F., 2009. Sustainable Water Utilization in Arid Region of Iran by Qanats. International Journal of Human and Social Sciences 4, 505–508.

Brinker, W., 1991. (in German) Zur Wasserversorgung von Resafa-Sergiupolis. Damaszener Mitteilungen 5 119 – 146.

Bruins, H.J., 2012. Ancient desert agriculture in the Negev and climate-zone boundary changes during average, wet and drought years. Journal of Arid Environments 86, 28–42.

Bruins, H.J., Evenari, M., Nessler, U., 1986. Rainwater-harvesting agriculture for food production in arid zones: the challenge of the African famine. Applied Geography 6, 13–32.

Brunner, U., 2000. The Great Dam and the Sabean Oasis of Ma'rib. Irrigation and Drainage Systems 14, 167–182.

Bull, L.J., Kirkby, M.J., 2002. Dryland Rivers: Hydrology and Geomorphology of Semi-Arid Channels. Wiley, England ; New York.

Cech, T.V., 2009. Principles of Water Resources: History, Development, Management, and Policy. John Wiley & Sons.

Costa, P., 1983. Notes on Traditional Hydraulics and Agriculture in Oman. World Archaeology 14, 273–295.

Critchley, W.R.S., Reij, C., Willcocks, T.J., 1994. Indigenous soil and water conservation: A review of the state of knowledge and prospects for building on traditions. Land Degradation & Development 5, 293–314.

Evenari, M., Shanan, L., Tadmor, N., Aharoni, Y., 1961. Ancient Agriculture in the Negev. Science, New Series 133, 979–996.

Evenari, M., Tadmor, N., 1982. The Negev: The Challenge of a Desert, 2nd Ed, New. ed. Harvard Univ Pr.

Frasier, G., Myers, l., 1984. Handbook of water harvesting. Washington D.C.

Frederick, C., Krahtopoulou, A., 2000. Deconstructing Agricultural Terraces: Examining the influence of Construction Method on Stratigraphy, Dating and Archaeological Visibility, in: Frederick, C., Halstead, P. (Eds.), Landscape and Land Use in Postglacial Greece. Continuum International Publishing Group, pp. 79 – 93.

Gale, S.J., Hunt, C.O., 1986. The hydrological characteristics of a floodwater farming system. Applied Geography 6, 33–42.

Genequand, D., 2006. Some Thoughts on Qasr al-Hayr al-Gharbi, its Dam, its Monastery and the Ghassanids. Levant 38, 63–84.

Gilbertson, D.D., 1986. Runoff (floodwater) farming and rural water supply in arid lands. Applied Geography 6, 5–11.

Giráldez, J.V., Ayuso, J.L., Garcia, A., López, J.G., Roldán, J., 1988. Water harvesting strategies in the semiarid climate of southeastern Spain. Agricultural Water Management 14, 253–263.

Goudie, A., Wilkinson, J.C., 1977. The Warm Desert Environment.

Guralnik, B., Matmon, A., Avni, Y., Porat, N., Fink, D., 2011. Constraining the evolution of river terraces with integrated OSL and cosmogenic nuclide data. Quaternary Geochronology 6, 22–32.

Hanson, G., Nilsson, Å., 1986. Ground-Water Dams for Rural-Water Supplies in Developing Countries. Ground Water 24, 497–506.

Helms, S.W., 1981. Jawa. Lost city of the black desert. London (Methuen) 1981.

Hill, J., Woodland, W., 2003. Contrasting Water Management Techniques in Tunisia: Towards Sustainable Agricultural Use. The Geographical Journal 169, 342–357.

Hooke, J.M., Mant, J., 2002. Floodwater use and management strategies in valleys of southeast Spain. Land Degradation & Development 13, 165–175.

Issar, A., 2001. The knowledge of the principles of groundwater flow in the ancient Levant. International Symposium OH2 Origins and History of Hydrology, Dijon.

Kamash, Z., 2012. Irrigation technology, society and environment in the Roman Near East. Journal of Arid Environments.

Lightfoot, D., 1996a. The Nature, History, and Distribution of Lithic Mulch Agriculture:

An Ancient Technique of Dryland Agriculture. The Agricultural History Review 44, 206 – 222.

Lightfoot, D.R., 1996b. Syrian qanat Romani: history, ecology, abandonment. Journal of Arid Environments 33, 321–336.

Lightfoot, D.R., 1996c. Moroccan khettara: Traditional irrigation and progressive desiccation. Geoforum 27, 261–273.

Lightfoot, D.R., 2000. The Origin and Diffusion of Qanats in Arabia: New Evidence from the northern and southern Peninsula. Geographical Journal 166, 215–226.

Mays, L., 2010a. A Brief History of Water Technology During Antiquity: Before the Romans, in: Mays, L. (Ed.), Ancient Water Technologies. Springer.

Mays, L., 2010b. Ancient Water Technologies, 1st ed. Springer.

Motiee, H., Mcbean, E., Semsar, A., Gharabaghi, B., Ghomashchi, V., 2006. Assessment of the Contributions of Traditional Qanats in Sustainable Water Resources Management. International Journal of Water Resources Development 22, 575–588.

Näser, C., 2010. The Great Hafir at Musawwarat es-Sufra: Fieldwork of the Archaeological Mission of Humboldt University Berlin in 2005 and 2006, in: Godlewski, W., Łajtar, A. (Eds.), Between the Cataracts. Proceedings of the 11th Conference of Nubian Studies, Warsaw University, 27 August – 2 September 2006, Part Two, Fascicule 1: Session Papers, PAM Suppl. Series 2.2/1. pp. 39–46.

Nasri, S., Albergel, J., Cudennec, C., Berndtsson, R., 2004. Hydrological processes in macrocatchment water harvesting in the arid region of Tunisia: the traditional system of tabias. Hydrological Sciences Journal 49, null–272.

Nicholson, S.E., 2011. Dryland Climatology. Cambridge University Press.

Ortloff, C.R., 2005. The Water Supply and Distribution System of the Nabataean City of Petra (Jordan), 300 BC– AD 300. Cambridge Archaeological Journal 15, 93–109.

Ortloff, C.R., 2009. Water Engineering in the Ancient World: Archaeological and Climate Perspectives on Societies of Ancient South America, the Middle East, and South-East Asia. Oxford University Press, USA.

Oweis, T.Y., Prinz, D., Hachum, A.Y., 2012. Rainwater Harvesting for Agriculture in the Dry Areas. Crc Pr Inc.

Prinz, D., 1994. Water Harvesting: Past and Future, in: Pereira, L. (Ed.), Sustainability of Irrigated Agriculture. pp. 135 – 144.

Prinz, D., 2002. The Role of Water Harvesting in Alleviating Water Scarcity in Arid Areas. Keynote Lecture, Proceedings, International Conference on Water Resources Management in Arid Regions. 23-27 March, 2002, Kuwait Institute for Scientific Research, Kuwait, (Vol. III, 107-122).

Pulido-Bosch, A., Sbih, Y.B., 1995. Centuries of artificial recharge on the southern edge of the Sierra Nevada (Granada, Spain). Environmental Geology 26, 57–63.

Roberts, N., 1977. Water Conservation in Ancient Arabia. Proceedings of the Seminar for Arabian Studies 7, 134–146.

Rosen, S.A., 2000. The decline of desert agriculture: a view from the classical period Negev, in: Barker, G., Gilbertson, D.D. (Eds.), The Archaeology of Drylands: Living at the Margin, One world archaeology. Routledge, London ; New York.

Shanan, L., 2000. Runoff, erosion, and the sustainability of ancient irrigation systems in the Central Negev desert., in: Hassan, M.A., Slaymaker, O., Berkowicz, S.M. (Eds.), The hydrology-geomorphology interface: rainfall, floods, sedimentation, land use. A selection of papers presented at the Conference on Drainage Basin Dynamics and Morphology

held in Jerusalem, Israel, May 1999. IAHS Press, pp. 75–106.
Spencer, J.E., Hale, G.A., 1961. Origin, Nature and Distribution of Agricultural Terracing. Pacific Viewpoint 1–40.
Tooth, S., 2000. Process, form and change in dryland rivers: a review of recent research. Earth-Science Reviews 51, 67–107.
Treacy, J., Denevan, W., 1994. The Craetion of Cultivated Land trough Terracing, in: Miller, N.F., Gleason, K.L. (Eds.), The Archaeology of Garden and Field. University of Pennsylvania Press, Philadelphia.
van Wesemael, B., Poesen, J., Solé Benet, A., Cara Barrionuevo, L., Puigdefábregas, J., 1998. Collection and storage of runoff from hillslopes in a semi-arid environment: geomorphic and hydrologic aspects of the aljibe system in Almeria Province, Spain. Journal of Arid Environments 40, 1–14.
Wade, A.J., Smith, S.J., Black, E.C.L., Brayshaw, D.J., Holmes, P.A.C., El-Bastawesy, M., Rambeau, C.M.C., Mithen, S.J., 2012. A new method for the determination of Holocene palaeohydrology. Journal of Hydrology 420–421, 1–16.
Wheater, H., Al-Weshah, A. (Eds.), 2002. Hydrology of wadi systems, Technical Documents in Hydrology. UNESCO, Paris.
Whitehead, P.G., Smith, S.J., Wade, A.J., Mithen, S.J., Finlayson, B.L., Sellwood, B., Valdes, P.J., 2008. Modelling of hydrology and potential population levels at Bronze Age Jawa, Northern Jordan: a Monte Carlo approach to cope with uncertainty. Journal of Archaeological Science 35, 517–529.
Wikander, O. (Ed.), 1999. Handbook of Ancient Water Technology. Brill Academic Pub.
Woodward, J. (Ed.), 2009. The Physical Geography of the Mediterranean. Oxford University Press.
Yair, A., Raz-Yassif, N., 2004. Hydrological processes in a small arid catchment: scale effects of rainfall and slope length. Geomorphology 61, 155–169.

4. Resafa

4.1 Runoff in two semi-arid watersheds in a geoarcheological context – a case study of Naga, Sudan and Resafa, Syria

Jonas Berking, Brian Beckers and Brigitta Schütt, 2010. Geoarcheology Vol. 25 No. 6, 815-836. DOI: http://dx.doi.org/10.1002/gea.20333

4.1.1 Introduction

The two ancient cities, the late Roman-early Islamic Resafa (~70 Common Era (CE) – 1400 CE) in the desert steppe of Syria and the Meroitic Naga (~300 Before Common Era (BCE) – 300 CE) in the dry savanna of Sudan were, during their heydays, both central places, located at the banks of major wadis and close to two big perennial rivers, the Euphrates and the Nile (Fig. 1).

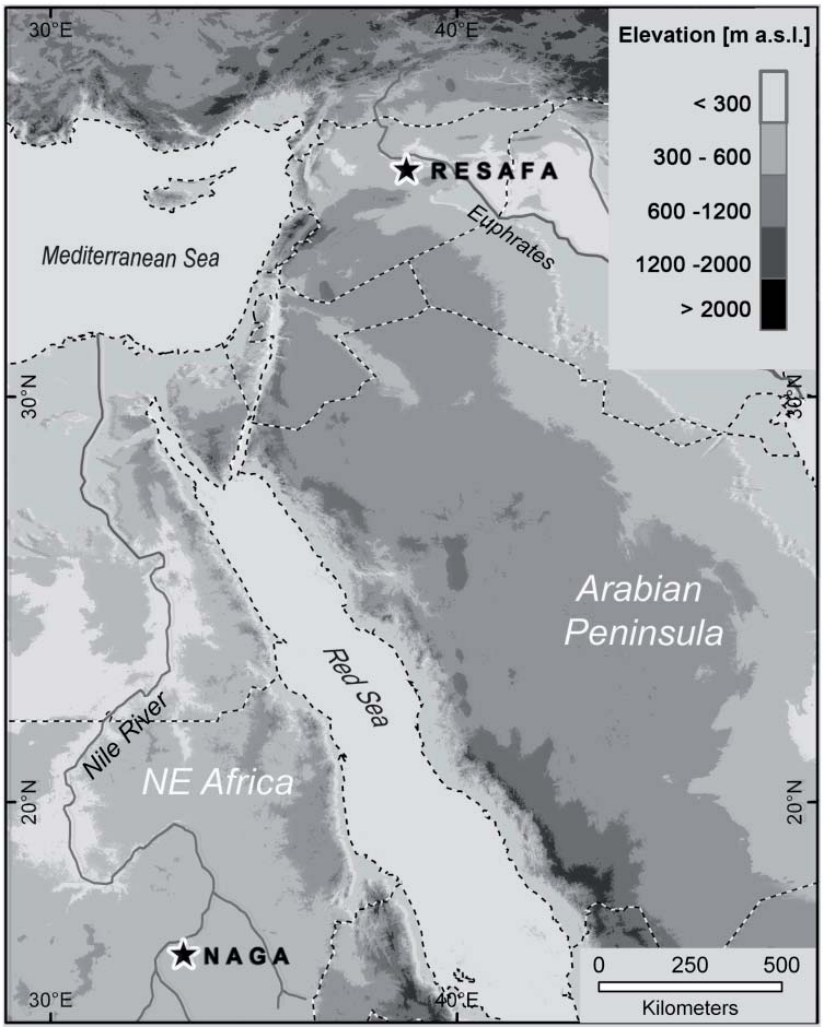

Fig. 1 Location of the two study sites: Resafa in Syria and Naga in Sudan (Mapping Basis GTOPO 30).

Nevertheless, both cities had additionally to rely on rainfall harvesting measures to ensure their water supply. Thus, at both sites dams and levees, subsurface or surface reservoirs were used to collect, control and store periodic, concentrated surface runoff. These systems were adapted to the local environmental conditions, i.e. the rainfall-runoff

behavior, which is highly dependent on the climate and physical characteristics of the respective catchment (Dunne, 1978).

The study's overall objective is to identify the environmental conditions required to run the water harvesting systems. On this basis it will be possible to assess the vulnerability of both systems to environmental changes. The presented paper focuses on the physical catchment characteristics and their parametrization, while the climatological component will be part of a forthcoming study (Fig. 2).

The challenge of this study is that both study sites are, like most locations in drylands, ungauged. Owing to their remote locations, information on the physical characters of the catchments is either scarce or coarsely resolved. Accordingly, we apply a lumped hydrological model to assess the catchments' rainfall runoff behavior, as is commonly done for regions with similar settings (Beven, 2003).

A plausibility check is made through the assumption that the current rainfall character is similar to that during the establishment of the water reservoirs and that the total amount of effective rainfall corresponds to the total volumes of the storage facilities.

The herein generated model queries are:

(i) Which minimum rainfall durations and rainfall amounts are necessary to produce surface runoff that reaches the water harvesting measures (threshold of effective rainfall)?

(ii) Which rainfall durations and rainfall amounts are necessary to fill up the water reservoirs at the respective sites?

(iii) What is the maximum likely storm event to be expected according to the magnitude-frequency analysis and how much water does it supply for water storage?

4.1.2 Background

Ancient cultures developed a variety of water technologies to sustain permanent settlements in arid or semi-arid environments. Among them were wells and conveyance systems that transported water to the settlements via conduits, channels and aqueducts

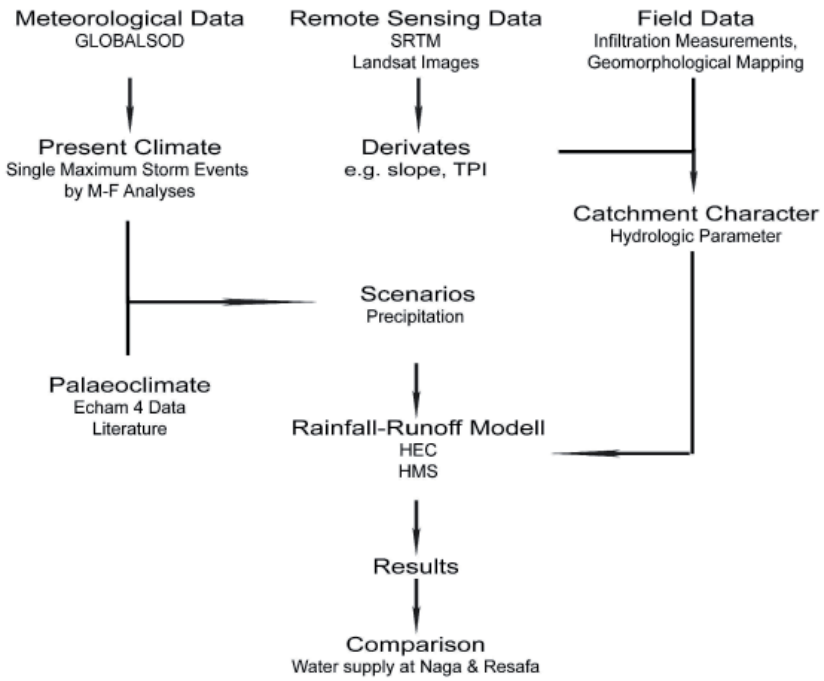

Fig. 2 The work structure of the study.

from perennial water sources such as rivers (Wikander, 2000). Additionally, water harvesting was a common method for water augmentation (Myers, 1975; Critchley, 1991). The harvested water served either for animal husbandry, for irrigation purposes, e.g. in the Negev (Evenari, 1961), or as drinking water, as was the case in Resafa and most likely in Naga.

In Resafa, the central facility for drinking water was a dam located along the right bank of the main wadi downstream from the inflow of a number of larger tributaries (Figure 3). This dam retained the periodic concentrated runoff of the channel and directed it into large subsurface cisterns inside the city walls (Brinker, 1991). In Naga surface ponds, locally called Hafirs (Hulme, 1996), were used to collect and store periodic surface runoff from the slopes and the channels. Periodic surface runoff and flood events were therefore the key factors of the freshwater supply of both cities.

In drylands, surface runoff is mainly generated when rainfall intensities exceed the infiltration capacity of the soil and is called Hortonian or infiltration excess overland flow (e.g., Dunne, 1978, Yair & Lavee, 1985). Infiltration capacity in arid and semi-arid areas is generally low owing to the lack of vegetation, shallow soils and incrustations (Baird, 1997). The rainfall character in drylands is in turn dominated by erratic, high-intensity, short-duration rainfall events with small spatial extension (Sharon, 1972). This combination generates episodic floods whose hydrographs directly correspond to the rainfall character (Wheater et al., 2007). Even though regional, low-intensity, steady rainfall may occur in drylands it is only rarely runoff-effective (Yair & Lvee, 1985).

Rainfall-runoff modeling is a common tool among hydrologists and engineers to cope with the uncertainties related to dryland hydrology. Wheater et al. (2007) provide a comprehensive introduction on the general issue (see also Bahat et al., 2008; Al-Qurashi et al., 2008; McIntyre & Al-Qurashi, 2009). Applied studies concern the feasibility of water harvesting for specific locations (e.g. Oweis & Taimeh, 1996; Critchley, 1991) and hazardous effects and mitigation of flash floods (e.g. Morin et al., 2008; Foody, 2004). Hydrological modeling tools are rarely applied in geoarcheology (Whitehead et al., 2008). Many of these studies consider the lack of detailed information on the spatial and temporal variability of rainfall to be the main problem of rainfall-runoff modeling in drylands (Wheater et al. 2007). Approaches to limit these uncertainties include developing stochastic rainfall intensity models using results of high density experimental rain gauge networks or conventional rain gauges (e.g., Wheater et al., 2007 and references therein; Tsubo et al., 2005), applying data from rainfall radar (Bahat et al., 2009), or using remote sensing precipitation estimations (Endreny et al., 2009).

4.1.3. The study sites

4.1.3.1 The study site of Resafa

Resafa (Rusafa, Ar-Rasafeh) was founded as a fortified post by the Romans in the northern steppe of Syria, 25 km south of the Euphrates, at about 75 CE. At this time Resafa was only one among hundreds of military and trading posts of the Limes Arabicus: the border defence system of the Eastern Roman provinces against the Parthian and later Sassanid Empire which extended from the Black Sea to the Red Sea (Ulbert, 1986; Konrad, 2001).

In the early 4th century CE a Roman officer named Sergius suffered martyrdom in Resafa for avowing himself a Christian. Subsequently a Sergius cult arose and Resafa, later also named Sergiupolis, became one of the most important Christian pilgrimage sites of the eastern Mediterranean (Fowden, 1999 and references therein).

This combination of strategic and religious importance made Resafa a prosperous city with a great city wall, churches and cisterns, despite the unfavorable environment (Karnapp, 1976). After the Islamic conquests, the Umayyad Caliph Hisham ibn 'Abd al-Malik chose Resafa as his residence (724-743 CE). In the following years Resafa remained a regional central place, but, like many cities along the Syrian Euphrates, was abandoned after the Mongol invasion in 1269 (Sack, 1996).

From the fertile floodplains of the Euphrates along the Limes to the south into the Syrian desert steppe, the terrain is monotonous and undulating, covered with scattered xeric shrubs and ephemeral grasses (Wirth, 1971). A prominent, if in parts indistinct, landmark on this route is the moderately sloping, low escarpment formed by the north-south striking Ar-Rasafah Fault (Asfahani & Radwan, 2007). The escarpment and the corresponding rolling plain, which gently ascends to the Jabal Bishri in the east, consist of gypsum with interbedded layers of limestone and marl (Ponikarov, 1966; Rössner, 1995). Locally the plain is covered by loess-like sediments. The escarpment is dissected by ephemeral channels tributary to the Wadi es Sélé, which drains the northern and western declivities of Jabal Abu Rujmayn and Jabal Bishri, respectively, into the Euphrates. Typically for channel systems in arid environments, the dendritic channel network of the Resafa Basin is a relict of the Pleistocene wet periods (Wirth, 1971). As described by Allison (1997), present-day runoff events in the Syrian Desert have a low degree of connectivity to wadi networks and predominantly percolate or drain into depressions. The Wadi es Sélé overflows only if triggered by low-frequency high-magnitude rainfall events (personal communication by local residents, 2008). The summer-dry and winter-wet Syro-Mesopotamian plain around Resafa is traditionally used for pasture. Tillage occurs only along the alluvial plain of the Wadi es Sélé and the lower courses of its major tributaries. At present annual precipitation averages 136 mm (Table 1). According to Roman and early Islamic sources that refer to Resafa as a "city in the desert," precipitation was not significantly different from today during the respective periods (Kellner-Heinkele, 1996). Considering the high transportation costs in past times, it is most likely that the settlements along the Limes Arabicus locally tried to cultivate crops (Schlumberger, 1950). Remains of small gardens along the alluvial plain of the Wadi es Sélé document

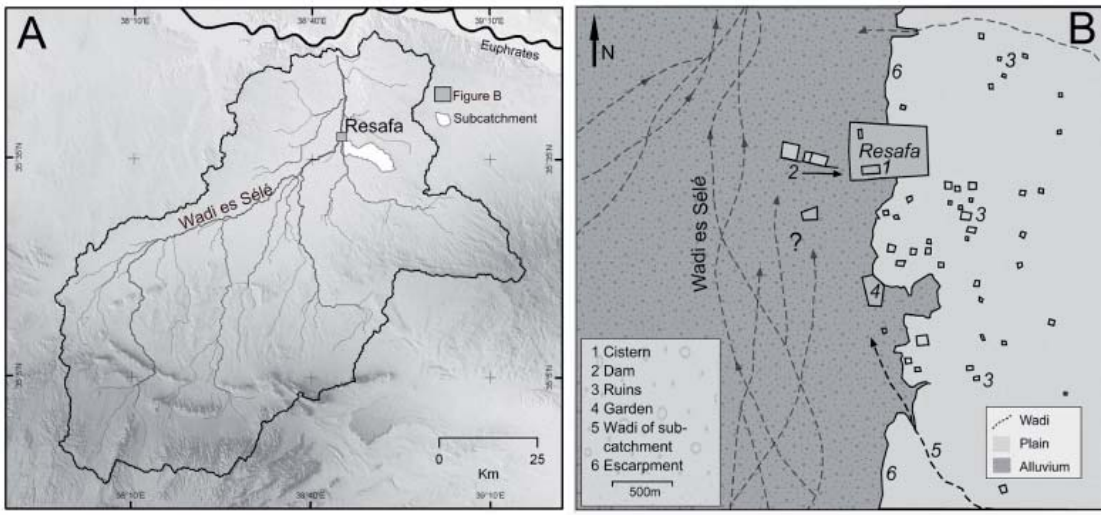

Fig. 3 (A) Map of the Resafa Basin. The catchment is outlined. Note that the wadis are highlighted and the drainage network only represents the topographic connectivity of the wadis. (B) Detail sketch of the hydrography and water supply system around Resafa.

that this area was used for agriculture during early settlement times already (Ulbert, 1986). However, until now there has been no evidence of irrigated fields big enough to supply the city with sufficient food.

The soils of the region are predominately xeric Gypsisols. Soil depths vary along topographic units. Soils deeper than 20 cm are found only in the Colluvisols of the depressions and foot-slopes and in the Fluvisols of the alluvium (Wirth, 1971; Furley et al., 1989; field observations in 2009).

The water supply of Resafa was based on three sources: about 60 m deep wells which delivered brackish groundwater due to the parent gypsum, rooftop water harvesting and storage in bottle-shaped cisterns, and, as the central facility, floodwater harvesting. Floodwater harvesting from the Wadi es Sélé channeled wadi floods along a 450 m long dam into large subsurface cisterns located inside the city walls. These cisterns had a total volume of $21*10^3$ m^3; the biggest of them had a capacity of $14.6*10^3$ m3. Chalky accumulations on top of the cistern walls show the maximum fill level. The dam along the Wadi es Sélé had a spillway to prevent floods from overtopping and destroying it. Additionally, a lock in the feeder channel of the cisterns could be used to control the inflow between the channel and the cisterns (Brinker, 1991, Fig. 3).

4.1.3.2 The study site of Naga

The ancient Meroitic civilization developed between 280 years BCE and 330 years CE The settlement of Naga is regarded as one of the bigger city complexes of the Meroitic phase, founded within the epoch of Kushite rule in Nubia. The dominion of the Meroitic state was located along the Nile between the 6th Cataract north of Khartoum and the 1st Cataract near Aswan. In this area a complex society, characterized by both Egyptian and African attributes developed since the early Bronze Age, reached its heyday around the beginning of the Common Era, and slowly declined in historical times until the end of the Roman period (Adams, 1974, Wildung & Kröper 2006).

The city of Naga is located at the Wadi Awatib, a tributary of the river Nile, which discharges into the Nile north of Naga between the 5th and the 6th cataract, close to the town of Shendi. Naga was located along the eastern bank of the Wadi Awatib, at the western foot of a ridge (Fig. 4). The city included many different building complexes, indicating a high number of permanent citizens. Today the area is only sparsely settled by peasants who mainly practise rain-fed agriculture, raise cattle and cultivate sorghum in the floodplains of Wadi Awatib (Gabriel, 1997).

The area‘s annual rainfall averages around 95 mm with the rainy season from May to October, maximum rainfall being expected in July and August (Berking & Schütt, in press). At present, Wadi Awatib is an ephemeral stream that drains an area of 2360 km^2 including the two main subcatchments of Wadi Abu Hashim and Wadi Abu Rihan as headstreams (Table 1). The main drainage divide runs along prominent sandstone ridges and plateaus. These plateaus and mesas dominate the edges of Wadi Awatib and rise up to 90 m above the valley bottom (Giraud et al., 1992). The river bed of Wadi Awatib is braided and broadens to a width of 10 km. The groundwater table in the wadi is recorded in 72 and 77 meters depth, measured in two wells close to the excavation site of Naga.

All over the study site the occurrence of sparse drought-resistant vegetation is controlled by climatic presetting and modified by human impact, such as grazing or clearing. Acacia tortilis and Acacia mellifera are the most prominent trees, occurring either as riverine forests or in little patches next to the riverbeds associated with Astrebla s. and Panicum turgidum (Aktar-Schuster & Mensching, 1993). Whereas in the middle and lo-

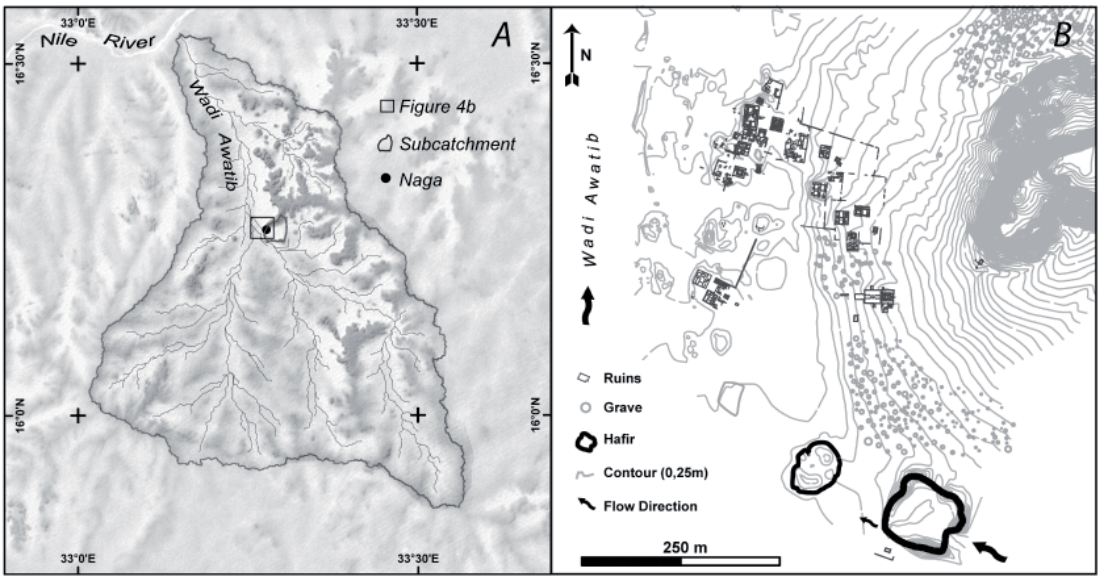

Fig. 4 Location of the study site of Naga (a) and (b) the detailed map of the ancient city with the "Great Hafir" highlighted.

wer course of Wadi Awatib the vegetation shows the typical contracted pattern of drylands, a more dense dry-savannah vegetation occurs in the remote areas of the upper course.

Soils in the region are predominantly red-brown Regosols (Berking & Schütt, in press). Along the river bed of Wadi Awatib and its tributaries, soil development is affected by erratic flooding. Especially in the Fluvisols of the alluvial plain, ascending translocation of soil water and finally its evaporation cause the formation of subsurface incrustations (Berking & Schütt, in press).

Table 1

	Catchment of Wadi Awatib	Resafa Basin
Area (km²)	2360	7120
Elevation range (m a.s.l.)	362 – 598	1240 - 270
Average elevation (m)	482	462
Slope range (°)	0 – 21	0 – 36
Average slope (°)	0.8	1.62
Stream length (km)	333	2347
Drainage density (km/km²)	0.14	0.33
Mean temperature (°C)	29.3	18.6
Annual precipitation (mm)	94	136
Max. daily precipitation (mm)	61	80
Rainy season	May - Sep	Oct. - Apr.
Stream length (km)	333	2347
Drainage density (km/km²)	0,14	0,33
Water reservoir (m3)	21.000	45.000
Subcatchment (km2)	14.2	126
Runoff threshold (mm/h)	39	18
Infiltration range (mm/h)	18 - 592	0 - 140

Table 1 Catchment (upper part) and climate (lower part) characteristics

Since Meroitic times floodwater harvesting in the area has collected surface water in superficial artificial basins, known as hafirs (Arabic: dig). Hafirs are dug into the ground, and the resulting depressions are encircled by walls built of the excavated material. The

storage capacity is given by the excavated depression and its surrounding wall. The use of hafirs is still common in the area; the water is predominantly used for irrigation and for cattle watering. The "Great Hafir of Naga", which is the subject of this paper, is located at the right river bank of Wadi Awatib about 1 km upstream of Naga at the inflow of a minor tributary. Its construction dates back to Meroitic times; at present it is inactive owing to siltation processes (Kleinschrot 1984, 1986; Hinkel, 1991). Nevertheless, the ancient water supply is indicated by the Hafir's calculated volume, totalling $45*10^3$ m3 (tachymetric data kindly provided by U. Weferling).

4.1.4. Data Processing And Methods

4.1.4.1 Model description and processing steps

The model applied is the Hydrological Modelling System (HMS), Version 3.3, developed by the Hydrologic Engineering Center of the US Army Corps of Engineers (HEC, 2008). HMS is a rainfall-runoff model suitable for dendritic watershed systems and is also applicable in semi-arid and arid catchments (Foody, 2004).The underlying algorithms and the model concept are described in detail in the manuals (HEC, 2000, 2008). To allow analysis of subcatchments, HMS is used in a semi-distributed manner. Subcatchments were delineated to represent the major tributaries of the main wadi in the respective catchment. In this study the focus is on the adjacent subcatchments of the water harvesting measurements (see Fig. 3, 4 and Table 1).

To derive topographic, topologic and hydrologic information, the ArcHydro tools of the Centre for Research in Water Resources at the University of Texas are applied in combination with GeoHMS (ArcHydro, 2009; HEC, 2000).

Applying HMS, the user is able to choose between various precipitation input options, infiltration loss parameterizations and flood routing methods. As final infiltration rates are attained quickly in arid and semi-arid areas (Greenbaum et al., 2006), the constant loss method is used to determine infiltration as done by Morin et al. (2008) and muskingum routing for flood routing (Chow et al., 1988) as done by Foody et al. (2004). The CN (Curve Number) Lag method is used to compute the time of concentration. The respective CNs are chosen based on the hydrological soil characteristics of the catchments and the landuse derived from field observations and satellite images, i.e. Landsat, Spot and Ikonos (for CN, see USDA–NRCS, 2005). In the Resafa Basin the CNs range between 63 and 85 and in Wadi Awatib between 55 and 63.

4.1.4.2 Relief data

The overall data base for the required topographic parameters is the Digital Elevation Model (DEM) as provided by the Shuttle Radar Topography Mission (SRTM) with a resolution of 90x90 m. On the basis of these topographic data, derivates were determined, parameterizing the geometric character of the relief. The derivates can be divided into the primary topographic attributes slope, aspect and curvature, and secondary topographic attributes, such as the Topographic Index (TI) or the Topographic Position Index (TPI), both used to extrapolate the infiltration measurements to area averages, as described in the Infiltration data paragraph (a comprehensive introduction is given by Wilson (2000)). The Topographic Index (TI) is defined as $\ln(\alpha/\tan\beta)$, in which α is the contributing area and $\tan\beta$ is the local downslope (Tagil et al. 2008). The Topographic Position Index (TPI) is frequently applied to separate landscape units. The TPI is the difference between the elevation of a cell and the average elevation of a user-defined number of

neighboring cells. Resulting values for valleys, for example, are lower than those of isolated hilltops (Weiss, 2001; Tagil et al., 2008).

4.1.4.3 Meteorological data

To compare the hypothetic storms with real rainfall observations and thus assess recurrence intervals of runoff events, daily precipitation data of the WMO (World Meteorological Organization) stations of Raqqa in Syria and Khartoum in Sudan were used because these are the only available long-term observations in the two regions. The datasets were checked for plausibility (Table 2) and then classified with a magnitude-frequency analysis as described by Ahnert (1982).

However, these records generally do not reflect the intensity of an individual rainfall event in drylands (see background chapter).To match the temporal resolution of the design storms, it is assumed that each record reflects a one-hour storm event of the recorded amount of precipitation. Moreover, a 15 min peak is incorporated as preset by HEC for sub-hourly variations of design storms (HEC, 2008). Because no such data are available for the two regions, we used values reported from a Negev desert test site, which total ~1 mm * min -1. (Kidron & Yair, 1997; Kidron, 2007; Yair, A., & Raz-Yassif, N., 2004; Bahat et al., 2009)

Apart from precipitation, real evaporation is the most important factor for any water balance calculations (Pilgrim et al., 1998) and is challenging to determine on a drainage basin scale especially in drylands (Beven, 2003). In the present study, evaporation is neglected because the focus lies on short and heavy rainfall events and the impact of evapotranspiration should be negligible compared to the presumed uncertainty in assuming a constant evapotranspiration loss per minute (Haan et al., 1994).

4.1.4.4 Infiltration data

Infiltration rates as hydrologic modelling input parameters belong to the most critical terms in semi-arid, sparsely vegetated areas (Coe et al., 2008). Infiltration is the gravitational entry of water into the soil, and different approaches exist to obtain infiltration rates by field measurements (Dane & Topp, 2002). Since infiltration rates cannot be measured directly in most situations, both numerical and empirical approximations of infiltration have been developed (Dane & Topp, 2002). Whereas short-term infiltration dynamics will be affected by both sorptivity and hydraulic conductivity, the real long-term infiltration rate will drop to a steady-state rate that is equal to the saturated conductivity (Ks). High variability of natural soil hydrodynamics has to be kept in mind, and estimates of sorptivity and hydraulic conductivity from field measurements can be wrong by up to 100% (Hillel, 1998).

To approximate the hydraulic conductivity, the application of mini-disk infiltrometers (MDI) shows good results in validation and comparison with other methods (Zhang,

Station	WMO ID	Period	Total days recorded	Valid data	Lat. ° N	Long. ° E	Altitude [m asl]	Distance to the study site
Raqqa	400390	1960 - 2009	31750	23.02%	35° 57′	39° 1'	250	30 km
Khartoum	62721	1994 - 1999	2190	47.00%	15° 35'	32° 33'	380	100 km

Table 2 Climate Stations used for magnitude-frequency analysis (source GLOBALSOD).

1997; Li et al., 2005). Here we used a mini-disk infiltrometer from Decagon Devices, Pullman, WA with a radius of 1.55 cm. Steady infiltration under tensions was determined at pressure heads of -1.0, -2.0 for all surfaces, and -6.0 cm at very permeable sandy sites (Li et al., 2005).

The method introduced by Zhang (1997) is applied to estimate the soil's near-saturated conductivity from the steady-state infiltration rates. The sorptivity part of the infiltration is estimated based on a texture analysis. Ks is determined as cumulative infiltration rate fitting a function to the square root of time (Decagon Devices, 2007). Ks is then extrapolated to areal averages.

Hence for both sites DEM derivates were correlated to the punctual infiltrometer measurements and then extrapolated to area averages (cf. Moore, 1993; Wilson, 2000; Florinsky et al., 2002). Several regression methods (i.e. exponential, polynominal) were tested, and the one was chosen that showed the best compromise between RMSE (root mean square error) coefficient of determination (r^2) and least complexity.

In the case of the Resafa Basin we found the best fit between experimental infiltration rates and the Topographic Index of the respective site (TI) using a linear function (r^2 =0.63, n=28, α <0.05) (Beven 2002; Fig. 5). Whereas in the Resafa Basin xeric Gypsisols with poor infiltration rates are the predominant soil types, on the plain the Colluvisols and Fluvisols have generally higher sand contents than the material on the backslopes.

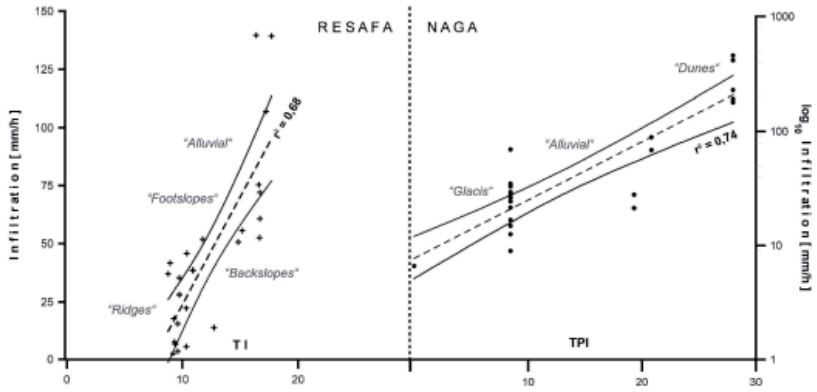

Fig. 5 Infiltration rates vs. Topographic Index (TI) for Resafa and Topographic Position Index (TPI) in the case of Naga represent values of 23 in-situ measurements (see also text for description). Regression fits are indicated by black dotted- and the 95% confidence interval by black continuous lines.

Accordingly infiltration rates are higher in the soils developed in the fluvial or hill wash deposits (Hillel, 1998).The function is then applied to calculate the infiltration rates of the drainage basin area based on the TI values as derived from the digital elevation model. The resulting data show locally negative infiltration rates. Data analysis shows that these locations correspond to areas with outcropping bedrock, so the negative values were set to zero.

In Naga the surfaces of elevated areas such as plateaus or mesas and escarpments consist of outcropping bedrock with very low infiltration rates. Around the escarpment, fan-like deposits due to hill wash processes built the footslope. This landform element is termed glacis and is composed of well-rounded pebbles up to 20 cm in diameter; they decrease in diameter with increasing distance to the escarpment. The pebbles are embedded in a sandy to loamy matrix which is highly compacted and locally cemented by iron oxides. These glacis also have a relatively low hydraulic conductivity, whereas the

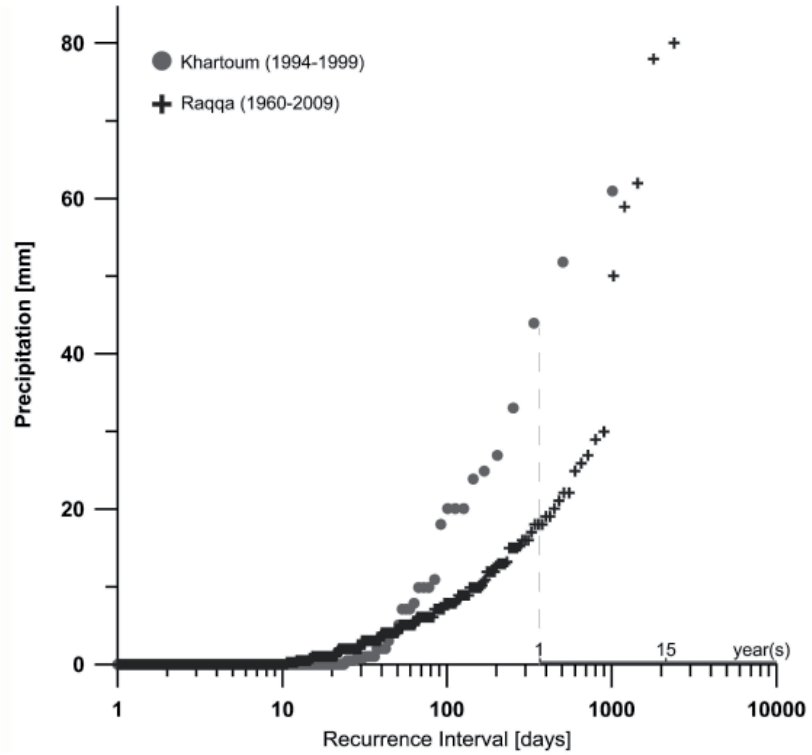

Fig. 6 Magnitude-frequency analysis of daily precipitation for the weather stations Khartoum (with n = 2190) and Raqqa (with n = 31720) (Data base see Table 2).

deposits on the adjacent floodplains have medium infiltration rates (Berking & Schütt, in press). North and south of the escarpment, the glacis are locally covered by dune deposits which show high infiltration rates. For the catchment of the Great Hafir the best fit of experimentally measured infiltration rates with topographic characters was found for the Topographic Position Index (TPI). The correlation between the measured infiltration rates and the corresponding TPI values is exponential ($r^2 = 0.74$, n=23). This reflects the high hydraulic conductivity of the dunes covering wide areas of the drainage basin. The function is applied to calculate the infiltration rates of the drainage basin area based on the TPI values as derived from the digital elevation model (Fig. 5).

Note that the relationship between the DEM derivates and infiltration rates as found in Resafa and Naga cannot be transferred to other regions without experimentally based adaption (Carol et al., 2003).

4.1.5. Results

4.1.5.1 Precipitation

Table 2 shows that for the Raqqa weather station only 23% and for the Khartoum weather station only 47% of the available data are valid precipitation data; all other values were not plausible or flagged as uncertain by the distributing National Oceanic and Atmospheric Administration (NOAA). The expected annual precipitation maximum totals 45 mm for Khartoum and 18 mm for Raqqa. The maximum precipitation for the given time periods (Table 3) peaks at 61 mm for Khartoum (10. April 1994) and at 80 mm for Raqqa (3. May 2007).The maximum frequency analysis reveals that a maximum rainfall of 61 mm can be expected once in 2.7 years in Naga and once in 3.9 years in Resafa (Fig. 6, Table 3).

4.1.5.2 Water availability and rainfall-runoff conditions

The contributing areas of the water harvesting facilities total 14.2 km2 for the Great Hafir of Naga and 126 km2 for the runoff diversions at Resafa. The associated infiltration rates in the Resafa Basin range from near zero up to 140 mm * h-1 (STD=37.6, n=28). In the Great Hafir Basin they range from 18 to 592 mm * h-1 (STD=234.5, n=23) (Table 1).

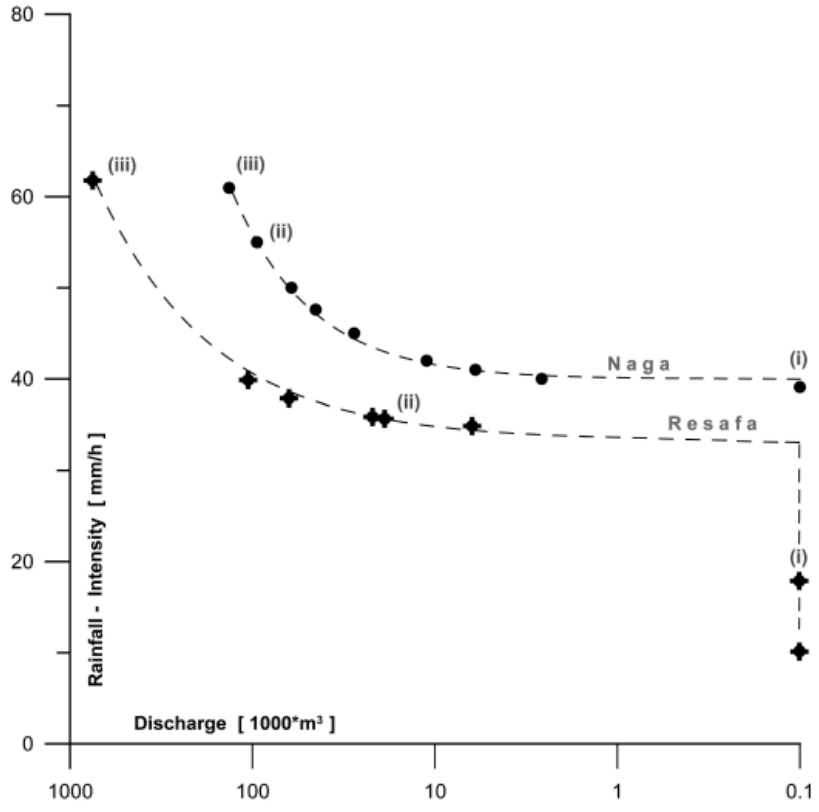

Fig. 7 Linear plot of rainfall intensity vs. discharge at the outlets of the derived subcatchments. (Note that the x-axis uses the logarithm to base 10 and plotted descending in terms of highlighting the values near zero.)

The minimum rainfall intensity required to produce surface runoff that reaches the water harvesting measures (query i) totals 10 mm of rainfall in one hour in Resafa and 39.1 mm rainfall in one hour in Naga. In Resafa a constant discharge of 100 m^3 is visible in Figure 7, independent of the rainfall depths. This is due to the 15 min storm peak which generates a constant amount of runoff until total rainfall depth exceeds 35 mm in one hour. Effective rainfall of this rate can be expected nearly annually at both sites.

With respect to the amount of water needed to fill up the water reservoirs, the second query (ii) shows that at Resafa a rainfall of 35.9 mm within one hour is required to fill up the city cisterns, which have a total volume of 21 000 m^3. At Naga a rainfall of 47.6 mm within one hour is required to fill up the Great Hafir, which has a total volume of 45 000 m3. The recurrence interval of such rainfall events is less than once in two years in Resafa and almost once a year at Naga.

Query (iii) shows that large overland flow and flashfloods are likely to occur when maximum rainfall intensity of 61 mm is adopted, leading to 134000 m^3 in Naga and 744000 m^3 in Resafa. The recurrence interval of such major events is 3.9 years at Resafa and 2.8 years at Naga (Figure 7, Table 3)

4.1.6 Discussion

In the Resafa Basin initial surface runoff is triggered at rainfall intensities of 10 mm * h-1 and a rainfall duration of one hour, whereas in the Great Hafir Basin, where the infiltration rates are much higher, surface runoff does not occur until rainfall reaches intensities of 39.1 mm * h-1 and lasts one hour (Table 3). These different behaviors are mainly controlled by the different infiltration capacities of drainage basins. In Resafa the estimated hydraulic conductivity rates Ks are in the range of infiltration studies in the Syrian Middle Euphrates region, which total between 5 and 341 mm * h-1 on comparable types of gypsiferous soils (Furley et al., 1989 and Mousli, 1980). In the drainage basin of the Great Hafir at Naga very high infiltration rates occur in particular in the unconsolidated dune sediments, whereas infiltration rates are fairly low on the fluvial and alluvial sediments and escarpment areas (Kidron, 2001; Berking & Schütt, in press).

	Resafa	Naga	Resafa	Naga	Resafa	Naga	Resafa	Naga	Resafa	Naga
$P_{intensity}$ [mm*h^{-1}]	18	18	35.9	35.9	39.1	39.1	47.6	47.6	61.9	61.9
Discharge [10^3 * m^3]	0.1	0	20.3	0	85.8	0.1	264.7	45.2	744	134
Query	i_a	i_a	i_b	i_b	ii_a	ii_a	ii_b	ii_b	iii_{a+b}	iii_{a+b}
Recurrence interval [yr^{*-1}]	>1	>3.5	<0.5	>1.5	<0.5	>1	<0.4	>0.9	<0.3	<0.2

Table 3 Comparison of the results from the Rainfall-Runoff Model (P = Precipitation; with a = Resafa; b = Naga). (i) min. rainfall intensity for runoff (ii) rainfall event to fill up water reservoirs (iii) max. rec. storm event and discharge volume (see also introduction).

Rainfall events with similar intensities of 40 - 55 mm * h-1 are reported for the Negev Desert by Yair (2004), with a recurrence interval of two years (see also: Yair & Lavee, 1985; Lange et al. 2000; Bahat et al., 2009). Rainfall durations of 30 and 60 minutes and intensities of 80 mm * h-1 and 75 mm * h-1 are reported from the semi-arid parts of Kenya by Rowntree (1998) and Sutherland & Brian (1990). Sutherland & Brian (1990) give threshold values of 6-9 mm * h-1 for Hortonian overland flow. A rainfall threshold value of 9 mm* h-1 is also discussed in Kidron & Yair (2001) and given by Martinez-Mena et al. (1998) for sandy soils in southern semi-arid Spain, where also higher threshold values of at least 20 mm * h-1 in 30 min rainfall duration are stated by Cammerat (2004). These studies are often based on spatial and temporal high resolution data or experimental designs with simulated sprinkler irrigations.

Even though the two study sites are located in two different climate regions (Figure 1) they show distinct similarities in terms of rainwater availability, rainfall probability and rainfall intensities (Figure 6, Table 3). Resafa is located in the Mediterranean climate regime, where rainfall is mainly associated with the Westerlies causing mostly advective rain during the winter months and bearing storm cells, associated with short duration heavy rainfalls (Dennett et al.,1984). By contrast, Naga is located at the fringe between the north-eastern Sahel and the eastern Sahara desert where precipitation comes with the northward shift of the ITC leading to convective rainfall during the summer months (Osman & Hastenrath, 1969; Walsh et al., 1988, Table 1).

However, the transfer of the current rainfall character to palaeoenvironmental conditions as well as its comparability with data from the Negev desert is not proved.

4.1.7 Conclusion

We know from many paleoenvironmental studies that the overall climate since the late Bronze Age in NE Africa and the Middle East was only slightly more humid than today (Farrand 1979; Gasse & Street, 1978; Hassan, 1980; Williams & Adamson, 1980; Gasse & van Campo, 1994; Hoelzmann et al. 2000; Gvirtzmann & Wieder, 2001). Additionally many authors postulate that paleoenvironmental conditions in these regions were not significantly different from today (among others: Sirocko et al., 1993; Pachur & Wünnemann, 1996; Bar-Matthews et al. 2003; Kröpelin et al., 2008).

The approach presented here shows that the local water reservoirs at both study sites could be filled at least once in two years under present-day climatic conditions. Minimum rainfall intensities required to fulfill these conditions are 35.9 mm *h-1 and a duration of one hour in the Resafa Basin and 47.6 mm*h-1 and a duration of one hour in the basin of the Great Hafir. It should be noted that the reliability and representativeness of the meteorological data suffer the problems of short-term and fragmentary observations (Hulme, 1996).

Moreover, the application of a rainfall-runoff model to test the effectivity of water harvesting facilities of the ancient cities proves to be a valuable tool to estimate the water supply of these cultures and may be extended to such questions in other regions.

Acknowledgments

This study is supported by the Cluster of Excellence Exc264 TOPOI. Fieldwork was made possible only by the logistic help and perfect setting at the excavation sites. Therefore special thanks go to the "Ägyptisches Museum Berlin" and the German Archaeological Institute (DAI).

References

Adams, W.Y. (1974). Sacred and Secular Polities in Ancient Nubia. World Archaeology. Political Systems, 6(1),. 39-51.

Ahnert, F. (1982). Untersuchungen über das Morphoklima und die Morphologie des Inselberggebietes von Machakos, Kenia. Catena Suppl.-Bd., 2, 1-72.

Aktar-Schuster, M. & Mensching, H. (1993): Desertification in the Butana. GeoJournal, 31, 1, 41-50.

Allison, R. (1997). Middle East and Arabia, in Thomas, D. (Ed) (1997). Arid Zone Geomorphology, Process Form and Change in Drylands (2nd ed). John Wiley and Sons.

Al-Qurashi, A.; McIntyre N.;. Wheater H & Unkrich C. (2008). Application of the Kineros 2 rainfall–runoff model to an arid catchment in Oman. Journal of Hydrology 355 (1–4), 91–105.

Asfahani, J. & Radwan, Y. (2007). Tectonic Evolution and Hydrogeological Characteristics of the Khanaser Valley, Northern Syria, Derived from the Interpretation of Vertical Electrical Soundings. Pure Applied Geophysics, 164, 2291–2311.

Bahat, Y.; Grodek, T.; Lekach, J.& Morin, E. (2009). Rainfall–runoff modeling in a small hyper-arid catchment. Journal of Hydrology, 373(1-2), 204-217.

Baird A. (1997). Overland flow generation and sediment mobilisation by water, in Thomas, M.S.T. (ed.):Arid Zone Geomorphology. John Wiley and Sons.

Bar-Matthews,M., Ayalon, A., Gilmour,M., Matthews,A., & Hawkesworth, C.J. (2003). Sea-land oxygen isotopic relationships from planktonic foraminifera and speleothems in the Eastern Mediterranean region and their implication for palaeorainfall during inter-

glacial intervals. Geochimica et Cosmochimica Acta, 67(17), 3181-3199.

Berking, J., & Schütt, B. (in press). Late Quaternary Morphodynamics in the Area of the Meroitic Settlement of Naga, Central Sudan. Zeitschrift für Geomorphologie,Suppl.-Bd.

Beven, K.J. (2002). Runoff Generation in Semi-Arid Areas. In: Bull, L.J., & Kirkby M.J (eds): Dryland Rivers: Hydrology and Geomorphology of Semi-arid Channels. John Wiley, Chichester. Pp. 388.

Beven, K.J. (2003). Rainfall-Runoff Modelling: The Primer. Wiley-Interscience.

Birkhead, A. L. & James, C.S. (2002). Muskingum river routing with dynamic bank storage. Journal of Hydrology, 264, 1, 113-132.

Brinker, W. (1991). Zur Wasserversorgung von Resafa-Sergiupolis. Damaszener Mitteilungen 5, 119-146.

Brinker, W. (1991): Zur Wasserversorgung von Resafa-Sergiupolis, Damaszener Mitteilungen 5.

Cammeraat, E. (2004). Scale dependent thresholds in hydrological and erosion response of a semi-arid catchment in southeast Spain. Agriculture, Ecosystems & Environment, 104(2), 317-332.

Carol, P., Harden, P.& Delmas S. (2003). Infiltration on mountain slopes: a comparison of three environments, Geomorphology, 55, I1-4, 5-24.

Carsel, R.F., Parrish, R.S. (1988). Developing joint probability distributions of soil water retention characteristics. Water Resour. Res., 24, 755-769.

Chow, V.T., Maidment, D.R., & Mays, L.W. (1988). Applied Hydrology. McGraw-Hill, New York.

Coe, J.A., Kinner, D.A., & Godt, J.W. (2008). Initiation conditions for debris flows generated by runoff at Chalk Cliffs, central Colorado. Geomorphology, 96, 270-297.

Critchley, W., & Siegert K. (1991). Water harvesting. A manual for the design and construction of water harvesting schemes for plant production. FAO Paper No. AGUmisc. 17/91. FAO, Rome

Dane, J.H.. & Topp, G.C. (eds) (2002). Methods of Soil Analysis Part 4 - Physical Methods. Soil Science Society of America, Madison, WI.

Davis, C.A., Hellweger, F.L. & Maidment, D.R. (1997). HEC-PREPRO: A GIS Preprocessor for Lumped Parameter Hydrologic Modeling Programs. Center for Research in Water Resources, University of Texas at Austin.

Decagon Devices (2007). Mini Disk User's Manual, Ver. 6. Decagon Devices, Inc., 2365 NE Hopkins Court, Pullman, WA 99163.

Dennett,M.D., Keatinge,J.D.H.& Rodgers, J.A. (1984). A comparison of rainfall regimes at six sites in northern Syria. Agricultural and Forest Meteorology, 31, 3-4, 319-328.

Dunne, T. (1978). Field studies of hillslope flow processes. In: Kirkby, M.J., & Chorley, R.J. (eds): Hillslope Hydrology. Wiley, Cichester, pp. 227-293.

Endreny, T., A., Kyle E.& Thomas, P.E (2009). Improving Estimates of Simulated Runoff Quality and Quantity Using Road-Enhanced Land Cover Data. Journal of Hydrologic Engineering. 14, 4, 346-351.

Evenari, M.; Shanan, L.; Tadmor, N.; Aharoni, Y. (1961). Ancient Agriculture in the Negev: Archeological studies and experimental farms show how agriculture was possible in Israel's famous desert. Science. 133(3457), 979-996.

Farrand, W. R. (1979): Chronology and Palaeoenvironment of Levantine Prehistoric Sites as Seen from Sediment Studies. Journal of Archaeoalogical Science 6: 369 - 392.

Florinsky, I.V.; Eilersc, R.G.; Manninga, G.R., & Fullerd, L.G. (2002). Prediction of soil pro-

perties by digital terrain modeling. Environmental Modelling and Software, 17(3), 295-311.

Foody, G.; Ghoneimm, E. Arnell, N. (2004). Predicting locations sensitive to flash flooding in an arid environment, Journal of Hydrology, Volume 292, Issues 1-4.

Fowden, E. (1999). The Barbarian Plain: Saint Sergius between Rome and Iran. Berkeley and Los Angeles. University of California Press.

Furley, P. and Zouzou, R. (1989). The origin and nature of gypsiferous soils in the Syrian Mid-Euphrates, Scottish Geographical Magazine.

Gabriel, B (1997). Zur quartären Landschaftsentwicklung der nördlichen Butana (Sudan). Mitteilungen der Sudanarchäologischen Gesellschaft zu Berlin, 7, 23-30.

Gasse, F. & Street, F. A. (1978): Late Quaternary Lake-Level Fluctuations and Environments of the Northern Rift Valley and Afar Region (Ethiopia and Djibouti). Palaeogeography, Palaeoclimatology, Palaeoecology 24:279 - 325.

Gasse, F. & Van Campo, E. (1994). Abrupt Post-Glacial Climate Events in West Asia and North Africa Monsoon Domains. Earth Planetary Science Letter, Vol. 126, pp. 435-456.

GHCN:Global Historical Climatology Networks. May 2008 (http://iridl.ldeo.columbia.edu /docfind/databrief/cat-atmos.html)

Giraud, B., Bussert, R., Schrank, E., (1992): A new Theacean wood from the Cretaceous of northern Sudan. Review of palaeobotany and palynology, 75, 3-4, 289-299.

GLOBALSOD, Global Surface Summary of Day. May 2008. (http://iridl.ldeo.columbia.edu /docfind/databrief/cat-atmos.html)

Greenbaum, N., Ben-Zvi, A., Haviv, I., & Enzel, Y. (2006). The hydrology and palaeohydrology of the Dead Sea tributaries. In: Enzel, Y. , Agnon A., & Stein, M. (eds): New frontiers in Dead Sea palaeoenvironmental research. Geological Society of America, pp. 63–93.

Gvirtzman, G. & Wieder, M. (2001): Climate of the last 53,000 Years in the eastern Mediterranean, based on soil-sequence Stratigraphy in the coastal plain of Israel. Quaternary Science Reviews, 20, 1827 - 1849.

Haan, C.T., Barfield, B.J., & Hayes, J.C. (1994). Design Hydrology and Sedimentology for Small Catchments. Academic Pr. Inc..

Hassan, F.A. (1980): Prehistoric settlements along the Main Nile. - In: WILLIAMS, M.A.J.& FAURE, H.(Hrsg.):Sahara and the Nile. Rotterdam: 421 - 450.

HEC (2000). Hydrologic Modeling System: Technical Reference Manual. US Army Corps of Engineers Hydrologic Engineering Center.

HEC (2008). Hydrologic Modeling System: User Manual. US Army Corps of Engineers Hydrologic Engineering Center, Davis,CA.

Hillel, D. (1998). Environmental Soil Physics: Fundamentals, Applications, and Environmental Considerations. Elsevier.

Hinkel, M. (1991). Hafire im antiken Sudan. Zeitschrift für ägyptische Sprache und Altertumskunde, 118, 32-48

Hoelzmann, P., Keding, B., Berke, H., Kröpelin, S. & Kruse, H., J. (2000). Environmental Change and Archaeology: Lake Evolution and Human Occupation in the Eastem Sahara During the Holocene. Palaeogeography Palaeoclimatology Palaeoecology, 169, 193-217.

Hulme, M. (1996): Climate Change Within the period of Meteorological Records. - In: Adams, W.M., Goudie, A.S.; Orme, A.R.: The Physical Geography of Africa, Oxford University Press,New York, 88-102.

Imeson, A.C., & Prinsen, H.A.M. (2004).Vegetation patterns as biological indicators for identifying runoff and sediment source and sink areas for semi-arid landscapes in

Spain. Agriculture, Ecosystems and Environment, 104(2), 333-342.
Karnapp W. (1976). Die Stadtmauer von Resafa in Syrien. Denkmäler Antiker Architektur, 11.
Kellner-Heinkele, B. (1996). Rusafa in den Arabischen Quellen. In D. Sack: Die Große Moschee von Resafa - Rusafat Hisham. Resafa IV.
Kidron G., J. & Yair, A.. (2001). Runoff-induced sediment yield over dune slopes in the Negev Desert. 1: Quantity and variability. Earth Surf. Process. Landforms, 26, 461–474.
Kidron G., J. & Yair, A.. (1997). Rainfall-runoff relationship over encrusted dune surfaces, Nizzana, Western Negev, Israel. Earth Surface Processes and Landforms, 22, 1169–1184.
Kidron, G.J. (2007). Millimeter-scale microrelief affecting runoff yield over microbiotic crust in the Negev Desert. Catena, 70(2), 266-273.
Kleinschroth, A. (1984). Wasserreservoirs im Sudan aus der Zeit der Antike. Mitteilungen aus Hydraulik und Gewaesserkunde der TUM, 41, 75-106.
Kleinschroth, A. (1986). Die Verwendung des Hafirs im meroitischen Reich. Beiträge zur Sudanforschung,1, 79-96.
Knebla ,M.R.; Yanga, Z.-L.; Hutchison, K. & Maidment, D.R. (2005). Regional scale flood modeling using NEXRAD rainfall, GIS, and HEC-HMS/RAS: a case study for the San Antonio River Basin Summer 2002 storm event. Journal of Environmental Management, 75, 325–336.
Konrad, M. (2001). Der spätrömische Limes in Syrien: Archäologische Untersuchungen an den Grenzkastellen von Sura, Tetrapyrgium, Cholle und in Resafa. Resafa, V.
Kröpelin, S., Verschuren, D., Lézine, A.-M., Eggermont, H., Cocquyt, C., Francus, P., Cazet, J.-P., Fagot, M., Rumes, M., Russell, J. M., Darius, F., Conley, D. J., Schuster, M., von Suchodoletz, H. & Engstrom,, D.R. (2008). Climate-Driven Ecosystem Succession in the Sahara: The Past 6000 Years. Science, 320, 5877, 765 – 768.
Ladoy, P., Lovejoy, S. and Schertzer, D., (1991). Extreme variability of climatological data: scaling and intermittency. In: Schertzer, D. and Lovejoy, S. Editors, 1991. Nonlinear variability in geophysics: scaling and fractals, Kluwer Academic Publishers, The Netherlands, pp. 241–250.
Lange; J., Liebundgut, C., Schick, A. (2000). The Importance of Single Events in Arid Zone Rainfall-Runoff Modelling, 25 (7), 673-677.
Legutke, S., & Voss, R. (1999). The Hamburg Atmosphere-Ocean Coupled Circulation Model ECHO-G. DKRZ-Hamburg, Technical Report, 21.
Li, X-Y., González, A., & Sole´-Benet, A. (2005). Laboratory methods for the estimation of infiltration rate of soil crusts in the Tabernas Desert badlands. Catena, 60, 255–266.
Martínez-Mena, M., Albaladejo, J., & Castillo, V. M. (1998). Factors influencing surface runoff generation in a Mediterranean semi-arid environment: Chicamo watershed, SE Spain. Hydrological Processes, 12(5), 741-754.
McIntyre, N. & Al Qurashi, A. (2009). Performance of ten rainfall-runoff models applied to an arid catchment in Oman. Environmental Modelling and Software. 24, 726-738.
Moore, I.D., Gessler, P.E., Nielsen, G.A., & Peterson, G.A. (1993). Soil attribute prediction using terrain analysis. Soil Science Society of America Journal, 57(2), 443–452.
Morin, E.; Jacoby, Y., Navon S., & Bet-Halachmi E. (2008). Towards flash-flood prediction in the dry Dead Sea region utilizing radar rainfall information. Advances in Water Resources, 32(7), 1066-1076.
Mousli, O.F. (1980). Methods of evaluation and classification of gypsiferous soils and suitability for irrigated agriculture. In: F.H. Beinroth and A. Osman (Eds.) (1980).

Proceedings of the 3rd International Soil Classification Workshop. The Arab Center for Studies of the Arid Zones and Dry Lands (ACSAD), Damascus, Syria: 278-307.

Mulligan, M. (1998). Modelling the geomorphological impact of climatic variability and extreme events in a semi-arid environment, Geomorphology, Volume 24, Issue 1 , Pages 59-78.

Myers, L.E. (1975). Water Harvesting and Management for Food and Fiber Production in the Semi-arid Tropics. AR/USDA: Berkeley, CA.

Nicolau, J.,M., Sole-Benet, A., Puigdefabregas, J., & Gutierrez-Elorza, M. (1996). Effects of soil and vegetation on runoff along a catena in semi-arid Spain. Geomorphology, 14(4), 297–309.

Osman, O.E., Hastenrath, S.L. (1969): On the Synoptic Climatology of Summer Rainfall over Central Sudan. Arch. Met. Geoph. Biokl., Ser. B 17, 297-324.

Oweis, T., & Taimeh, A. (1996). Evaluation of a small basin water-harvesting system in the arid region of Jordan. Water Resource Management, 10(1), 21-34.

Pachur H.-J. & Wünnemann, B. (1996). Reconstruction of the paleoclimate along 30°E in the eastern Sahara during the Pleistocene/Holocene transition. Palaeoecology of Africa 24,1-32.

Parker, A., & Goudie, A. (2008). Geomorphological and palaeoenvironmental investigations in the southeastern Arabian Gulf region and the implication for the archaeology of the region. Geomorphology, 101(3), 458-470.

Pilgrim, H., Chapman, T.G., & Doran, D.G.D. (1998). Vegetation Problems of rainfall-runoff modelling in arid and semiarid regions.Hydrological Sciences. Journal des Sciences Hydrologiques, 33, 4.

Ponikarov, V. P. (ed.) (1966). The Geological Map of Syria, Scale 1:200000, Sheet I-37-XX (Salamiyeh).Moscow.

Reid, I., Laronne, J.B., & Powell, M.D. (1998). Flash-flood and bedload dynamics of desert gravel-bed streams. Hydrological Processes, 12, 543–557.

Riehl, S., Bryson, R., & Pustovoytov, K. (2008). Changing growing conditions for crops during the Near Eastern Bronze Age (3000–1200 BC): the stable carbon isotope evidence. Journal of Archaeological Science, 35(4), 1011-1022.

Rösner, U. (1995). Zur quartären Landschaftsentwicklung in den Trockengebieten Syriens. Relief Boden Paläoklima, 10.

Rowntree, K. M. (1988). Storm rainfall on the Njemps flats, baringo district, Kenya. International Journal of Climatology, 8(3), 297-309.

Sack , D. (1996). Die Große Moschee von Resafa - Rusafat Hisham. Resafa IV.

Schlumberger, D. (1950): La Palmyrene du Nord-Ouest. Recherches archaeologiques sur la mise en valeur d'une region du desert par las Palmyrens. Bibl. Archeol. Et Hist. Bd. 49. – Thése d´Etat, Paris.

Sharon, D. (1972). The spottiness of rainfall in a desert area. Journal of Hydrology, 17, 161–175.

Sirocko, F., Sarnthein, M., Erleneuser, H., Lange, H., Arnold, M., & Duplessy, J. C. (1993). Century-scale events in monsoonal climate over the past 24,000 years. Nature 364: 322–324.

Sugar, C. & James, G., (2003). Finding the number of clusters in a data set: an information theoretic approach. Journal American.Statistic Association, 98,750 – 763.

Sutherland, R. & Brian, R. B. (1990). Runoff and erosion from a small semiarid catchment, Baringo district, Kenya. Applied Geography, 10(2), 91-109.

Tagil, S. & Jenness, J. (2008). GIS-Based Automated Landform Classification and Topographic, Landcover and Geologic Attributes of Landforms Around the Yazoren Polje, Turkey. Journal of Applied Sciences 8(6), 910-921.

Tooth, S. (2000). Process, form and change in dryland rivers: a review of recent research: Earth-Science Reviews, 51, 67-107.

Tsubo, M.; Walker, S., & Hensley, M. (2005). Quantifying risk for water harvesting under semi-arid conditions: Part I. Rainfall intensity generation. Agricultural Water Management, 76(2), 77-93.

Ulbert T. (1986). Die Basilika des Heiligen Kreuzes in Resafa-Sergiupolis. Resafa II. Zabern. Pp. 230.

USDA–NRCS (ed.) (2005). US Department of Agriculture Natural Resources and Conservation Service, National Engineering Handbook. National Technical Information Service, Washington, DC.

Wagstaff, K. (2001). Constrained K-means Clustering with Background Knowledge. Proceedings of the Eighteenth International Conference on Machine Learning. 577 - 584.

Walsh, R.P.D., Hulme M. & Campbell M.D. (1988). Recent rainfall changes and their impact on hydrology and water supply in the semi-arid zone of the Sudan. The Geographical Journal 154(2): 181–198.

Weiss, A. (2001). Topographic Position and Landforms Analysis. Poster presentation, ESRI User Conference, San Diego, CA.

Wheater, H., Sorooshian, S. & Sharma, K. D. (2007).Hydrological modelling in arid and semi-arid areas. 195 pages. Cambridge.

Whitehead, P., Smith, S., Wade, a., Mithen, S., Finlayson, B. & Sellwood, B., (2008). Modelling of hydrology and potential population levels at Bronze Age Jawa, Northern Jordan: a Monte Carlo approach to cope with uncertainty. Journal of Archaeological Science, 35(3), 517-529.

Wikander, O. (ed.) 1999: Handbook of Ancient Water Technology. Brill Academic Publishers, Leiden.

Wildung, D.& Kröper, K. (2006). Naga, Royal City of Ancient Sudan. Staatliche Museen zu Berlin – Stiftung preußischer Kulturbesitz.

Williams, M. A. J. & Adamson, D.A. (1980): Late Quaternary depositional history of the Blue and White Nile rivers in central Sudan. In: Williams, M.A.J. & Faure, H.: Sahara and the Nile, 281-304.

Williams, M., & Nottage, J. (2006). Impact of extreme rainfall in the central Sudan during 1999 as a partial analogue for reconstructing early Holocene prehistoric environments. Quaternary International, 150, 1, 82-94.

Wilson, J. P. & Gallant, J.C. (2000). Secondary Topographic Attributes. Terrain Analysis: Principles and Applications. John Wiley and Sons. New York.

Wirth, E. (1971). Syrien, Eine Geographische Landeskunde. Wissenschaftliche Buchgesellschaft Darmstadt.

Wun, S.; Lib, J. & Huang, G.H. (2008). A study on DEM-derived primary topographic attributes for hydrologic applications: Sensitivity to elevation data resolution . Applied Geography, 28(3), 210-223.

Yair, A. & Lavee, H. : (1985). Runoff Generation in arid and semi-arid zones. In: Anderson, M.G. & Burts, T.P. (eds): Hydrological Forecasting. Wiley Chichester, pp. 183 – 220.

Yair, A., & Raz-Yassif, N. (2004). Hydrological processes in a small arid catchment: scale

effects of rainfall and slope length. Geomorphology, 61, 155–169.
Zhang, R. (1997). Determination of soil sorptivity and hydraulic conductivity from the disk infiltrometer. Soil Science Society of America Journal, 61, 1024-1030.

4.2 The elaborated floodwater harvesting system of Resafa – Construction and reliability

Brian Beckers, Brigitta Schütt, 2013. Journal of Arid Environments, 96, 31-47.
DOI: http://dx.doi.org/10.1016/j.jaridenv.2013.04.004

4.2.1 Introduction

"[...] ar-Ruṣāfa [Resafa] has neither creek nor springs and [...] its inhabitants drink from the town cisterns. When the cisterns give out at the end of the summer, they haul water from the Euphrates [...]. The wells at ar-Ruṣāfa have a depth of 120 ells [~ 65 m] but their water is brackish." (Al-Aṣma´i (~ 740 - 828 AD), cited by Musil, 1928, 270 ff).

The above quote summarizes quite well the water supply problems of the Roman/ Early Islamic town of Resafa ([ar-] Rusafa, also Sergiupolis, Ruṣāfat Hišhām), which are the main topic of this study. The Romans founded the town as a fortified settlement in the 1st century AD in the Syrian desert steppe at the eastern bank of the Wadi es-Sélé (Fig. 1 and 2). It was part of the Eastern Limes, the Roman border defense system against the Parthian and later Sassanid Empire (Fig. 2). The settlement became one of the most important Christian pilgrimage sites in the eastern Mediterranean after a Roman officer named Sergios suffered martyrdom in Resafa in the 4th century AD (Fowden, 1999). In the following century, as the population and the numbers of pilgrims grew, great city walls, churches and sophisticated water supply facilities were built (Fig. 3 a/b). In the 7th cen-

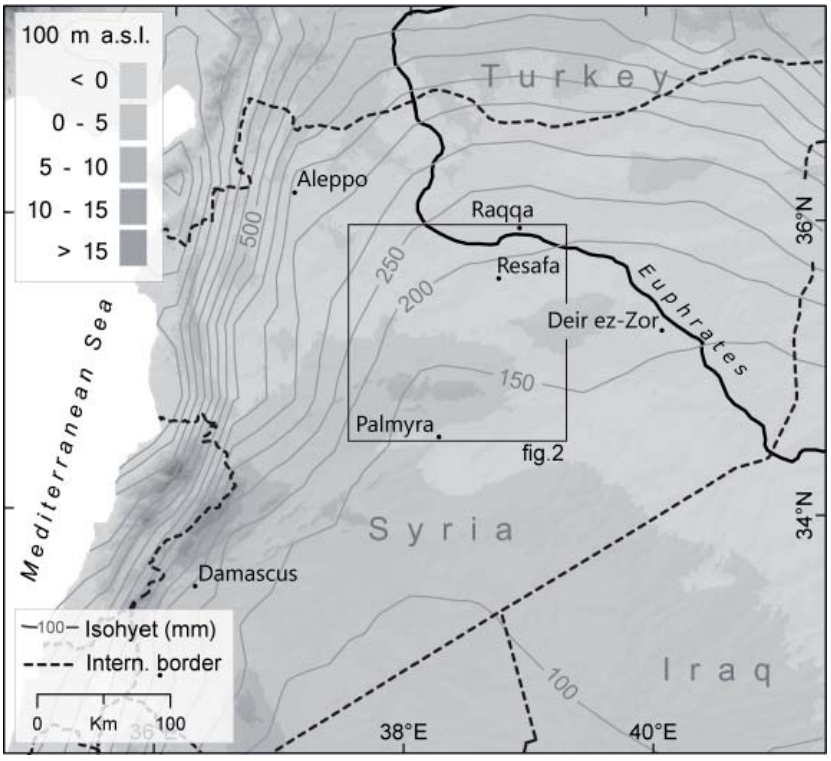

Fig. 1 Location of the research area in modern Syria with isohyets. (Data sources: topography: SRTM, Isohyets are based on the GPCC dataset (1951 - 2000)).

tury AD, after the Islamic conquest, the Umayyad caliph Hišām ibn ʿAbd al-Malik (691 – 743 AD) took residence in Resafa and expanded the settlement extra muros (outside the city walls). Throughout its history Resafa was a prominent nodal point of commercial ca-

ravans and nomadic tribes (Musil, 1928). After a gradual decline in importance, the city was finally abandoned in the 14th century AD after the Mongol invasion (Sack, 1996).

In contrast to other ancient settlements in the region such as the oasis of Palmyra or Raqqa at the Euphrates (Fig. 2), Resafa had and has no perennial water sources (Fowden, 1999). The brackish water from the several wells inside and outside the city walls could be used almost only for agricultural and domestic purposes (Brinker, 1991). Its dominant drinking water source was rainfall and runoff, which were collected and stored in cisterns. Two techniques were applied: (i) rainfall falling on roofs was collected and stored in bottle-shaped cisterns (rooftop harvesting) and (ii) floods, occurring during or shortly after sufficient rainfall events were retained and channeled to large subsurface cisterns (floodwater harvesting) (see e.g. Critchley et al., 1994 for a general introduction to traditional water harvesting methods). Thus the water supply of the city was highly vulnerable to rainfall variability. Interannual and longer term variability of rainfall, however, is nowadays a distinctive feature of the climate of the Syrian steppe and, according to the chronicles of Michael the Syrian (1166 – 1199 AD), had also been during Late Roman/Early Islamic times (Morony, 2000). Consequently the question arises as to the reliability of the water supply system and especially the floodwater harvesting facility as the major source of water.

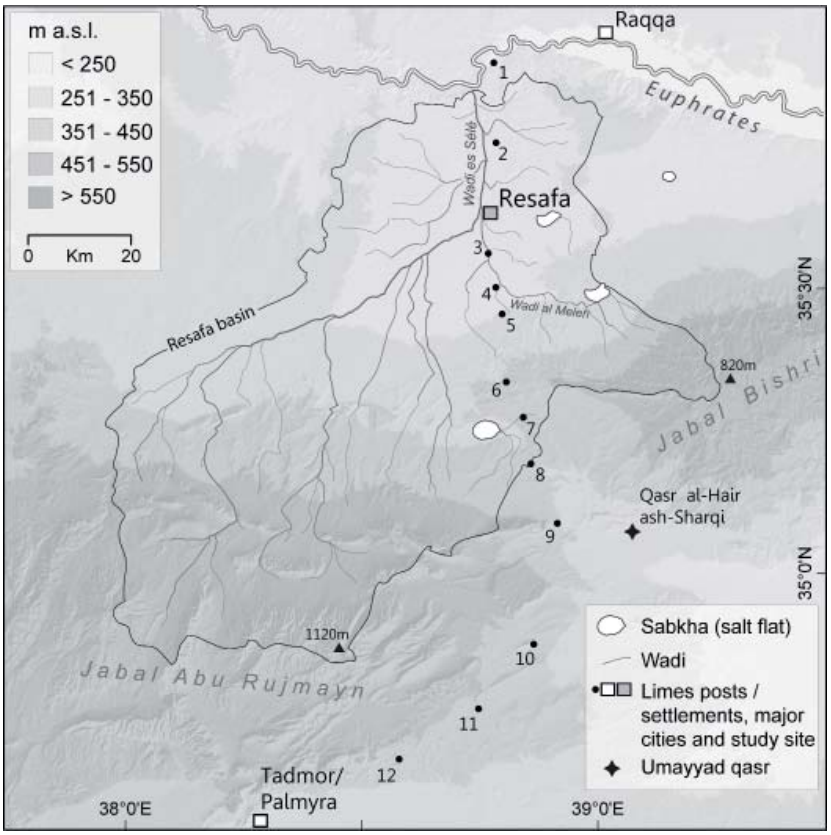

Fig. 2 Topography of the Resafa basin with general wadi system, Limes posts, settlements and major ancient cities. 1. Sura 2. Tetrapyrgium 3. Al - Qusair 4. Unnamed Roman military post 5. Cholle 6. Tall Fhada 7. Al – Qudair 8. Al – Kum 9. Oresa (al - Taiyiba) 10. As – Suhna 11. Al – Hulaiha 12. Aracha. Data sources: topography: SRTM, names and locations: Musil (1928), Konrad (2001).

A recent study by Berking et al. (2010) estimates the minimum hourly rainfall intensity that is necessary to generate runoff in the catchment of Resafa´s floodwater harvesting system. However, the reliability of this system has not yet been analyzed in detail (Beckers et al., 2012). The most comprehensive archaeological study on the water supply of Resafa was conducted by Brinker (1991). The study focuses on the city cisterns and the hydraulic structures next to the city walls. Aerial photos from the early 20th century indicate that linear structures parallel to the dominant flow direction existed and facilitated the floodwater harvesting system (Fig. 3 A/B). These structures have so far not been associated with the floodwater harvesting facilities. We assume that such structures were part of an embankment system that channeled the floodwaters towards the city and protected buildings from flooding, a technique frequently reported for ancient sites in the Middle East and beyond (Mayerson et al., 1961; Bruins et al., 1986; Critchley et al., 1994; van Wesemael et al., 1998). However, modern road construction, earth works for irrigation and farming, and erosion have leveled or destroyed large parts of these presumed structures and recent excavations could only reveal parts of them (Beckers et al., 2012).

The main objectives of this paper are to:

(i) assess the reliability of the floodwater harvesting system of Resafa by applying a hydrological model and current rainfall data. Two main assumptions underlie this approach. First, it is assumed that the current rainfall regime can be used as a proxy for the rainfall climatology that prevailed in the region during the Roman/Early Islamic period. Second, it is assumed that the general physical characteristics of the catchments have not changed significantly since that time (for a discussion on these assumptions see section 2 and 3).

(ii) examine the hypothesis of a closed embankment system along the eastern margin of the Wadi es-Sélé by applying a hydraulic model and preliminary results from excavations and a previous geomorphological survey.

The time frame under consideration is the 6th to the 14th century AD, the period during which the existence of a floodwater harvesting system in Resafa is historically and archaeologically attested (Brinker, 1991).

4.2.2. Study Site

4.2.2.1 Geology, hydrology, and vegetation

The following section summarizes the environmental conditions in the Syrian desert steppe (Mean Annual Rainfall (MAR) < 200 mm, Wirth, 1971) and in particular of the Resafa Basin, the catchment of the Wadi es-Sélé (Fig. 2). Two quotes of Arabic scholars illustrate the ancient and, as shown below, present landscape around Resafa:

"Ar-Ruṣāfa lies in a desert1 so flat that the view is bounded only by the horizon. […]" (Ibn Buṭlān (died in c. 1064 AD), cited by Musil, 1928). And Fowden (1999) quotes al-Isfahani (c. 900 – 970 AD) : *„[Hisham] had gone out with his family […]. And he camped on a barren, stony plain that was elevated and extensive, in a year when the rain had fallen early and abundantly and the land had taken its adornment from the variety of the colors of its vegetation of pretty spring blooms, which were […] well watered on a plateau whose soil seemed like pieces of camphor."*

Camphor, a white, crystalline organic compound, most likely refers to the abundant gypsum bedrock which builds large parts of the surface around Resafa. The gypsum be-

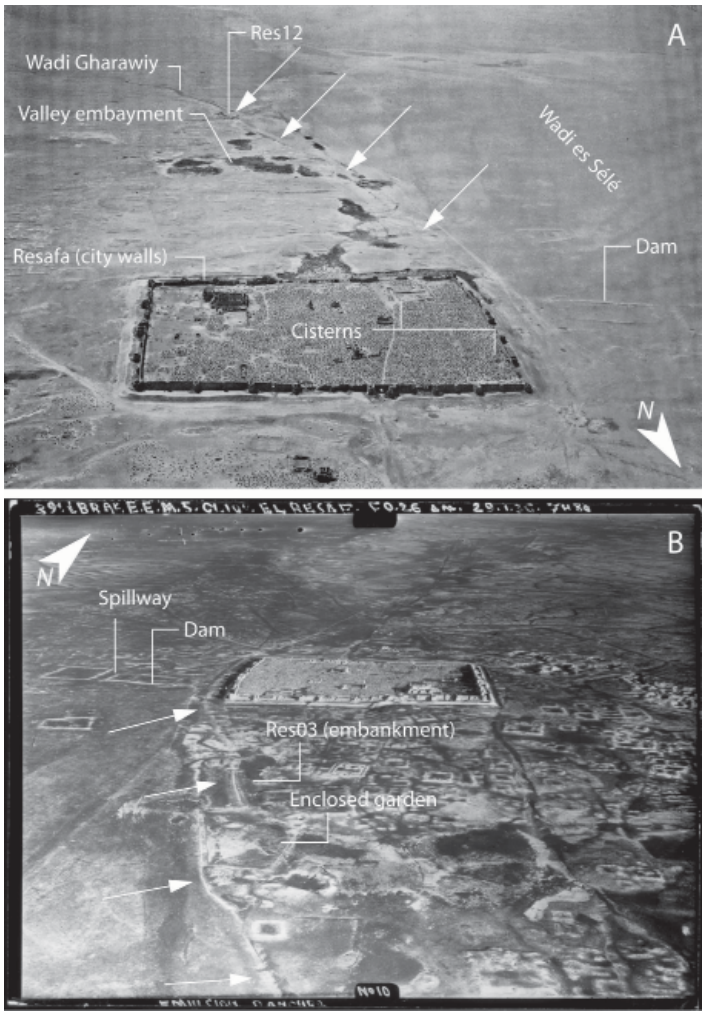

Fig. 3 A/B Edited aerial pictures of Resafa and surroundings with landscape and building features mentioned in the text. The rectangular structures to the south of the enclosed city, clearly visible in photo B, are predominantly building remains of the Ummayyad period. Res12 and RES03 are excavation sites where archaeological evidence of parts of the embankment system was found. The arrows indicate the location of the presumed embankment system.

drock is interbedded with limestone and marl layers. These evaporites are part of the Miocene Lower Fars formation and constitute the upper geological formations of the undulating monotonous tableland to the east and west of Resafa (Ponikarov, 1966; Wolfart, 1967). Karst features such as dolines (some of them with diameters of 200 – 300 m) are present in the vicinity of Resafa. The southern and eastern gently rolling divides of the Resafa basin consist of Cretaceous and Paleogene limestone and marls. The wide, non-entrenched valley of the Wadi es-Sélé is covered by Pleistocene pebbles and sands which are intermittently overlain by Holocene fluvial deposits, mostly composed of silty sands (Wolfart, 1967). The floodplain of the lower course of Wadi es-Sélé is bordered to the east by the gently sloping and low escarpment of the north-south running Ar-Rasafeh [Resafa] -Fault (Sbeinati et al., 2009).

The hilltops and ridges of the region (most of them are flat or moderately sloping) show bedrock outcrops, whereas the middle and foot slopes are covered by a thin colluvial mantle. Alluvial sediments cover the valleys and depression bottoms. The sediments are mostly composed of fine-textured, in some parts gravelly, weathering residues of the gypsiferous bedrock, mixed with loess-like sediments which are deposited by the frequent dust storms passing across the region (Masri et al., 2003). Accordingly, the soils of the region predominantly consist of xeric gypsisols (Reifenberg, 1952).

The caternary variation in sediment cover thickness is reflected by the vegetation density. The vegetation of the Syrian drylands mainly consists of xeric shrubs and grasses which are moderately dense along the valley bottoms and scattered on the slopes and

hilltops (Wirth, 1971; Zohary, 1973). Only after sufficient winter rains annual plants cover wide parts of the steppe (Zohary, 1973). The region is traditionally used for pasture (Lewis, 2009), and the vegetation is nowadays heavily degraded predominantly due to century-long overgrazing (Louhaichi et al., 2012).

The well-established dendritic channel system of the Resafa Basin (Fig. 2) is a relict of Pliocene to Pleistocene wet periods (Wolfart, 1967). At present, perennial streams are absent in the basin, and the major wadis such as the Wadi es-Sélé lack distinct channels. By contrast, most of the steeper tributaries descending from the divides and the escarpment have well-defined channels. Allison (1998) states that present-day runoff events in the Syrian steppe have a low degree of connectivity and predominantly percolate or drain into depressions or salt flats and the floodplains of the major wadis (Berking et al., 2010). Also the Wadi es-Sélé overflows only irregularly about once in ten years (personal communication by the local residents, 2008).

4.2.2.3 Present and past climate

Large parts of Syria´s present climate can be classified as Mediterranean with a continental character, especially in the summer months. The summers (June – September) are hot and dry, the winters (November - March) mild and relatively wet, and the transition periods (October, April, May) are short (Wirth, 1971) (Fig. 4). The seasonal variations of the Syrian climate are mainly governed by the cyclic movement of the global circulation system and the location of Syria between the subtropical high pressure belts and the Westerlies (Bolle, 2003). In winter Syria is under the influence of the Westerlies, which support the movement of Atlantic depressions to the region and facilitate cyclogenesis in the eastern Mediterranean. These west-east tracking storms are the main source of moisture for the region (Trigo et al., 1999; Harding et al., 2009). In summer, rainfall is scant in the western parts and almost absent in the eastern parts of Syria largely owing to the location of the subtropical high pressure belts over Syria during this time. The summer

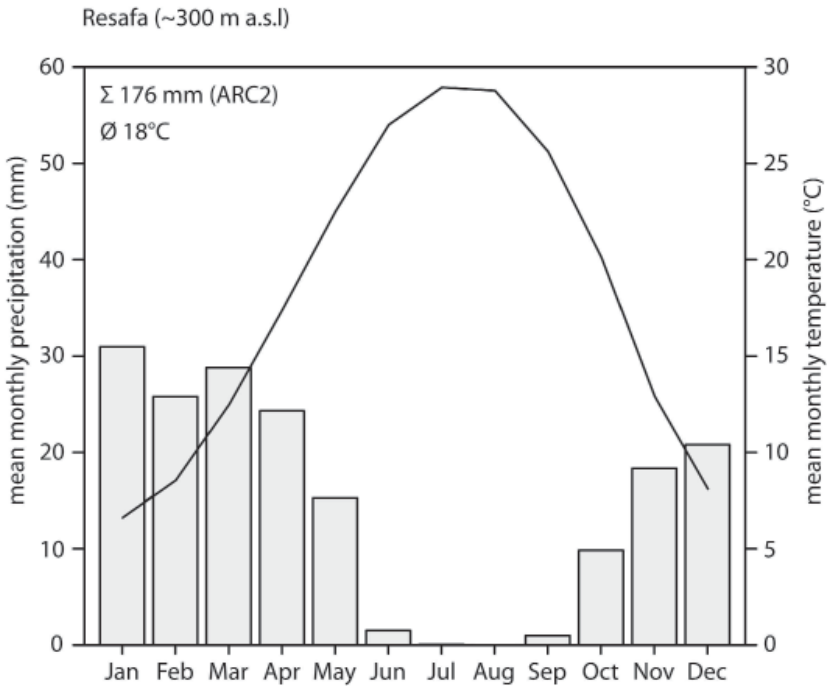

Fig. 4 Climate diagram of Resafa 1983 - 2011 (Precipitation data from the Arc 2 dataset and temperature data from the UEA – CRU dataset (Mitchell and Jones, 2005)).

dryness in Syria and especially in the interior parts is further enhanced by the descending movement of the Etesian winds from the summer hot and dry Anatolian plateau (Wirth, 1971; Bolle, 2003; Raicich et al., 2003). Monthly mean temperatures in winter range between 10 and 15 °C. Monthly minimum temperatures drop to 0 - 4 °C in this region with mean annual minima of -2 to -5 °C. On rare occasions cold northern air masses move into northern Syria, causing several days or weeks of severe frost. These cold spells can be a threat to the livestock and crops. In summer the mean monthly temperatures vary between 25 and 30 °C and rarely drop below 10° C during the night (Wirth, 1971).

The precipitation regime is the main distinctive feature of the climate regions in Syria and constitutes the major limiting factor for human activities and ecosystems (Wirth, 1971; Luterbacher et al., 2006). The country has a steep west-east precipitation gradient with about 800 mm*yr-1 in the coastal mountains to below 150 mm*yr-1 in the Syrian Desert (Fig. 1). The months with the highest rainfall amounts are on long term average January and February in the eastern parts of Syria (Trigo et al., 2010). However, the Syrian desert steppe receives the most intense rainfall on average in March due to frequent thunderstorms which are triggered by unstable air masses, caused by the rapid heating of the land masses during that time (Wirth, 1971). After the summer the first precipitation events in the eastern parts of Syria occur between mid-October and mid-November.

Given that the eastern Mediterranean is a climatic transition zone and owing to the interannual differences in the dominating large-scale circulation and pressure patterns, the annual rainfall amounts, precipitation characteristics, and the onset and end of the rainy season vary considerably on interannual and decadal time scales (Luterbacher et al., 2006). Droughts and exceptionally wet years are common phenomena in the region (e.g. Trigo et al., 2010), and the variability tends to increase with decreasing mean annual precipitation (Wirth, 1971). The main teleconnection patterns that influence these variations in parts of the eastern Mediterranean and the Middle East are said to be the North Atlantic Oscillation (NAO), El Niño Southern Oscillation (ENSO), the South Asian Monsoon and the East Atlantic/West Russia pattern (reviewed in e.g. Alpert et al., 2006; Luterbacher et al., 2006; Xoplaki et al., 2012). The influence of these patterns on the eastern Mediterranean climate have most likely been present throughout the Holocene (Schmidt et al., 2004). However, the impact of these phenomena on precipitation variations are spatially and temporally not uniformly distributed in the region (Roberts et al., 2012; Xoplaki et al., 2012). In the Syrian desert steppe, their influence is in general weak or statistically not significant (e.g. Krichak and Alpert, 2005; Roberts et al., 2012; Xoplaki et al., 2012).

The large-scale atmospheric circulation patterns that govern the eastern Mediterranean and the Middle Eastern climate are assumed to have been established between 5000 - 3500 yrs BP (Jalut et al., 1997). Palaeoclimatic proxy studies and climate modeling results generally agree that the eastern Mediterranean became dryer since the Mid-Holocene, around 6500 – 6000 yrs. BP (reviewed in e.g. Robinson et al., 2006; Roberts et al., 2011). Since the beginning of the late Holocene (c. 2500 yrs. BP) a similar climate to that of the present day has prevailed in the Eastern Mediterranean (Finné et al., 2011). However, palaeoclimate proxy records from the Eastern Mediterranean and Middle East indicate that centennial climate fluctuations occurred during that time interval. The most significant ones were: the Roman warm period (c. 400 AD – 400 AD) with warmer and dryer conditions; a period of wetter conditions from 400 AD to 800 AD; the Medieval climate anomaly (c. 950 AD – 1250 AD) with warmer and wetter conditions, and the Little Ice Age (c.

1400 AD – 1700 AD) with cooler and dryer conditions (Finné et al., 2011; Kaniewski et al., 2012; Roberts et al., 2012). However, the aforementioned studies and contemporary sources suggest that the general characteristics of the climate during the focused period resemble those of the present. The chronicles of Zuqnin and of Michael the Syrian (spanning from 488 to 775 AD and from about 600 to 1200 AD, respectively), for example, document that rain fell predominantly from October to the end of May, droughts as well as wet years were common, and the onset and end of the rainy season were variable (Morony, 2000; Widell, 2007). Moreover, the regional ancient settlement pattern of the Syrian steppe was similar to the present pattern, and the water supply strategies of the ancient settlements in the region were adapted to an arid or semi-arid climate (Wirth, 1971; Rösner, 1995; Kamash, 2012; Riehl, 2012).

4.2.2.3 The location, layout, and water supply system of Resafa

Details on the history and archaeology of Resafa can be found in Musil (1928), Sack (1996), and Fowden (1999), for example, and on the Roman/Early Islamic settlement history of the region in Poidebard (1934), Konrad (2001), and Kamash (2012). Resafa is located downstream of the confluence of several major tributaries of the Wadi es-Sélé (Fig. 2). Parts of the enclosed city lie on the elevated plain that extends from the escarpment of the Ar-Rasafeh fault to the Jebel Bishri and partly in the floodplain of the Wadi es-Sélé (Fig. 5). Most buildings extra muros are built south of the enclosed city on the elevated plain and date to the Ummayyad period (8th to the 9th century AD) (Sack, 1996). However, some buildings and structures were built on the alluvial plain of the Wadi es-Sélé dating from the Late Antique to the Ummayad period (Mackensen, 1984) e.g. an enclosed garden in the valley embayment to the south of Resafa (Fig. 3/5) and several buildings to the south of the city walls (Fig. 5).

The water supply infrastructures of the enclosed city was studied by Brinker (1991) and the paper is published in German only. Thus the most relevant aspects of this paper will be summarized in the next few paragraphs and supplemented with observations by other authors. Rooftop harvesting constituted an important part of the drinking water supply of the city throughout its existence. However, it was likely the only source of drinking water while Resafa was just a small Roman military fort (until about the beginning of the 6th century) (Brinker, 1991). The collected water was stored in bottle-shaped cisterns. Brinker (1991) counted 27 cisterns of this kind intra muros (inside the city walls) with each having a capacity of about 20 – 30 m^3. More cisterns of this kind can be found extra muros in the Wadi es-Sélé which were most likely associated with buildings (Fig. 5). Brinker (1991) argues that the sum of about 700 m^3 of water that could be stored in these cisterns was not sufficient to supply a city of the size of Resafa after the beginning of the 6th century and therefore a much larger water source had to be harnessed. Thus, the central water harvesting facility was the floodwater harvesting system. Owing to the low degree of connectivity of the wadi system of the Resafa basin, the sub-catchments which regularly contribute to the floodwater harvesting systems are likely those in the vicinity of Resafa. In Resafa this is the catchment of the Wadi Gharawiy (Fig. 5B). The rare occasions when floods of the remoter tributaries flowed pass Resafa are assumed to have a minor role in the water supply (Berking et al., 2010). Brinker (1991) describes the construction and history of the system as follows: when Resafa developed from a solely military station and gathering point for caravans to an important pilgrimage site, Anastasius I (r. 491 – 518 AD) initiated the building of great city walls most likely in 499/500 AD. After war-related disruptions the walls were completed under Justinian I (r. 518 – 527 AD) in the early 520s AD (Hof, 2008). The layout of the enclosed city is excep-

tional in the region and most likely adapted to hydraulic constraints (Garbrecht, 1996). It allowed the building of protected cisterns in the thalweg of the Wadi, thereby obviating the necessity of raising the floodwater up to the level of the plain (Garbrecht, 1996). Four large cisterns (total capacity ~ 21,000 m^3) were successively built during a period of about 200 years, the first and smaller ones at about the same time as the city walls. By far the largest cistern, with a capacity of 14,600 m^3, was built between the end of the 7th and the beginning of the 8th century AD (Westphalen and Knötzele, 2004). Chalky water marks at the upper walls of the cisterns attest that they were at least occasionally filled up to their total capacity (Brinker, 1991). The cisterns were connected to the floodplain by a channel that led via a culvert built into the city wall to an artificial shallow reservoir built by an earthen dam. This dam was about 450 m long and up to 3 m tall and blocked parts of the thalweg of the Wadi es-Sélé. The foot of the dam was protected by a wall made of gypsum blocks. A 38 m wide spillway with a capacity of about 80 – 120 m^3*s-1 was built in the middle of the dam. The spillway floor is on the level of the upper side of the culvert, thus preventing the channel from overflowing. Two large open water basins are attached to the north of the dam and the left and the right of the spillway. These basins were most likely filled when excess water flowed along the spillway (Fig. 3) (Musil, 1928). The channel leading to the cisterns is about 4.5 m wide. Garbrecht (1996) proposes that the channel was blocked by a wall towards the basin, thus allowing only the upper part of the water column with little sediment load to flow into the channel. Two opposite stones in the channel show grooves, and Brinker (1991) assumes that they are remains of a sluice gate to control the water flowing into the channel. The filling of the cisterns is described by Garbrecht (1996) as follows: arrival of the flood and filling of the basin downstream of the dam; rising of the water level up to the level of the inlet of the channel (~ 50 cm, as deduced from the height of the channel walls); start of the filling of the cisterns with a maximum rate of 5m^3*s-1 (as deduced from the dimensions of the

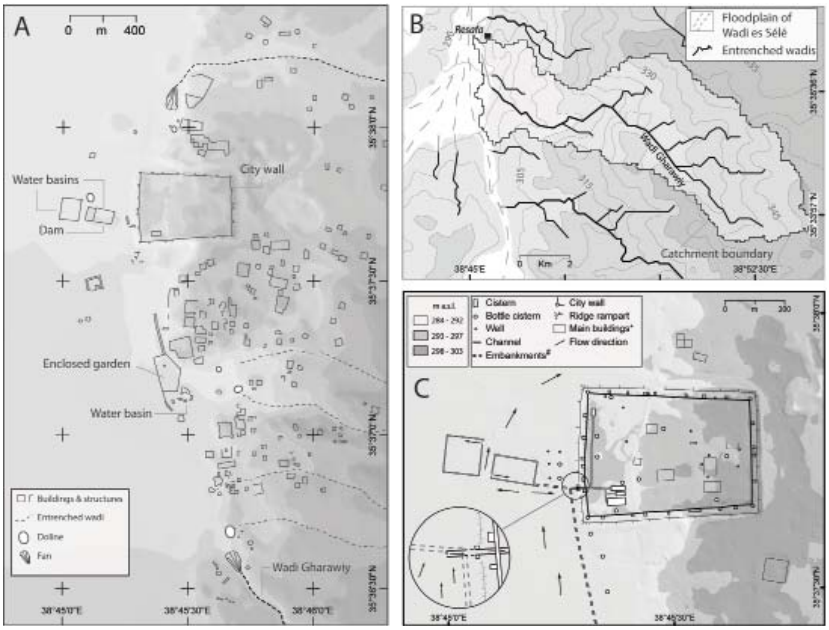

Fig. 5A: Map of the archaeological finds, basic hydrography and topography of Resafa. 5B: Catchment of the Wadi Ghuraby and hydrography 5C: Detail sketch of the floodwater harvesting system of Resafa. The dashed lines indicate the presumed embankments in the northern part. Note that the number of cisterns and wells intra muros is not accurate correct because we lacked information on the location of some of the structures (section 2.3).

culvert). If the water level continues to rise, the excess water is channeled downstream via the spillway and most likely partly channeled into the basins to the east and west of the spillway (Fig. 3/5).

How many residents and visitors had to be supplied from the cisterns is not known, and to the best of our knowledge no reliable estimate exists. However, given the dimensions of the cisterns the number of residents and visitors in Resafa may have frequently been in the thousands at least after the 7th century AD (21,000 m^3 of stored water could have served about 11,500 adults for one year if one assumes a consumption of 5 l/day/adult (cf. Whitehead et al., 2008).

4.2.3. Data, Methods and Analysis

4.2.3.1 Study approach

The major aim of this study is to assess the reliability of the floodwater harvesting system of Resafa. In this study we consider reliability as "a characteristic of an item, expressed by the probability that the item will perform its required function under given conditions for a stated time interval" (Birolini, 2007). The required function of the floodwater harvesting system is to collect and store as much water as necessary to supply the drinking water demand of the city until the cisterns are refilled by a flood event. Given that the water demand of the city is not known, we somewhat arbitrarily assume that the minimum requirement for the system had been its ability to refill the cisterns at least once per rainy season (for the sake of simplicity we set the maximum capacity of 21,000 m^3 as the target volume (section 2.3). Human aspects and the performance of the built structures of the system are considered ideal (Birolini, 2007). Hence, it is assumed that every sufficient runoff event could have been harvested. Consequently, the reliability of the system in our study is a function of runoff occurrence and runoff volume. Gauging data of the wadis in the Resafa basin are lacking. A runoff time series to study the frequency and volumes of flood events had thus to be generated by applying a hydrological model as in several recent studies that estimated the water availability of ancient settlements in the Mediterranean and Middle East (van Wesemael et al., 1998; Whitehead et al., 2008; Crook, 2009; Berking et al., 2010; Harrower, 2010; Wade et al., 2012). The environmental conditions and the stated time interval under which the reliability is tested is the rainfall and runoff regime of the past 29 years (section 3.3). During this period severe droughts as well as exceptionally wet years are reported for the region (Trigo et al., 2010; Kaniewski et al., 2012) and should thereby capture the range of climate conditions that prevailed from the 6th to the 14th century AD (section 2.2) (cf. Bruins, 2012). The results of the investigated period are then qualitatively discussed on the basis of results from paleoclimatic studies and climate-related chronologies in the region. We favored this approach over the application of precipitation data from GCMs because of the large uncertainties inherent in these models, especially regarding local scale water availability analysis in the study region (Hemming et al., 2010). Moreover, the climate variability in the time frame under consideration is said to be rather small and often not adequately captured by GCMs (Gonzalez-Rouco et al., 2011, section 2.2).

The study consists of the following major methodological steps:

- Analyzing rainfall data to assess the rainfall regime in Resafa and the character of short-term rainfall intensities during rainy seasons with different characters.

- Applying a hydrological model to generate a runoff time series. The runoff data were analyzed concerning return periods of events relevant for floodwater harvesting and examining the annual and interannual temporal distribution of those events.

- Running a hydraulic model to assess the influence of the assumed hydraulic structures on the flow patterns of floods. Potential changes in terrain properties–for example owing to alluviation or erosion–were examined on the basis of results from a previous geomorphological study. The results of the hydraulic modeling have no influence on the results of the reliability study described above.

4.2.3.2 Archaeological excavations, geomorphological survey, and age determination

The initial aim of the geomorphological survey was to reconstruct the ancient landscape and land use around Resafa, and the excavations targeted the built structures presumably related to the water supply system of Resafa. The preliminary results from these studies served three purposes in this study: (i) to provide input variables to the hydrological model (ii) to assess terrain changes in the alluvium of the Wadi es-Sélé (iii) to assess the age of supposed hydraulic structures. The geomorphological survey was conducted between 2008 and 2009. Excavations were performed on behalf of the German Archaeological Institute under the direction of Prof. Dr. Dorothée Sack (TU Berlin). The methods applied in the geomorphological survey will be briefly summarized in the following paragraphs as the studies are largely unpublished.

A geomorphological map of the catchments in the vicinity of Resafa was created by surveying and by visual analysis of satellite images (Ikonos, Corona). Sediment cores were extracted from the floodplain of the Wadi es-Sélé at six locations using a hand-operated vibracorer (for locations see Fig. 7). The drillings had a depth of ~ 1.5 to 6 m, and the extracted sediments were described and sampled directly in the field. Additionally, two sediment profiles that were exposed in dolines were described and sampled. All sediments were physically and chemically analyzed in the geomorphological laboratory at the Department of Earth Sciences - Freie Universität Berlin. The analysis included the determination of sediments' total (TC mass-%) and organic carbon content (TOC mass-%) with a Woesthoff Carmhograph and the analysis of the sediments' grain size distribution applying laser diffractometry. The results of the laser diffractometry were statistically analyzed with the GRADISTAT program (Blott and Pye, 2001). Details on the methods can be found in Schütt et al. (2010) and Beckers et al. (2013). Topographic wadi cross profiles were measured at the outlet of the Wadi Gharawiy using a measuring tape and an inclinometer. In order to estimate the saturated hydraulic conductivity (Ksat), infiltration measurements using a minidisk infiltrometer were made on representative terrain units as mapped in the field. Details of the method are described in Berking et al. (2010).

Age determination had to rely on radiocarbon dating only, because we were not allowed to export sealed samples (a prerequisite for Optical Stimulated Luminescence dating) and because the investigated profiles and sediment cores lacked datable artifacts. Charcoal fragments were extracted from profiles, sediment cores, and the charcoal-rich mortar of selected built structures. The samples were sent to the Poznań Radiocarbon Laboratory in Poland, which uses accelerator mass spectrometry. All radiocarbon ages were calibrated using the OxCal v.4.1 software (Bronk Ramsey, 2009) and the IntCal04 calibration curve (Reimer et al., 2009).

4.2.3.3 Meteorological data and analysis

Data

We used data of meteorological stations which report to the World Meteorological Organization Global Telecommunication System (GTS) and secondary datasets which are based on or make use of these data. Only few GTS stations cover the Syrian desert steppe and adjacent areas. Three meteorological stations are located in a similar climate zone as Resafa´s (Fig. 1). Of these, Deir ez Zor and Palmyra have contributed to the GTS network on a monthly basis since 1946, and Raqqa has participated with large gaps since 1956. Daily data from these stations are fragmentary. Palmyra is the station with the longest periods of continuous daily records (Jan. 1983 - Apr. 1999). Thus we applied daily satellite precipitation estimates which are frequently used for hydrological modeling in data-sparse regions (Stisen and Sandholt, 2010 and references cited). In this study daily precipitation estimates were obtained from the daily gridded RFE (NOAA-CPC Rainfall Estimator) - ARC 2 (African Rainfall Climatology Version 2) rainfall estimates which also cover Syria and have a spatial resolution of 0.1° × 0.1° (Love et al., 2004; Novella and Thiaw, 2012). We analyzed the spatial average of the two cells which cover Resafa and the catchment of the Wadi Gharawiy. The dataset is generated by merging gauge measurements and satellite infrared measurements using the RFE2 algorithm (Xie and Arkin, 1996). It was chosen because it has the longest continuous record and the highest spatial resolution of comparable datasets. It covers the period from 1983 to present (we analyzed the January 1989 – December 2011 period) and performs especially well in homogenous, relatively flat areas such as the Resafa basin (Novella and Thiaw, 2010). Satellite precipitation estimates need validation as they are not direct measurements of precipitation (Stisen and Sandholt, 2010). We used the GPCC (Global Precipitation Climatology Centre) dataset version 5 for gridded (0.5°) monthly time series and the daily records of the Palmyra station as reference datasets. The GPCC dataset is generated by spatially interpolating meteorological station data (Rudolf et al., 2010). The performance of the ARC 2 rainfall estimates is assessed by two methods: (i) temporally (monthly sums) and spatially (area averages) matched data are compared with the GPCC data by applying standard validation techniques, i.e. mean error (ME), root-mean-square error (RMS), linear correlation coefficient (CC) and coefficient of variation (R^2) as done by Dinku et al. (2010); (ii) in order to evaluate the reliability of the ARC 2 daily precipitation estimates, i.e. number of rainy days and daily rainfall intensities, the data of the ARC 2 cell covering Palmyra are compared with the statistical characters of daily precipitation records of the Palmyra station as it provides the longest continuous record of daily precipitation. Direct comparison of gauge measurements with spatial averages as delivered by the satellite estimates can be problematic (e.g. Cherubini et al., 2002; Wang and Wolff, 2010). However, as stated by Cohen Liechti et al. (2012), the comparison can indicate whether the satellite estimates are reasonable. All datasets were downloaded via the IRI/LDEO Climate Data Library (http://iridl.ldeo.columbia.edu/). Many studies show a recent shift in rainfall regimes of regions across the Mediterranean basin and the Middle East and attribute this to the recent global warming. We applied a Mann-Kendall test to detect trends in seasonal amounts and mean daily intensities to assess whether the rainfall regime in Resafa has changed significantly during the past 29 years.

Analysis

Paleoclimate studies and chronicles often give information on medium- or long-term climatic conditions (Morony, 2000; Luterbacher et al., 2006). However, short-term rainfall intensities, the most important factor for runoff generation in drylands (Wainwright and Bracken, 2011), do not necessarily vary uniformly with medium- or long-term variations of precipitation amounts (Alpert, 2002). We therefore analyzed the relationship of daily

rainfall intensities according to their character in normal, wet, and dry rainy seasons. The rainy season, i.e. the hydrological year, was considered to last from October to May as defined by Trigo et al. (2010). The rainy seasons were classified according to the standardized precipitation index (SPI) of the eight-month SPI of May (see McKee et al., 1995, for a general introduction to the SPI). The SPI was calculated with the SPEI package v. 1.2. in R using the default settings (Vicente-Serrano et al., 2010) and classified according to McKee et al. (1995). Daily rainfall intensities were categorized in accordance with Gallego et al. (2005) to discuss their character in the respective rainy season. The 90% percentile was taken as the light/moderate - heavy boundary and the 95% percentile as the heavy - torrential boundary. The light/moderate – heavy boundary in this study is approximately the daily rainfall threshold for runoff to be generated, and the heavy – torrential boundary is the one where modeled runoff volumes exceed the critical volume of 10,000 m^3 (section 3.4.2). Additionally, the mean daily intensity of each rainy season was calculated to assess the relationship between rainy season totals and mean daily intensities by linear correlation analysis. A rainy day is here defined as a day with > 0.1 mm precipitation, a threshold commonly applied in rainfall analysis (Vicente-Serrano and Beguería-Portugués, 2003).

4.2.3.4 Hydrological modeling

Model and Data

A comprehensive introduction to hydrological modeling in drylands can be found in Wheater (2007) and to dryland hydrology in general in Wainwright and Bracken (2011). Lumped hydrological modeling was applied to generate a rainfall-runoff time series of the major catchment of the floodwater harvesting system (Fig. 6, section 2.3) and to compute hydrographs as an input variable to a hydraulic model. We applied the Hydrologic Engineering Center - Hydrological Modeling System (HEC HMS) (HEC, 2000) using the empirical Soil Conservation Service (SCS) runoff Curve Number (CN) as the loss method and to calculate the time of concentration. The SCS unit hydrograph was chosen as the transfer function to transform excess precipitation into direct runoff (SCS, 1964). We did not account for evapotranspiration losses as did Berking et al. (2010). In the absence of gauging data no calibration was conducted. The CN method produces reasonable results in small to medium-sized dryland catchments with ephemeral drainage and little information on the drainage basin physical characteristics (van Wesemael et al., 1998; Foody et al., 2004; Hammouri and El-Naqa, 2007; Rozalis et al., 2010; El-Hames, 2012). A critical review of the method can be found in Ponce and Hawkins (1996). A digital elevation model (DEM) obtained from the Shuttle Radar Topography Mission (SRTM) with a resolution of 90 m was used to delineate the (sub-) catchment(s) and to derive the drainage network and secondary topographic attributes (see below). In order to assign Curve Numbers to the respective sub-catchments, the terrain was first separated into three land units that reflect the caternary variation in sediment/vegetation cover, soil type and saturated hydraulic conductivity (section 2.1). The Topographic Position Index (TPI) was applied for separation of the terrain units. The TPI was calculated using the Land Facet Corridor Tools, an add-on in ArcMap 10 (Jenness et al., 2011). The TPI was subsequently classified by using an unsupervised Iso cluster algorithm as provided in the Spatial Analyst of ArcMap 10. The three terrain units were labeled: hilltops and backslopes, middle and footslopes, and alluvium (Fig. 6). The hydrological soil group was assigned to each terrain unit according to the average Ksat values found on each terrain unit and the approximated depth of the sediment cover as mapped in the field. The hydrolo-

gical soil group and Curve Numbers were selected using common look-up tables (table 1). Finally, the Curve Number was spatially averaged over the respective sub-catchment. Following Rozalis et al. (2010), the antecedent moisture conditions (AMC) were set at AMC2. The spatial average of the initial abstraction is about 7 mm (table 1) and matches with values of other studies in semi-arid and arid catchments with similar physical

Table 1. Hydraulic properties of the terrain units and the modeled catchment.

Terrain unit	ksat[1] (mm/h±1σ)	n[2]	Dominant texture	Depth to impermeable layer[3]	Hydrol. Condition[3]	Hydrol. soil group[3]	CN[4]	S (mm)[5]	Ia (mm)[6]
Hilltops and backslopes	5 ± 2	6	silt/bedrock	< 50 cm	poor	D	93	20	4
Middle- and footslopes	21 ± 6	6	sandy silt	< 100 cm	poor	C	87	44	8
Alluvium	47 ± 9	12	silty sand	> 100 cm	fair	B	72	100	20
Modeled catchment	NA	NA	NA	NA	NA	NA	88	35	7

[1] saturated hydraulic conductivity

[2] number of (minidisk) infiltration measurements

[3] Criteria according to U.S. Department of Agriculture (2007)

[4] Curve Number for arid and semiarid rangelands (U.S. Dep. of Agriculture, 2007)

[5] Potential maximum retention, S = 25.4*(1000/CN - 10)

[6] Initial abstraction, Ia = 0.2*S

characteristics (van Wesemael et al., 1998; Ben-Zvi and Shentsis, 2000; Shanan, 2000; Berking et al., 2010).

The model was run on an event basis driven by the ARC 2 daily rainfall estimates. However, assuming constant daily rainfall intensities is unrealistic and could lead to a underestimation of peak discharge values (Awadallah and Younan, 2012), especially in arid and semi-arid climates where rainfall events tend to be short and intense (Nicholson, 2011). Lacking short duration (sub-daily) rainfall data for the study site, we applied the ratio of the SCS storm type II to convert daily precipitation to design storms. The SCS design storm method (HEC, 2000) is implemented in HEC HMS, and its type II is recommended for the arid and semi-arid environments of the U.S. but is also suitable for drylands

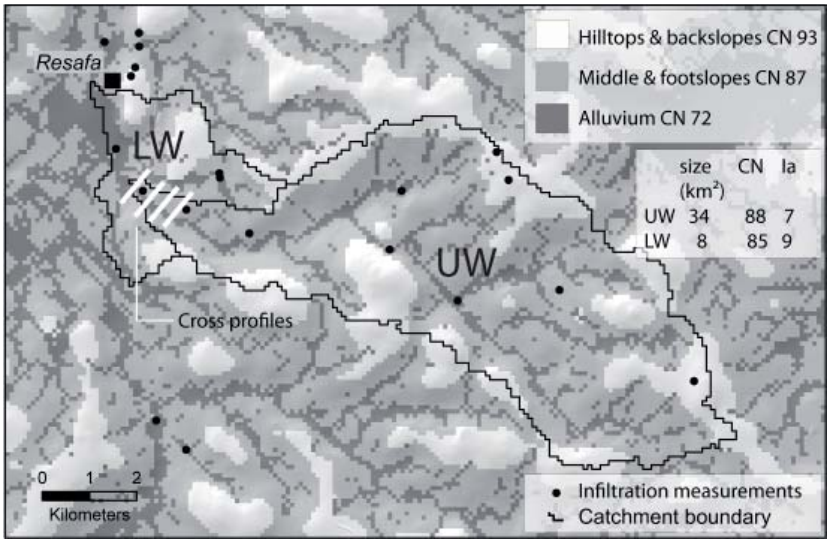

Fig. 6 The main catchment of the floodwater harvesting system consists of the upper watershed (UW) and the lower watershed (LW). The UW is that of the Wadi Gharawiy. The catchments are delineated and topographically classified based on the SRTM digital elevation model. Curve Numbers were assigned based on field survey (infiltration measurements). For cross profiles see Fig. 9. UW: upper watershed, LW: lower watershed, CN: curve number, Ia: initial abstraction.

worldwide (Awadallah and Younan, 2012). To estimate the hydrograph at the outlet of the Wadi Gharawiy, the catchment was split into two sub-catchments (Fig. 6).

As the Wadi Gharawiy is ungauged, the results were validated by comparing them with results from other studies on runoff yields in semi-arid and arid catchments (c.f. Wagener et al., 2004). In order to validate computed peak discharge values, we additionally compared those with high-water marks found at four successive cross-sections at the outlet of the Wadi Gharawiy applying the hydraulic model HEC RAS (HEC River Analysis System, HEC, 2010). This validation method is often used in poorly gauged and ungauged catchments (Greenbaum, 2007; Morin et al., 2009; Koutroulis and Tsanis, 2010). Details on the method and its problems can be found in Jarret and England (2002) and HEC (2010). The high-water marks were relatively fresh and consisted of plant debris and sheep excrements deposited along the lowest wadi terrace. The material was deposited between two consecutive field campaigns conducted in September 2008 and April 2009. The highest rainfall event recorded (in the ARC 2 dataset) between these field campaigns was about 15 mm per day on 29 Oct. 2008, and it is assumed that the associated runoff event caused the deposition. The modeled peak discharge corresponding to this rainfall event was taken as the input in HEC RAS with a Manning roughness coefficient of 2.5 as estimated in the field. Subsequently the computed water levels were compared to the water levels as indicated by the high-water marks. In addition, the cross-sectional extent of the maximum predicted discharge value was modeled in order to test whether the channel would accommodate the flood or overtop the banks.

Analysis

Garbrecht (1996) emphasizes that the water level needs to rise before it is able to flow into the canal supplying Resafa with water (section 2.3). The minimum volume of runoff necessary for effective harvesting is estimated to be about 10,000 m^3. This is approximately the amount necessary to raise the water table immediately upstream of the dam up to 50 cm (section 2.3). In the following we refer to the runoff events exceeding this threshold as “effective runoff”. Thus a runoff event which would fill the cisterns to their full capacity would have to have at least a volume of about 30,000 m^2 (~ 20,000 m^3 cistern capacity + ~ 10,000 m^3 necessary minimum volume of runoff).

The modeled runoff time series was analyzed regarding the probability of occurrence (expressed by the annual recurrence interval) of effective runoff in a rainy season by conducting a frequency analysis of rainy season runoff volume maxima. The timing of occurrence of effective runoff events during the hydrological year and the length of periods between the occurrences was analyzed using simple descriptive statistics.

4.2.3.5 2D - Hydraulic modeling

Model and Data

Incision and aggregation are regular and alternating processes which occur in ephemeral streams and especially in wadis with low gradients and a wide floodplain such as the Wasi es-Sélé. In consequence, flow patterns on these plains may constantly change. When floods emerge on the plains usually transmission losses increase (Tooth, 2000). Hence the flow length affects the amount of water which can be harvested downstream. Hydraulic modeling is a commonly applied tool to simulate flow pattern and floodplain inundation and to estimate the effect of hydraulic structures on flood behavior (Bates et al., 2010). Here we applied the 2D raster based hydraulic model Lisflood – FP (Bates et al., 2010). A 2D raster based model was favored over a one-dimensional model because

a distinct channel in the Wadi es-Sélé is lacking, and the aim was to simulate the flow paths across the floodplain (Kandasamy and Hannan, 2008). We applied the Lisflood model as implemented in the CAESAR-Lisflood landscape model v.1.2x (e.g. Coulthard et al., 2007). CAESAR-Lisflood was chosen because it has an easy to use graphical user interface and is open source. The source code can be downloaded from http://code.google.com/p/caesar-lisflood/. The main purpose of CAESAR is to model landscape evolution, but it is also capable of modeling flood events via the Lisflood module. We ran the model in reach and flow only mode and a Mannings roughness parameter of 3 as determined in the field. The terrain information was obtained by digitizing the contour lines of a 1:5000 topographic map (contour interval 1 m) which is based on aerial photos from 1961 and from land survey results. Processing and survey were conducted by the Faculty of Geomatics, University of Applied Sciences Karlsruhe; the data were kindly provided by Prof. Dr. Günter Hell. A raster DEM with a horizontal resolution of 10 m was generated by using the Topo-to-Raster algorithm according to Hutchinson (1989) and omitting heights of modern built structures such as the north-south running road embankment next to Resafa. The DEM therefore approximately represents the terrain as it was in the early 1960s before larger earthworks for irrigation and road construction were made. The presumed embankments were integrated in the DGM by raising the height of the DEM pixels which are approximately located on the presumed structures by 1.5 m (this value is somewhat arbitrary; however, it is the height of the embankment excavated at RC3, see Fig. 7 b). Possible changes in terrain properties since the Roman/Early Islamic period were assessed on the basis of the results from the geomorphological survey (section 3.2). For each scenario, the model was driven by the output hydrograph of the hydrological model calculated at the outlet of the Wadi Ghurabi (section 3.4). The runoff event used for both scenarios was an event which can be expected about every rainy season (peak discharge ~ 1.5 m^3*s-1, see Fig. 12).

Analysis

We modeled the flow pattern of floods in two scenarios: (1) under present conditions and those structures which are archaeologically attested (2) including a system of embankments that reached from the outlet of the Wadi Gharawiy to the dam (section 1). A prerequisite for a quantitative assessment of the difference in runoff yield at the dam would be the modeling of transmission losses for each scenario. However, reliable estimation of transmission losses is challenging and data-intensive (Wheater and Al Weshah, 2002). As we lack adequate data, we did not account for transmission losses in the hydraulic model. The results from the two scenarios were thus only qualitatively assessed under consideration of the aforementioned factors, i.e. flow patterns and whether buildings would have been affected by the floods.

4.2.4. Results and Discussion

4.2.4.1 Sedimentology, excavations, and radiocarbon dates

At excavation site Res12 a rectangular structure almost completely buried by sediments and a most recently built levee were excavated. The structure is 20 m long, 4 m wide, and 3.5 m high (for location and picture see Fig. 7 a/b/c). The walls are made of large hewn gypsum blocks. On top of the flat structure, a 50 cm high wall is attached, and to the south and north of the platform up to 1 m high walls of gypsum blocks are connected. The structure is aligned parallel to the main flow direction. The dimensions and construction of the structure make it unlikely that its purpose was solely for channeling water as ini-

tially suggested. It may also have been a cistern, and its upper western side and the wall extension could have served to channel the flood water towards the dam. Assuming it is a cistern, an intentional burying of the structure, as opposed to alluviation, would facilitate a filling without the necessity of lifting water (see also discussion below). A charcoal fragment taken from the thick mortar bed of the lowermost stone row has an age of 710 ± 60 cal AD (Res 12_2). Northwards, a trench was dug at the inlet of an earthen water basin (Fig. 5/7). At a depth of 30 cm, a bell-shaped mortar layer interbedded with thick layers of charcoal was excavated. The charcoal was dated to 710 ± 60 cal AD (RC2). A few meters north, the base of the western garden wall was excavated (Fig. 3/5/7). It consists of unhewn gypsum ashlar built on a thick mortar bed which was found a few centime-

Table 2 Summary of the radiocarbon ages.

Sample ID	Depth (cm)	Sample Context	Lab. ID	Radiocarbon Date (year BP ± 1σ)	$\delta^{13}C$ values*	Calibrated Ages (2σ - range)	Calibrated Median Ages
Res01_1	80	Alluvium	Poz-31152	2705 ± 35	-26.2	915 - 804 calBC	857 calBC
Res01_2	100	Alluvium	Poz-31151	1895 ± 30	-23.8	33 - 215 calAD	107 calAD
Res02_1	50	Garbage dump	Poz-31154	1265 ± 35	-24.6	665 - 866 calAD	737 calAD
Res02_2	90	Garbage dump	Poz-31155	1295 ± 30	-19.5	662 - 774 calAD	713 calAD
Res02_3	140	Garbage dump	Poz-31157	1270 ± 30	-24.9	664 - 855 calAD	730 calAD
Res03_1	40	Alluvium	Poz-33977	1730 ± 50	-30.5	140 - 420 calAD	308 calAD
Res03_2	120	Alluvium	Poz-33888	1375 ± 35	-19	600 - 763 calAD	654 calAD
Res05_1	340	Pool	Poz-31158	1410 ± 30	-22.7	590 - 666 calAD	634 calAD
Res05_2	390	Pool	Poz-31159	35000 ± 1000	-29.4	40132 - 35915 calBC	38128 calBC
Res08	60	Basin fill	Poz-31162	1250 ± 30	-18.3	676 - 870 calAD	745 calAD
Res10_1	140	Alluvium	Poz-31164	225 ± 30	-9.7	1640 - 1955 calAD	1764 calAD
Res10_2	150	Alluvium	Poz-31165	480 ± 30	-25.3	1407 - 1453 calAD	1431 calAD
Res10_3	160	Alluvium	Poz-31166	260 ± 30	-23.6	1520 - 1954 calAD	1647 calAD
Res_12_1	80	Alluvium	Poz-33862	35500 ±900	-29	40194 - 36833 calBC	38615 calBC
Res_12_2	150	Alluvium	Poz-33887	2405 ± 35	-13.8	747 - 396 calBC	485 calBC
Res_12_2	300	Mortar	Poz-32964	1320 ± 30	-22.4	652 - 771 calAD	688 calAD
RC1	0	Mortar	MAMS-11011	1313 ± 22	-26	656 - 770 calAD	687 calAD
RC2	40	Ash pit	MAMS-11009	1312 ±22	-12.1	657 - 770 calAD	688 calAD
RC3	20	Mortar	MAMS-11012	1316 ± 23	-4.9	655 - 770 calAD	685 calAD

Poz: Poznan Radiocabon Laboratory

MAMS: CEZ Archäometrie GmbH

All ages were calibrated using OxCal 4.2 (Bronk and Ramsey, 2009) and the IntCal04 calibration curve (Reimer et al., 2009)

* see section 3.2 for important note on the δ13C-values

ters under the present surface. The wall is reinforced with buttresses. The probable upper rows of the wall are now missing. An earthen embankment with a height of about 1.50 m is connected to the north of the garden wall. The surface of the embankment was coated with mortar, and a charcoal sample taken from the mortar was dated to 710 ± 60 cal AD (RC3). The excavated structures are all aligned in approximately south-north direction and connect to an imaginary line from the outlet of the Wadi Gharawiy toward the southeastern edge of the city wall. The radiocarbon dates fall within the period where contemporary sources attest a maintenance and development of the water supply of Resafa under Hišām ibn ʿAbd al-Malik and the building of the largest cistern in Resafa (Musil, 1928; Westphalen and Knötzele, 2004). The construction of the system would therefore fall within the construction period of various elaborate hydraulic structures in

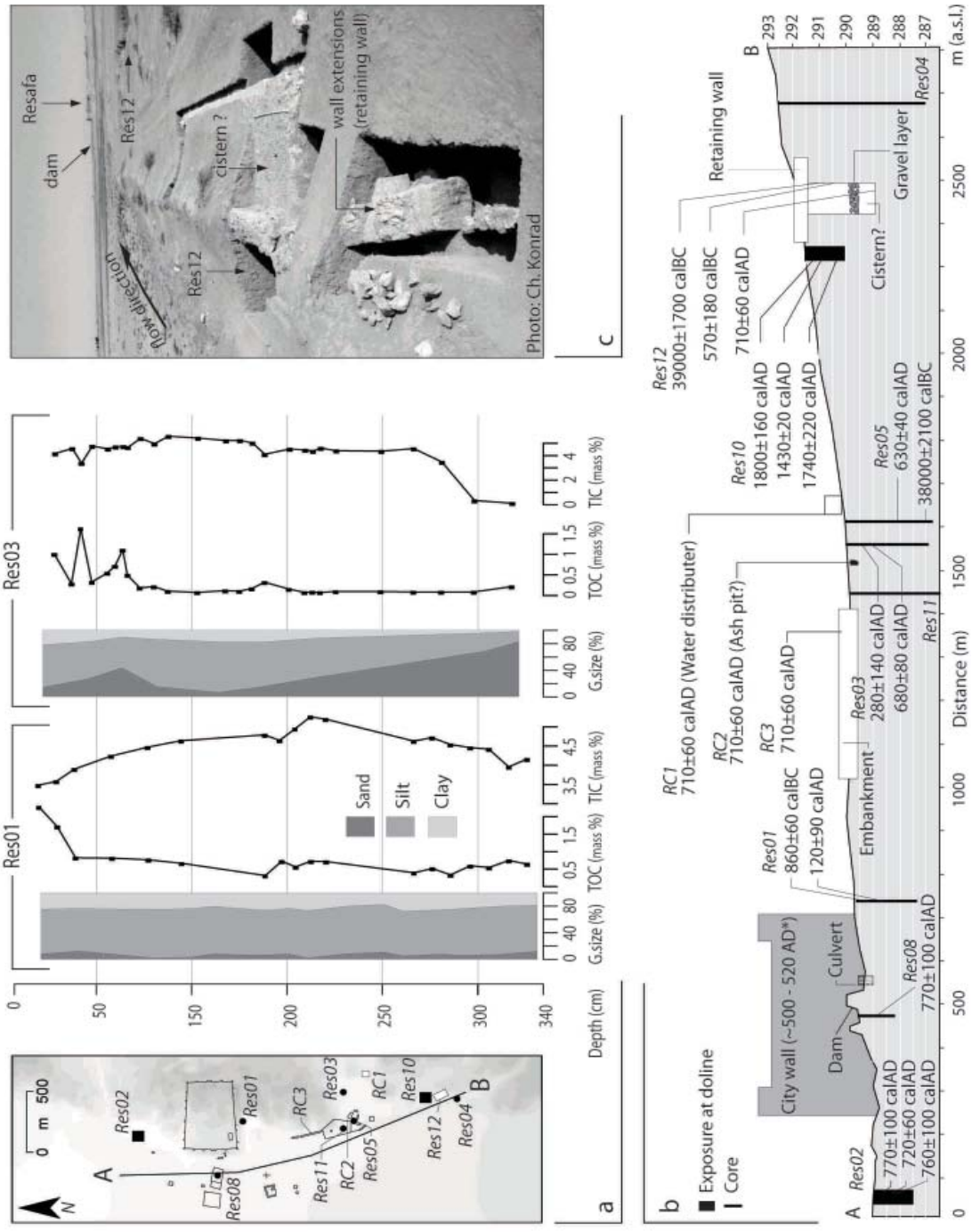

Fig. 7 a: Overview of the Resafa site showing the locations of exposures and drillings and the results of grain size analysis and carbon contents of drillings Res01 and Res03, 7 b: Longitudinal profile of the floodplain of the Wadi es Sélé stretching from the outlet of the Wadi Gharawiy to north of the dam (A – B, fig 7 a) based on the detailed DEM (see section 3.5). Note that the vertical exaggeration is >1:100. For visualization the buildings are not vertical exaggerated.7 c: Photo of the excavated structure at Res 12 looking north.

the Ummayad period in the region such as in Qasr al Hayr ash-Sharqi (Fig. 2) and Qasr al Hayr ash – Gharbi, including the massive Harbaqa dam (Genequand, 2006, 2009).

The location of the cores and exposures, contents of total organic carbon (TOC mass-%) and total inorganic carbon (TIC mass-%), and the grain size distribution of cores Res01 and Res03 are documented in Fig. 7 a/b. All of the samples from the cores and the exposures at dolines show similar low TOC and TIC values with little variations below the

common topsoil TOC peak (Fig. 7 a). These values are typical for gypsiferous soils in arid environments (Schütt, 1998a, 1998b, 2000; Dixon, 2009) and show that the dominant sediment sources are the weathering residues of the gypsum bedrock. The texture of the samples is predominantly poorly sorted sandy mud, indicating a fluvial or colluvial depositional environment. Moreover, the lack of the coarse grain size fraction in almost all the extracted sediments (even in those which are located in the thalweg of the Wadi es-Sélé, Res01/Res05) indicates that the floods running down the wadi were predominantly sheet floods with a limited transport capacity. It also has to be considered that coarser gypsum pebbles deposited in the channel bed decay quickly in the temporarily water-saturated environment of the channel infills. The gradual increase of the sand fraction content in core Res03 (Fig. 7 a) reflects the increasing influence of the gravelly-sandy in-situ gypsum saprolith. This pattern was also observed in core Res05 at a depth of about 3.50 m. Drilling Res04 was drawn from the fan of the Wadi Gharawiy and resembles the typical alternation between finer and coarser alluvial fan deposits of an ephemeral stream (Harvey, 2011). The alluvial infill of the Wadi es-Sélé is thus about 3 – 5 m thick at its eastern margin. The most remarkable sediment profile was exposed in a trench which was dug to excavate the massive rectangular structure (see above and Fig. 7 a/b/c). At a depth of 2.5 m, a 30 cm thick and ungraded gravel layer embedded in sandy mud was found next to the structure in the western trench (Fig. 7 b). In the eastern trench this gravel layer does not occur. The layer is most likely the continuation of the fan of Wadi Gharawiy or was deposited following an extreme flood event. Additional layers indicating high-energy fluvial transport are absent in the profile. The radiocarbon data of the charcoal taken from the exposure give little indication of the deposition chronology because of stratigraphic age inversion. Both radiocarbon dates are older than the age of the charcoal fragment extracted from the mortar of the structure. We assume the following scenario: Shortly after the excavation of a trench and the building of the structure, a high flood event deposited the gravel layer. Subsequently the trench was either backfilled by the constructers or refilled by sedimentation.

The radiocarbon ages of the exposures and cores range between 860 ± 60 calBC and 1800 ± 160 calAD, with the exception of two samples which date to roughly 40,000 calBC (table 2). Almost all of the few charcoal remnants in the exposures were found in the upper 1.5 m of the sediment profiles. In general the results yield stratigraphically inconsistent ages, a pattern typical for detrital charcoal derived from alluvial and colluvial sediments (Lang and Hönscheidt, 1999). The results document a highly dynamic environment along the floodplain of the Wadi es-Sélé. The ages of the charcoal fragments found at the exposures in the dolines indicate that they are relatively recent features (Res02, Res10) and may post-date the ancient occupation of the site. A relationship between surface runoff and doline development is likely as the dolines in the Wadi es-Sélé predominantly occur in areas with high flow accumulation, where ponding occurs and where water was artificially concentrated (e.g. the doline in the continuation of the spillway) (c.f. De Waele et al., 2009).

Palaeochannels or “stable” palaeosurfaces could not be deduced from our data. Given that almost all the archaeological finds (with the exception of the structure at Res12) are either located on the present surface or within the upper few decimeters of the alluvial fill, we assume that the current surface approximately resembles that of the past 1500 years within a dynamic range of about ± 1.50 m. The application of the detailed DEM which is based on recent elevation data (section 3.5) for the estimation of ancient flow patterns seems therefore justifiable.

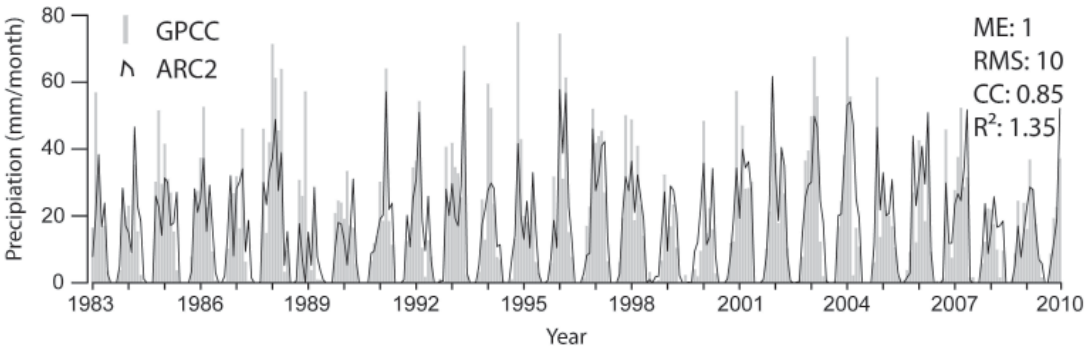

Fig. 8 Monthly time series of the GPCC and the Arc2 dataset with results from the error statistics.

4.2.4.2 Rainfall and runoff

Validation of satellite estimates and the hydrological model

The GPCC and the temporally and spatially averaged ARC 2 datasets are highly correlated (correlation coefficient 0.85, $\alpha < 0.05$, Fig. 7). The other error statistics indicate that the ARC 2 dataset performs reasonably well (Fig. 8) (cf. Dinku et al., 2010). Moreover, the ARC 2 precipitation estimates are in accordance with other rainfall studies conducted in the region (Wirth, 1971; Dennett et al., 1984). However, the ARC 2 estimates tend to estimate lower precipitation amounts compared to the GPCC for most of the years. This differences might arise from the sparse distribution of GPCC stations in the climatic region of Resafa. As emphasized by Hemming et al. (2010), this problem might lead to a bias towards unrepresentative GPCC stations located in the wetter and more densely gauged parts of western Syria. The statistical properties of the ARC 2 generated daily rainfall

Table 3 Comparison of the Arc2 dataset with the Palmyra station data.

	Rainy days*	Mean rainfall (mm/d)[§]	50% *Q* (mm/d)	75% *Q* (mm/d)	90% *Q* (mm/d)	95 % *Q* (mm/d)	Max (mm/d)
Arc2_Res[&]	977	3	2	3	6	9	60
Arc2_Palm[£]	771	3	2	4	7	11	58
Palmyra	706	3	1	4	7	13	35[$] / 69[#]

Q refers to the % quantile.

[&] spatial average of the two cells covering the modeled catchment (38.8°E - 39.0°E | 35.6°N - 35.7°N)

* number of rainy days (> 0.1 mm) in the period 01.01.1983 to 04.30.1999

[§] Mean rainfall on rainy days (> 0.1 mm)

[$] max rainfall recorded in the period 01.01.1983 to 04.30.1999

[#] max rainfall recorded in the period 01.01.1965 to 04.30.1999

estimates that cover the Palmyra station are in good agreement with the rainfall data measured at Palmyra weather station (table 3). The differences most likely arise from the different spatial scales of the two datasets (cf. Stisen and Sandholt, 2010).

According to the Mann – Kendall test, no significant trends in seasonal precipitation amounts (trend = +0.18, p-value = 0.17) and mean seasonal rainfall intensities (trend = (-0.04), p-value = 0.77) could be detected. This is in contrast to various studies which observed an increase in rainfall intensities and decrease of annual rainfall amounts in the Middle East and worldwide during the past few decades (Alpert, 2002 and referen-

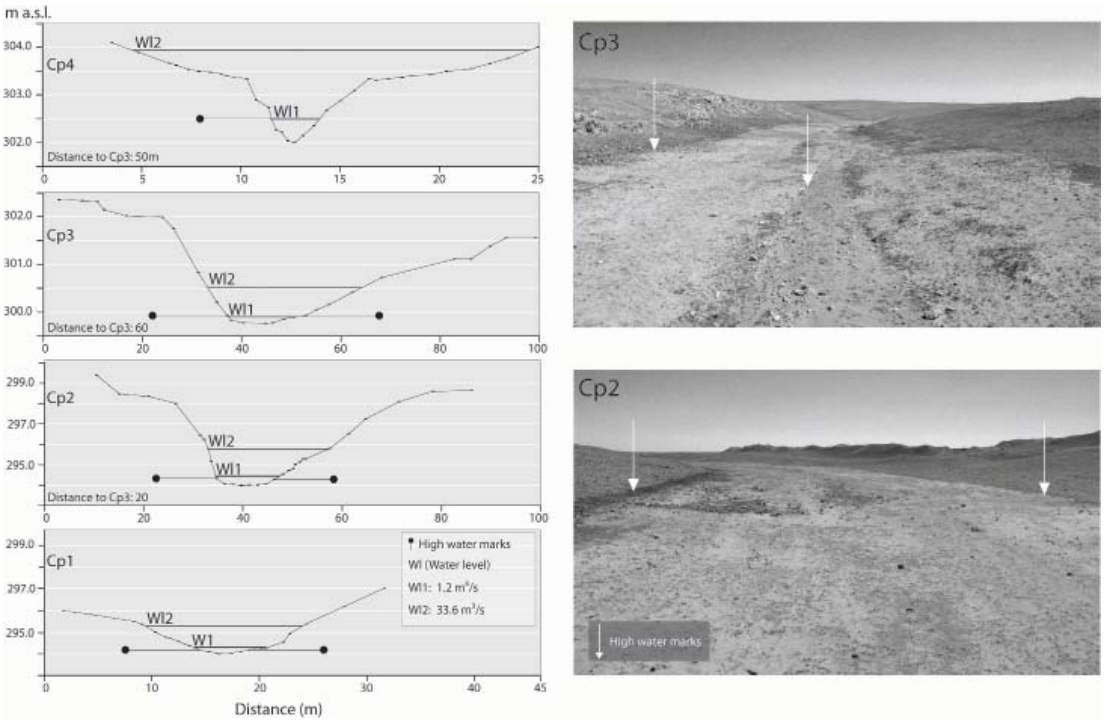

Fig. 9 Left side: Superelevated cross profiles of Wadi Gharawiy with modeled water levels and high water marks. For locations see Fig. 6. Right side: Sample photos of the Wadi Gharawiy looking upstream. Arrows indicate the high water marks.

ces cited). A probable bias of the rainfall data due to present climate change is, however, assumed negligible.

The hydrological model estimated a maximum discharge of 37 m^3*s-1 and maximum volume of 1800,000 m^3. These values approximately matches with maximum recorded discharge values reported from studies in comparable environmental settings and catchment sizes (Meirovich et al., 1998; Al-Qurashi et al., 2008; Morin et al., 2009). The water levels in the channel modeled by HEC RAS are in good agreement with the ones indicated by the high water marks on all the four cross-sections (differences of ~ ± 5 - 10 cm, Fig. 9). The channel would accommodate the maximum predicted flood. That agrees with our

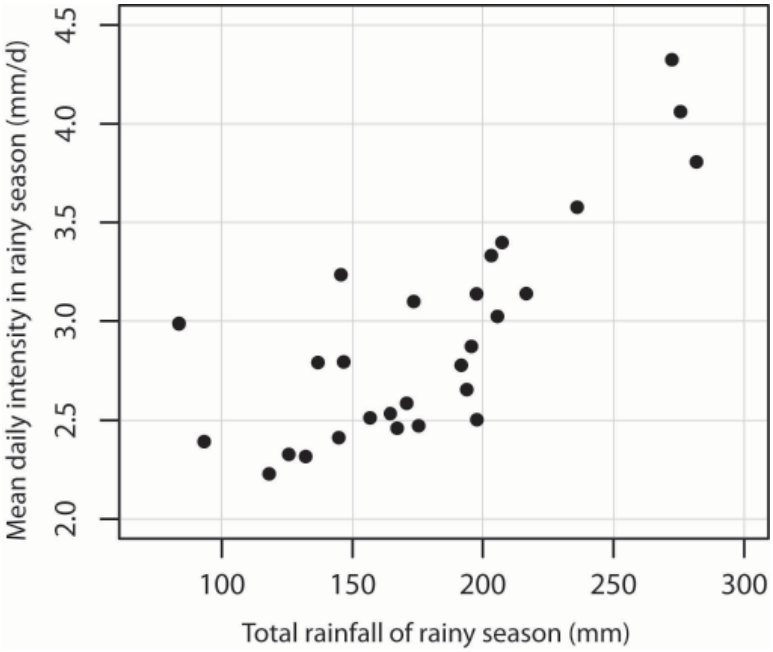

Fig. 10 Scatter plot of the rainy season total precipitation (mm) and mean daily rainfall intensity during rainy season (mm*d-1) (data base: ARC 2 rainfall estimates).

observations in the field where we found no indications of channel overtopping such as bars or slackwater deposits in higher locations than mentioned. The results of the hydrological model are therefore considered reliable.

4.2.4.2 Rainfall regime and water availability

The results of the rainfall and runoff analysis are summarized in Fig. 10, 11 and table 4. The rainy season totals (RST), and the mean daily intensities (MDI) have a significant correlation of 0.8 at a significance level of 0.01 (Fig. 10).

This agrees with the overall positive correlation between RST and MDI reported for many dryland regions in the Mediterranean and the Middle East (Easterling et al., 2000 and references cited). This relationship is also reflected by the contribution of the respective rainfall categories to the RST. In normal to wet years the contribution of the moderate to heavy, runoff-generating rainfall events to the RST tends to be higher than in dryer years. In only one severely dry year the daily rainfall intensities did not exceed the light rain category (1989/90). In all of the other wet seasons at least one heavy rainfall event occurred, even in the extremely dry rainy season of 1988/89.

Obviously owing to the event-based and deterministic hydrological modeling approach, this relationship is directly reflected by the numbers and volumes of runoff events per

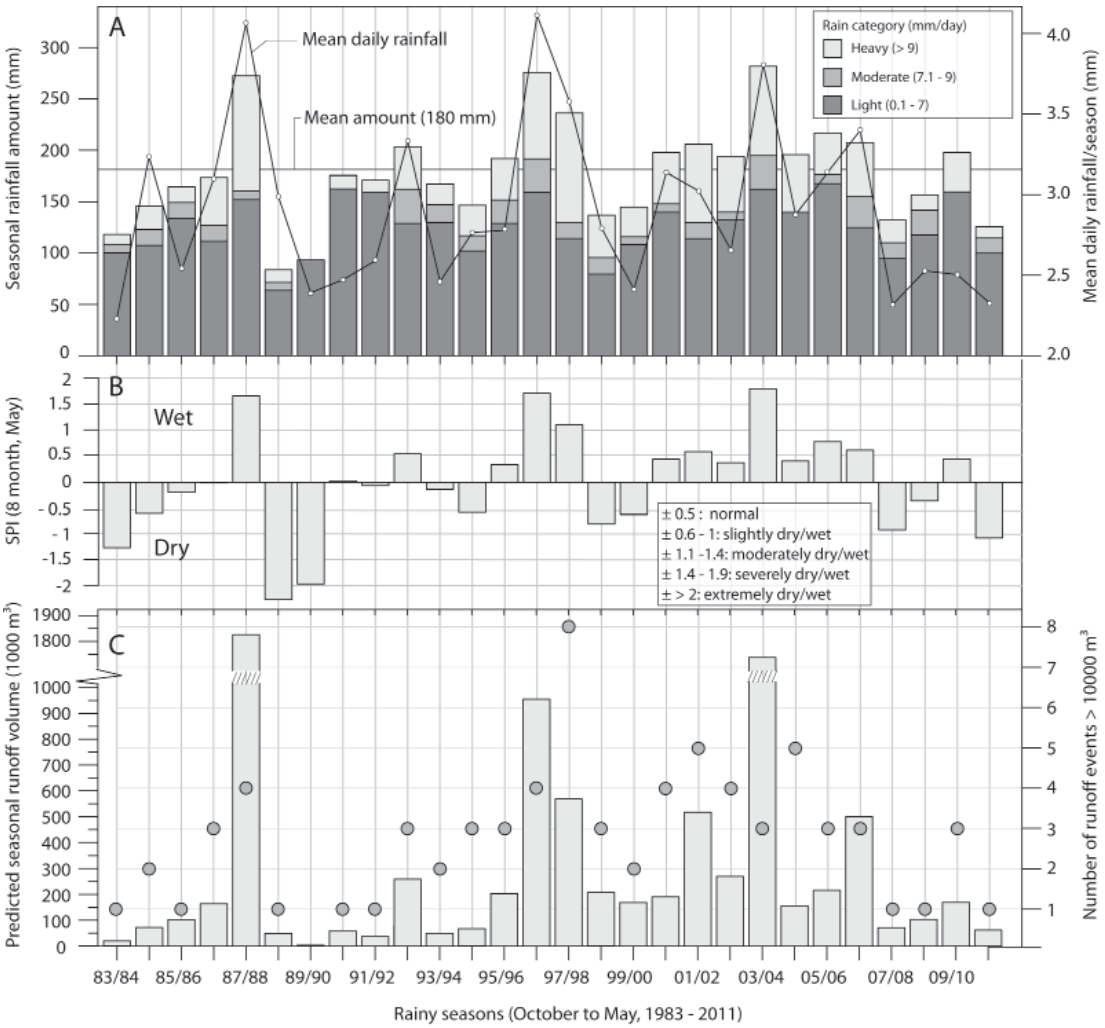

Fig. 11 Results of the rainfall and runoff analysis. A. Seasonal rainfall amounts with volumetric contribution of rainfall category and mean daily rainfall. B. Standardized precipitation index (SPI) of the rainy seasons. C: Seasonal runoff totals and number of efficient runoff events.

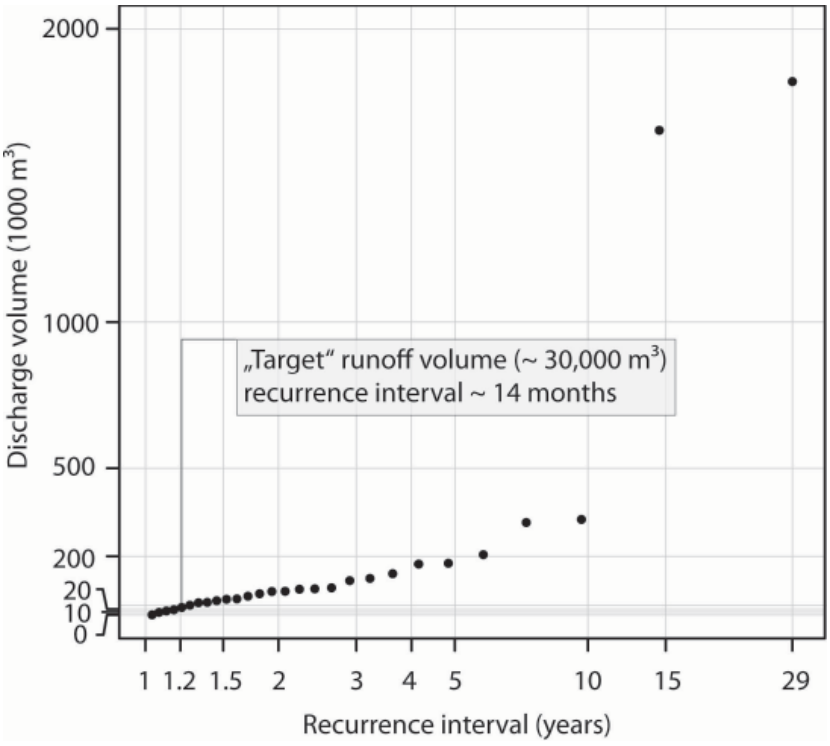

Fig. 12 Empirical flood frequency curve of maxima runoff event in the hydrological year (Oct - May). "Target" volume refers to the runoff volume necessary to fill the cisterns in Resafa to their full capacity (section 2.3).

rainy season predicted by the hydrological model (Fig. 11). In normal to severely wet rainy seasons, the total volume of runoff would far exceed the water storage capacities of Resafa, and on average four effective runoff events were predicted to occur during one rainy season. In slightly - moderately dry rainy seasons the cisterns of Resafa would have been filled to their total capacity at least once (rainy seasons 1983/84 and 2010/11). In the single recorded severely dry rainy season of 1989/90, no effective runoff was modeled. In the extremely dry rainy season of 1988/89 the cisterns could have been filled by one intensive storm and subsequent runoff event. Accordingly, the probability that the cisterns could have been filled once to their full capacity during a rainy season is 96%, and the risk of failure is 4%.

The recurrence interval of runoff events that fill the cisterns is roughly 14 months (Fig. 12). However, the temporal distribution of efficient runoff events during a rainy season is highly variable and depends on the character of the rainy season (wet - dry); a no runoff event was modeled during the dry season (June - August) in either of the modeled years.

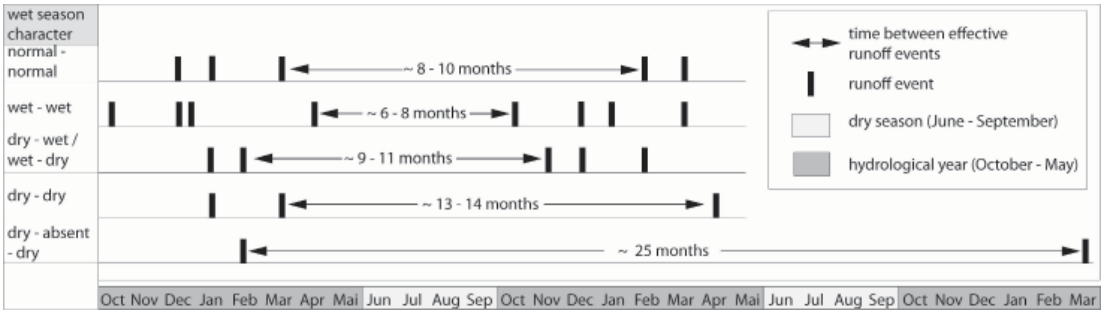

Fig. 13 Typical maximum periods between effective runoff events during wet season sequences of different character. The lengths of the periods are averages as deduced from the predicted runoff time series. Normal, wet, dry refers to the broader classification of the rainy season character according to the standardized precipitation index. The lowermost sequence indicates the single case when effective runoff was "absent" in a hydrological year.

Table 4 Results of the rainfall analysis

SPI class	n	n (%)	mean daily intensity (mm ± 1σ)	contribution light rain (% ± 1σ)	contribution moderate rain (% ± 1σ)	contribution heavy rain (% ± 1σ)	nr. runoff events >10 000 m³ (range)	mean runoff vol/season (1000 m³ ± 1σ)
severely wet	3	10	4 ± 0.26	57 ± 1	9 ± 4	34 ± 6	4-3	1753 ± 734
moderately wet	1	4	3.57	50	5	45	8	565
slightly wet	4	14	3.22 ± 0.17	64 ± 9	10 ± 5	25	3-5	369 ± 159
normal	11	40	2.7 ± 0.24	76 ± 10	6 ± 6	17 ± 9	1-5	134 ± 73
slightly dry	5	18	2.7 ± 0.37	70 ± 7	9 ± 2	20 ± 6	1-3	112 ± 68
moderately dry	2	6	2.2 ± 0.07	82 ± 4	14 ± 9	8 ± 4	1	19 ± 0.1
severely dry	1	4	2.39	100	0	0	0	0.3
extremely dry	1	4	2.99	76	9	15	1	46
overall	28	100	2.9*	71*	8*	21*	0 -8	336*

* weighted mean

In general most of the efficient runoff events occur in the first quarter of the year. The month with the highest probability of an efficient runoff event occurrence is March. This is also the month when intense thunderstorms are most likely to occur (section 2.2). In normal to wet years, efficient runoff events occur on average 3 – 4 times during the rainy season (table 4), and the first ones frequently appear between October and December. In most of the dryer rainy seasons, runoff only occurs between January and April. The annual maximum lengths of periods between the fillings of the cisterns are therefore determined by the character of the rainy season. Fig. 13 shows the average lengths of periods between effective runoff events during wet season sequences of different character.

The annual maximum lengths between the filling of the cisterns range between 6 and 25 months. On average the water reserves of the cisterns would have to have last for about 12 to 14 months before being refilled. The longest modeled period between effective runoff events was 25 months, when no effective runoff event was generated in the rainy season of 1989/90.

The present climate is relatively dry compared to certain periods during the past 1500 years (Finné et al., 2011). Moreover, the climate during the implementation and utilization of the floodwater harvesting system was relatively wet compared to today (section 2.2). Under the present, significantly dryer conditions the risk of failure of filling the cisterns at least once during a rainy season is only 4 %. Based on the assumption that the relationship between precipitation intensities and seasonal totals has not changed significantly, this implies that the runoff harvesting system was reliable. The constant maintenance and development of the floodwater harvesting system between the 6th and the 14th century AD as evident from the archaeological record confirms this result (Brinker, 1991; Westphalen and Knötzele, 2004). According to the Chronicles of Michael the Syrian severe droughts occurred irregularly, but throughout the Late Antique and Early Islamic period (Morony, 2000). Some of those drought years may have been the years when the cisterns were not refilled and the inhabitants of Resafa had to travel to the Euphrates or send their servants to transport water to Resafa as described in Arabic sources (section 1).

4.2.4.3 Reconstruction of flow patterns

The reconstruction of the flow pattern considering local micro-relief included processing of two scenarios developed on the basis of field survey and analysis of satellite images (Fig. 14). Analysis of aerial and satellite images (Ikonos, Spot, Corona) repeatedly shows

dark soil marks indicating subrecently flooded areas (e.g. Fig. 3) (c.f. Wilkinson, 1993). Under scenario 1 a flow pattern is generated as found by this image analysis including flood marks and geomorphological indicators from field survey. It shows that the flood spreads laterally about 400 m downstream of the outlet of Wadi Gharawiy and divides into one northeastward and one northward pushing branch. The main flow direction is towards the valley embayment to the east, where it inundates a small plain and subsequently passes through the garden. The two branches meet at the northwestern edge of the garden and flow into a moat south of the city wall where the flood is retained by the dam. Subsequently the excess water is channeled through the spillway and the flood

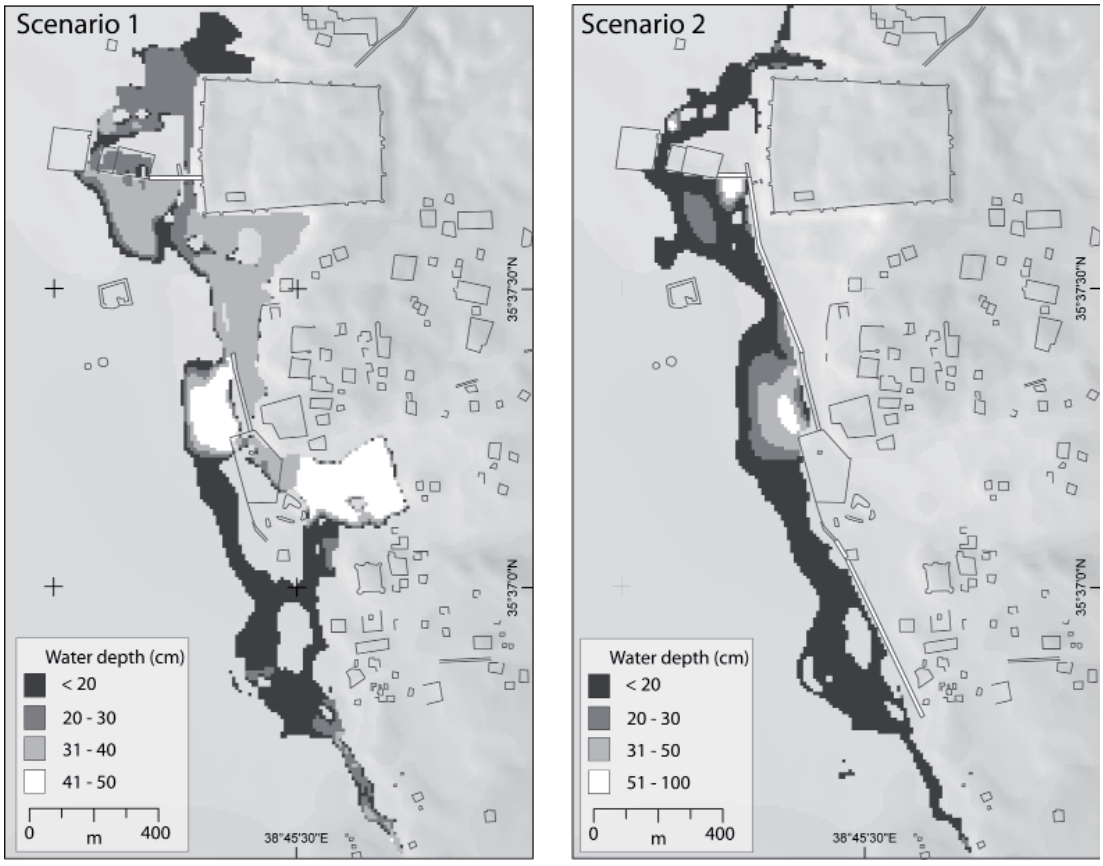

Fig. 14 Result of the flow pattern analysis. Scenario 1 shows the simulated flow pattern under current conditions and those structures implemented which are archaeologically attested. Scenario 2 shows the flow pattern with the presumed embankment system implemented in the model.

finally flows into a depression north of the city wall. The flood would submerge at least two of the once settled areas south of the city walls, including the southern garden and an associated garden pavilion (cf. Mackensen, 1984).

The effect of the embankments on the flow pattern becomes obvious by comparing the result from scenario 1 with scenario 2 (Fig. 14): the flood flows relatively straight northwards towards Resafa, where it is retained by the dam and the excess water is channeled via the spillway to the north of the city. The construction would thereby potentially reduce ponding, shorten the flood path, and therefore reduce transmission losses compared to the unchanneled scenario 1. In consequence, the embankment system would increase the runoff yield and protect settled areas from flooding. A similar system can be found at the Ummayad Qasr al Hayr ash-Sharqi about 65 km southeast of Resafa (Fig. 2) where embankments channeled floodwater of nearby wadis to storage facilities and

agricultural fields (Genequand, 2009). According to the aerial pictures, the excavation results, and the reconstructed flow patterns, the existence of the embankment system seems plausible, at least since the Ummayyad period. Another fragmentary Arabic quote on Resafa apparently confirms this assumption: *"(...) They built cisterns for it (Resafa) and a path for the water from the other end of the desert [steppe]"* (the quote is cited by Brinker (1991) and is recorded in the Fragmenta Historicum Araboricum). This path, initially interpreted as the Wadi es-Sélé by Brinker (1991), may have described this very embankment system.

4.2.5. Conclusions

The most important conclusions of this study are:

1. The floodwater system of Resafa is relatively reliable (the risk of failure is 4%) under current rainfall conditions, which are relatively dry compared to various periods since the Antiquity. Even during most of consecutive dryer rainy seasons the cisterns could have been refilled at least once every 13 to 14 months.

2. According to archaeological findings, it is likely that an extended embankment system existed that facilitated the floodwater harvesting system of Resafa at least since the Ummayyad occupation of the area. It would have potentially increased the runoff yield and protected settled areas from flooding. Yet its existence can ultimately only be validated by further excavations or geophysical surveys. The radiocarbon ages confirm previous studies which indicate extended construction and maintenance work of the water harvesting facilities during the Ummayyad period.

Nonetheless, to supply a city of the size of Resafa with drinking water relying almost exclusively on flood water harvesting is exceptional in the region. The success of the water supply might be explained by two factors: Resafa is located at the margin of a climate region whose precipitation regime has a strong Mediterranean character. This means that sufficient rainfall events triggering runoff occurred quite regularly with low variability. Farther east the Mediterranean character of the precipitation regime diminishes and the occurrence of precipitation is far more erratic (Wirth, 1971). Water harvesting measures are rather unreliable and risky in those regions. Moreover, if the system failed and severe droughts occurred, the inhabitants could have traveled to the Euphrates which was a one day journey by foot. The unlikely failure of the water supply system was therefore not life threatening.

Acknowledgements

This study was supported by the Cluster of Excellence TOPOI Exc 264. Special thanks to Prof. Dr. Dorothée Sack and her team for their support in the field and for sharing data and information. We would also like to thank the Syrian Department of Antiquities for their support and for granting survey permissions.

References

Allen, T., 1988. Five Essays on Islamic Art. Solipsist Pr.

Allison, R., 1998. Middle East and Arabia, in: Thomas, D.S.G. (Ed.), Arid Zone Geomorphology 2nd: Process, Form and Change in Drylands. John Wiley & Sons.

Alpert, P., 2002. The paradoxical increase of Mediterranean extreme daily rainfall in spite of decrease in total values. Geophysical Research Letters 29.

Alpert, P., Baldi, M., Ilani, R., Krichak, S., Price, C., Rodó, X., Saaroni, H., Ziv, B., Kishcha, P.,

Barkan, J., Mariotti, A., Xoplaki, E., 2006. Chapter 2 Relations between climate variability in the Mediterranean region and the tropics: ENSO, South Asian and African monsoons, hurricanes and Saharan dust, in: Mediterranean. Elsevier, pp. 149–177.

Al-Qurashi, A., McIntyre, N., Wheater, H., Unkrich, C., 2008. Application of the Kineros2 rainfall–runoff model to an arid catchment in Oman. Journal of Hydrology 355, 91–105.

Awadallah, A.G., Younan, N.S., 2012. Conservative design rainfall distribution for application in arid regions with sparse data. Journal of Arid Environments 79, 66–75.

Bates, P.D., Horritt, M.S., Fewtrell, T.J., 2010. A simple inertial formulation of the shallow water equations for efficient two-dimensional flood inundation modelling. Journal of Hydrology 387, 33–45.

Beckers, B., Berking, J., Schütt, B., 2012. The Elaborated Ancient Water Supply System of Resafa. Risk and Uncertainty of Water Harvesting in the Syrian Desert Steppe. eTopoi. Journal for Ancient Studies 0.

Beckers, B., Schütt, B., Tsukamoto, S., Frechen, M., 2013. Age determination of Petra´s engineered landscape – optically stimulated luminescence (OSL) and radiocarbon ages of runoff terrace systems in the Eastern Highlands of Jordan. Journal of Archaeological Science.

Ben-Zvi, A., Shentsis, I., 2000. Runoff events in the Negev, Israel. Proceedings of the Jerusalem Conference, May 1999 53–71.

Berking, J., Beckers, B., Schütt, B., 2010. Runoff in two semi-arid watersheds in a geoarcheological context: A case study of Naga, Sudan, and Resafa, Syria. Geoarchaeology 25, 815–836.

Birolini, A., 2007. Reliability Engineering: Theory and Practice, 5th ed. ed. Springer Berlin Heidelberg.

Blott, S.J., Pye, K., 2001. GRADISTAT: a grain size distribution and statistics package for the analysis of unconsolidated sediments. Earth Surface Processes and Landforms 26, 1237–1248.

Bolle, H.-J., 2003. Mediterranean Climate: Variability and Trends. Springer.

Brinker, W., 1991. (in German) Zur Wasserversorgung von Resafa-Sergiupolis. Damaszener Mitteilungen 5 119 – 146.

Bruins, H.J., 2012. Ancient desert agriculture in the Negev and climate-zone boundary changes during average, wet and drought years. Journal of Arid Environments 86, 28–42.

Bruins, H.J., Evenari, M., Nessler, U., 1986. Rainwater-harvesting agriculture for food production in arid zones: the challenge of the African famine. Applied Geography 6, 13–32.

Cherubini, T., Ghelli, A., Lalaurette, F., 2002. Verification of Precipitation Forecasts over the Alpine Region Using a High-Density Observing Network. Weather and Forecasting 17, 238–249.

Cohen Liechti, T., Matos, J.P., Boillat, J.-L., Schleiss, A.J., 2012. Comparison and evaluation of satellite derived precipitation products for hydrological modeling of the Zambezi River Basin. Hydrol. Earth Syst. Sci. 16, 489–500.

Coulthard, T.J., Hicks, D.M., Van De Wiel, M.J., 2007. Cellular modelling of river catchments and reaches: Advantages, limitations and prospects. Geomorphology 90, 192–207.

Critchley, W.R.S., Reij, C., Willcocks, T.J., 1994. Indigenous soil and water conservation: A review of the state of knowledge and prospects for building on traditions. Land Degradation & Development 5, 293–314.

Crook, D., 2009. Hydrology of the combination irrigation system in the Wadi Faynan,

Jordan. Journal of Archaeological Science 36, 2427–2436.
De Waele, J., Plan, L., Audra, P., 2009. Recent developments in surface and subsurface karst geomorphology: An introduction. Geomorphology 106, 1–8.
Dennett, M.D., Keatinge, J.D.H., Rodgers, J.A., 1984. A comparison of rainfall regimes at six sites in northern Syria. Agricultural and Forest Meteorology 31, 319–328.
Dinku, T., Connor, S., Ceccato, P., 2010. Comparison of CMORPH and TRMM-3B42 over Mountainous Regions of Africa and South America, in: Gebremichael, M., Hossain, F. (Eds.), Satellite Rainfall Applications for Surface Hydrology. pp. 193–204.
Dixon, J.C., 2009. Aridic Soils, Patterned Ground, and Desert Pavements, in: Abrahams, A.D., Parsons, A.J. (Eds.), Geomorphology of Desert Environments. Springer, New York.
Easterling, D.R., Evans, J.L., Groisman, P.Y., Karl, T.R., Al, E., 2000. Observed variability and trends in extreme climate events: A brief review. Bulletin of the American Meteorological Society.
El-Hames, A.S., 2012. An empirical method for peak discharge prediction in ungauged arid and semi-arid region catchments based on morphological parameters and SCS curve number. Journal of Hydrology 456–457, 94–100.
Finné, M., Holmgren, K., Sundqvist, H.S., Weiberg, E., Lindblom, M., 2011. Climate in the eastern Mediterranean, and adjacent regions, during the past 6000 years – A review. Journal of Archaeological Science 38, 3153–3173.
Foody, G.M., Ghoneim, E.M., Arnell, N.W., 2004. Predicting locations sensitive to flash flooding in an arid environment. Journal of Hydrology 292, 48–58.
Fowden, E.K., 1999. The barbarian plain: Saint Sergius between Rome and Iran, The transformation of the classical heritage. University of California Press, Berkeley.
Gallego, M.C., Garca, J.A., Vaquero, J.M., 2005. The NAO signal in daily rainfall series over the Iberian Peninsula. Clim Res 29, 103–109.
Garbrecht, G., 1996. (in German) Der Staudamm von Resafa-Sergiupolis, in: Garbrecht, G. (Ed.), Historische Talsperren II. Wittwer Konrad GmbH.
Genequand, D., 2006. Some Thoughts on Qasr al-Hayr al-Gharbi, its Dam, its Monastery and the Ghassanids. Levant 38, 63–84.
Genequand, D., 2009. Économie de production, affirmation du pouvoir et dolce vita : aspects de la politique de l'eau sous les Omeyyades au Bilad al-Sham, in: Al-Dbiyat, M., Mouton, M. (Eds.), Collections électroniques de l'Ifpo. Livres en ligne des Presses de l'Institut français du Proche-Orient. Institut français du Proche-Orient, pp. 157–177.
Gonzalez-Rouco, F., Fernandez-Donado, L., Raible, C., Barriopedro, D., Luterbacker, J., Jungclaus, J., Swingedouw, D., Servonnat, J., Zorita, E., Wagner, S., Ammann, C., 2011. Medieval Climate Anomaly to Little Ice Age transition as simulated by current climate models. PAGES news Vol 19.
Greenbaum, N., 2007. Assessment of dam failure flood and a natural, high-magnitude flood in a hyperarid region using paleoflood hydrology, Nahal Ashalim catchment, Dead Sea, Israel. Water Resour. Res. 43, W02401.
Hammouri, N., El-Naqa, A., 2007. Hydrological modeling of ungauged wadis in arid environments using GIS: a case study of Wadi Madoneh in Jordan. Revista Mexicana de Ciencias Geológicas 24, 185–196.
Harding, A., Palutikof, J., Holt, T., 2009. The Climate System, in: Woodward, J.C. (Ed.), The Physical Geography of the Mediterranean, The Oxford Regional Environments Series. Oxford University Press, Oxford ; New York.
Harrower, M.J., 2010. Geographic Information Systems (GIS) hydrological modeling in

archaeology: an example from the origins of irrigation in Southwest Arabia (Yemen). Journal of Archaeological Science 37, 1447–1452.

Harvey, A., 2011. Dryland alluvial fans, in: Thomas, D.S.G. (Ed.), Arid Zone Geomorphology: Process, Form and Change in Drylands. John Wiley & Sons.

HEC, 2000. Hydrologic Modeling System: Technical Reference Manual. US Army Corps of Engineers Hydrologic Engineering Center, Davis, CA.

HEC, 2010. HEC River Analysis System: Hydraulic Reference Manual. US Army Corps of Engineers Hydrologic Engineering Center, Davis, CA.

Hemming, D., Buontempo, C., Burke, E., Collins, M., Kaye, N., 2010. How uncertain are climate model projections of water availability indicators across the Middle East? Philos Transact A Math Phys Eng Sci 368, 5117–5135.

Hof, C., 2008. (in German) Die Stadtmauer von Resafa - Spuren früher Planänderung und deren Datierungsrelevanz, in: Bericht über die 45. Tagung für Ausgrabungswissenschaft und Bauforschung vom 30. April bis 4. Mai in Regensburg. Koldewey-Gesellschaft 45, pp. 233–248.

Hutchinson, M.F., 1989. A new procedure for gridding elevation and stream line data with automatic removal of spurious pits. Journal of Hydrology 106, 211–232.

Jalut, G., Esteban Amat, A., Mora, S.R. i, Fontugne, M., Mook, R., Bonnet, L., Gauquelin, T., 1997. Holocene climatic changes in the western Mediterranean: installation of the Mediterranean climate. Comptes Rendus de l'Académie des Sciences - Series IIA - Earth and Planetary Science 325, 327–334.

Jarrett, R., England, J., 2002. Relation of paleostage indicators for paleoflood studies, in: House, P.K. (Ed.), Ancient Floods, Modern Hazards: Principles and Applications of Paleoflood Hydrology. American Geophysical Union.

Jenness, J., Brost, B., Beier, P., 2011. Land Facet Corridor Designer: Extension for ArcGIS. Jenness Enterprises.

Kamash, Z., 2012. Irrigation technology, society and environment in the Roman Near East. Journal of Arid Environments.

Kandasamy, J., Hannan, J., 2008. Experience of 1D and 2D flood modelling in Australia – a guide to model selection based on channel and floodplain characteristics, in: Allsop, W., Samuels, P., Harrop, J., Huntington, S. (Eds.), Flood Risk Management: Research and Practice. CRC Press.

Kaniewski, D., Campo, E.V., Weiss, H., 2012. Drought is a recurring challenge in the Middle East. PNAS 109, 3862–3867.

Konrad, M., 2001. Der spätrömische Limes in Syrien. Resafa 5. Zabern.

Koutroulis, A.G., Tsanis, I.K., 2010. A method for estimating flash flood peak discharge in a poorly gauged basin: Case study for the 13–14 January 1994 flood, Giofiros basin, Crete, Greece. Journal of Hydrology 385, 150–164.

Krichak, S.O., Alpert, P., 2005. Decadal trends in the east Atlantic-west Russia pattern and Mediterranean precipitation. International Journal of Climatology 25, 183–192.

Lang, A., Hönscheidt, S., 1999. Age and source of colluvial sediments at Vaihingen–Enz, Germany. CATENA 38, 89–107.

Lewis, N.N., 2009. Nomads and Settlers in Syria and Jordan, 1800-1980, Reissue. ed. Cambridge University Press.

Louhaichi, M., Ghassali, F., Salkini, A.K., Petersen, S.L., 2012. Effect of sheep grazing on rangeland plant communities: Case study of landscape depressions within Syrian arid steppes. Journal of Arid Environments 79, 101–106.

Love, T., Kumar, V., Xie, P., Thiaw, W., 2004. A 20-Year Daily Africa Precipitation Climatology using Satellite and Gauge Data. AMS Conference on Applied Climatology, AMS 1–4.

Luterbacher, J., Xoplaki, E., Casty, C., Wanner, H., Pauling, A., Küttel, M., Rutishauser, T., Brönnimann, S., Fischer, E., Fleitmann, D., Gonzalez-Rouco, F.J., García-Herrera, R., Barriendos, M., Rodrigo, F., Gonzalez-Hidalgo, J.C., Saz, M.A., Gimeno, L., Ribera, P., Brunet, M., Paeth, H., Rimbu, N., Felis, T., Jacobeit, J., Dünkeloh, A., Zorita, E., Guiot, J., Türkes, M., Alcoforado, M.J., Trigo, R., Wheeler, D., Tett, S., Mann, M.E., Touchan, R., Shindell, D.T., Silenzi, S., Montagna, P., Camuffo, D., Mariotti, A., Nanni, T., Brunetti, M., Maugeri, M., Zerefos, C., Zolt, S.D., Lionello, P., Nunes, M.F., Rath, V., Beltrami, H., Garnier, E., Ladurie, E.L.R., 2006. Chapter 1 Mediterranean climate variability over the last centuries: A review, in: Mediterranean. Elsevier, pp. 27–148.

Mackensen, M., 1984. (in German) Resafa: Eine befestigte spätantike Anlage vor den Stadt-mauern von Resafa. Resafa 1. Zabern.

Masri, Z., Zöbisch, M., Bruggeman, A., Hayek, P., Kardous, M., 2003. Wind erosion in a marginal Mediterranean dryland area: a case study from the Khanasser Valley, Syria. Earth Surface Processes and Landforms 28, 1211–1222.

Mayerson, P., Evenari, M., Aharoni, Y., Shanan, L., Tadmor, N., 1961. Ancient Agriculture in the Negev. Science 134, 1751 –1754.

McKee, T.B., Doesken, N.J., Kleist, J., 1995. Drought Monitoring with Multiple Time Scales. Paper presented at the 9th AMS Conference on Applied Climatology. American Meteorological Society, Dallas, Texas.

Meirovich, L., Ben-Zvi, A., Shentsis, I., Yanovich, E., 1998. Frequency and magnitude of runoff events in the and Negev of Israel. Journal of Hydrology 207, 204–219.

Mitchell, T.D., Jones, P.D., 2005. An improved method of constructing a database of monthly climate observations and associated high-resolution grids. International Journal of Climatology 25, 693–712.

Morin, E., Jacoby, Y., Navon, S., Bet-Halachmi, E., 2009. Towards flash-flood prediction in the dry Dead Sea region utilizing radar rainfall information. Advances in Water Resources 32, 1066–1076.

Morony, M., 2000. Michael The Syrian as a Source for Economic History. Journal of Syriac Studies 3.2, 141–172.

Mouterde, R., Poidebard, A., 1945. Le limes de Chalcis; organisation de la steppe en haute Syrie romaine, Bibliothèque archéologique et historique. P. Geuthner, Paris.

Musil, A., 1928. Palmyrena, a topographical itinerary. American Geographical Society of Oriental Explorations and Studies No. 4, Ed. J.K. Wright, Czech Academy of Sciences and Arts, New York.

Nicholson, S.E., 2011. Dryland Climatology. Cambridge University Press.

Novella, N., Thiaw, W., 2010. Validation of Satellite-Derived Rainfall Products over the Sahel. Wyle Information Systems / CPC / NOAA 1–9.

Novella, N., Thiaw, W., 2012. Africa Rainfall Climatology Version 2. NOAA/NWS/NCEP/ Climate Prediction Center/Wyle Information Systems 1–8.

Poidebard, A., 1934. La Trace de Rome dans le désert de Syrie. Bibliothèque Archéologique et Historique. Délégation général de la France au Levant 38, Paris.

Ponce, V.M., Hawkins, R.H., 1996. Runoff Curve Number: Has It Reached Maturity? Journal of Hydrologic Engineering 1, 11.

Ponikarov, V., 1966. The geological map of Syria, scale 1:200000, sheet I-37-XX (Salamiyeh).

Raicich, F., Pinardi, N., Navarra, A., 2003. Teleconnections between Indian monsoon and

Sahel rainfall and the Mediterranean. International Journal of Climatology 23, 173–186.
Reifenberg, A., 1952. The Soils of Syria and the Lebanon. Journal of Soil Science 3, 68–88.
Riehl, S., 2012. Variability in ancient Near Eastern environmental and agricultural development. Journal of Arid Environments 86, 113–121.
Roberts, N., Brayshaw, D., Kuzucuoğlu, C., Perez, R., Sadori, L., 2011. The mid-Holocene climatic transition in the Mediterranean: Causes and consequences. The Holocene 21, 3 –13.
Roberts, N., Moreno, A., Valero-Garcés, B.L., Corella, J.P., Jones, M., Allcock, S., Woodbridge, J., Morellón, M., Luterbacher, J., Xoplaki, E., Türkeş, M., 2012. Palaeolimnological evidence for an east–west climate see-saw in the Mediterranean since AD 900. Global and Planetary Change 84–85, 23–34.
Robinson, S.A., Black, S., Sellwood, B.W., Valdes, P.J., 2006. A review of palaeoclimates and palaeoenvironments in the Levant and Eastern Mediterranean from 25,000 to 5000 years BP: setting the environmental background for the evolution of human civilisation. Quaternary Science Reviews 25, 1517–1541.
Rösner, U., 1995. Zur quartären Landschaftsentwicklung in den Trockengebieten Syriens (in German, English summary). Borntraeger.
Rozalis, S., Morin, E., Yair, Y., Price, C., 2010. Flash flood prediction using an uncalibrated hydrological model and radar rainfall data in a Mediterranean watershed under changing hydrological conditions. Journal of Hydrology 394, 245–255.
Rudolf, B., Becker, A., Schneider, U., Meyer-Christoffer, A., Ziese, M., 2010. The new "GPCC Full Data Reanalysis Version 5" providing high-quality gridded monthly precipitation data for the global land-surface. Global Precipitation Climatology Centre (GPCC), DWD, internet publication 1–7.
Sack, D., 1996. (in German) Die Große Moschee von Resafa-Rusafat Hisam. Resafa 4. Zabern.
Sbeinati, M.R., Darawcheh, R., Mouty, M., 2009. The historical earthquakes of Syria: an analysis of large and moderate earthquakes from 1365 B.C. to 1900 A.D. Annals of Geophysics 48.
Schmidt, G.A., Shindell, D.T., Miller, R.L., Mann, M.E., Rind, D., 2004. General circulation modelling of Holocene climate variability. Quaternary Science Reviews 23, 2167–2181.
Schütt, B., 1998a. Reconstruction of Holocene Paleoenvironments in the Endorheic Basin of Laguna de Gallocanta, Central Spain by Investigation of Mineralogical and Geochemical Characters from Lacustrine Sediments. Journal of Paleolimnology 20, 217–234.
Schütt, B., 1998b. Reconstruction of palaeoenvironmental conditions by investigation of Holocene playa sediments in the Ebro Basin, Spain: preliminary results. Geomorphology 23, 273–283.
Schütt, B., 2000. Holocene paleohydrology of playa lakes in northern and central Spain: a reconstruction based on the mineral composition of lacustrine sediments. Quaternary International 73–74, 7–27.
Schütt, B., Berking, J., Frechen, M., Frenzel, P., Schwalb, A., Wrozyna, C., 2010. Late Quaternary transition from lacustrine to a fluvio-lacustrine environment in the northwestern Nam Co, Tibetan Plateau, China. Quaternary International 218, 104–117.
SCS, 1964. SCS National Engineering Handbook Soil Conservation Service. US Department of Agriculture, Washington DC.
Shanan, L., 2000. Runoff, erosion, and the sustainability of ancient irrigation systems in

the Central Negev desert., in: Hassan, M.A., Slaymaker, O., Berkowicz, S.M. (Eds.), The hydrology-geomorphology interface: rainfall, floods, sedimentation, land use. A selection of papers presented at the Conference on Drainage Basin Dynamics and Morphology held in Jerusalem, Israel, May 1999. IAHS Press, pp. 75–106.

Stisen, S., Sandholt, I., 2010. Evaluation of remote-sensing-based rainfall products through predictive capability in hydrological runoff modelling. Hydrological Processes 24, 879–891.

Tooth, S., 2000. Process, form and change in dryland rivers: a review of recent research. Earth-Science Reviews 51, 67–107.

Trigo, I.F., Davies, T.D., Bigg, G.R., 1999. Objective Climatology of Cyclones in the Mediterranean Region. Journal of Climate 12, 1685–1696.

Trigo, R.M., Gouveia, C.M., Barriopedro, D., 2010. The intense 2007–2009 drought in the Fertile Crescent: Impacts and associated atmospheric circulation. Agricultural and Forest Meteorology 150, 1245–1257.

van Wesemael, B., Poesen, J., Solé Benet, A., Cara Barrionuevo, L., Puigdefábregas, J., 1998. Collection and storage of runoff from hillslopes in a semi-arid environment: geomorphic and hydrologic aspects of the aljibe system in Almeria Province, Spain. Journal of Arid Environments 40, 1–14.

Vicente-Serrano, S.M., Beguería, S., López-Moreno, J.I., 2010. A Multiscalar Drought Index Sensitive to Global Warming: The Standardized Precipitation Evapotranspiration Index. Journal of Climate 23, 1696–1718.

Vicente-Serrano, S.M., Beguería-Portugués, S., 2003. Estimating extreme dry-spell risk in the middle Ebro valley (northeastern Spain): a comparative analysis of partial duration series with a general Pareto distribution and annual maxima series with a Gumbel distribution. International Journal of Climatology 23, 1103–1118.

Wade, A.J., Smith, S.J., Black, E.C.L., Brayshaw, D.J., Holmes, P.A.C., El-Bastawesy, M., Rambeau, C.M.C., Mithen, S.J., 2012. A new method for the determination of Holocene palaeohydrology. Journal of Hydrology 420–421, 1–16.

Wagener, T., Wheater, howard S., Gupta, H.V., 2004. Rainfall-Runoff Modelling In Gauged And Ungauged Catchments. World Scientific Publishing Company.

Wainwright, J., Bracken, L., 2011. The work of water, in: Thomas, D.S.G. (Ed.), Arid Zone Geomorphology: Process, Form and Change in Drylands. John Wiley & Sons.

Wang, J., Wolff, D.B., 2010. Evaluation of TRMM Ground-Validation Radar-Rain Errors Using Rain Gauge Measurements. Journal of Applied Meteorology and Climatology 49, 310–324.

Westphalen, S., Knötzele, P., 2004. Water Supply of Resafa, Syria - Remarks on the Chronology of the Big Cisterns, in: Bienert, H.D., Häser, J. (Eds.), Men of Dikes and Canals. The Archaeology of Water in the Middle East. International Symposium Held at Petra, Wadi Musa (H. K. of Jordan). Verlag Marie Leidorf.

Wheater, H., Al Weshah, R., 2002. Hydrology of wadi systems - IHP regional network on wadi hydrology in the Arab region. UNESCO- Technical documents in hydrology vol. 55.

Wheater, H., Sorooshian, S., Sharma, K.D., 2007. Hydrological Modelling in Arid and Semi-Arid Areas, 1st ed. Cambridge University Press.

Whitehead, P.G., Smith, S.J., Wade, A.J., Mithen, S.J., Finlayson, B.L., Sellwood, B., Valdes, P.J., 2008. Modelling of hydrology and potential population levels at Bronze Age Jawa, Northern Jordan: a Monte Carlo approach to cope with uncertainty. Journal of Archaeological Science 35, 517–529.

Widell, M., 2007. Historical Evidence for Climate Instability and Environmental Catastrophes in Northern Syria and the Jazira: The Chronicle of Michael the Syrian. Environment and History 13, 47–70.

Wilkinson, T., 1993. Linear hollows in the Jazira, Upper Mesopotamia [WWW Document]. URL http://antiquity.ac.uk/ant/067/Ant0670548.htm

Wirth, E., 1971. (in German) Syrien: eine geographische Ländeskunde. Wissenschaftliche Buchgesellschaft.

Wolfart, R., 1967. (in German) Geologie von Syrien und dem Libanon, Beiträge zur regionalen Geologie der Erde. Borntraeger, Berlin-Nikolassee.

Xie, P., Arkin, P.A., 1996. Analyses of global monthly precipitation using gauge observations, satellite estimates, and numerical model predictions. Journal of climate 9, 840–858.

Xoplaki, E., Trigo, R.M., García-Herrera, R., Barriopedro, D., D'Andrea, F., Fischer, E.M., Gimeno, L., Gouveia, C., Hernández, E., Kuglitsch, F.G., Mariotti, A., Nieto, R., Pinto, J.G., Pozo-Vázquez, D., Saaroni, H., Toreti, A., Trigo, I.F., Vicente-Serrano, S.M., Yiou, P., Ziv, B., 2012. 6 - Large-Scale Atmospheric Circulation Driving Extreme Climate Events in the Mediterranean and its Related Impacts, in: The Climate of the Mediterranean Region. Elsevier, Oxford, pp. 347–417.

Zohary, M., 1973. Geobotanical Foundations of the Middle East. Taylor & Francis.

5. Petra

5.1 The chronology of ancient agricultural terraces in the environs of Petra in Jordan

Brian Beckers, Brigitta Schütt, 2012, in Stefan Schmid and Michel Mouton (eds.): Early Petra, Logos Verlag.

5.1.1 Introduction

Barren rocks, steep slopes and deep canyons characterise the semi-arid environs of the Nabataean/Roman city of Petra. Yet abundant remains of ancient agricultural and hydraulic structures attest that this unfavourable environment has been extensively used as farmland.

Some parts of the region have been reclaimed by installing so called runoff terraces. The main component of these terraces is a wall often made of hewn stones called riser. Risers are usually built either across the ephemeral channels of minor wadis or along the floodplains of major wadis. The occasional floods running down the wadis are retained by the risers and, due to the reduced flow velocity, transport capacity decreases and the transported sediments are deposited upstream of the risers. In consequence, a flat area upstream of the risers gradually develops, composed of loose sediments, which can subsequently be used for growing crops (called the terrace fill or tread). These risers are occasionally raised by adding new courses of stones, thereby enlarging the fields and the water storage capacity of the terrace. Hence, the three main purposes of such terraces are to moderate flood waves, to level steep areas and to preserve soil and water (Mayerson et al. 1961). Such terraces often occur in rows and create step-like adjoining fields that cover the valley floors (Fig. 3). Nowadays, most of the terraces show a considerable amount of damage, with collapsed risers and fields dissected by gullies. However, some of the agricultural terraces are still in use and new ones are even being built by the local population.

Most scholars attribute the construction of these terraces to the Nabataeans and Romans (Lindner et al. 2000; Tholbecq 2001; Kouk, 2006; Gentell, 2009; Lavento 2010). However, these conclusions are solely based on surface pottery and relative age determination, while the chronology of the cultural landscape has remained under debate.

The purpose of this chapter is to briefly summarise the results of a study which determined the age of agricultural terraces by applying Optical Stimulated Luminescence (OSL) and radiocarbon (14C) dating. The agricultural terraces investigated are located in the catchment of Wadi al-Ghurab, next to the Neolithic settlement of Beidha, and in the Roman Gardens along Seil Wadi Musa (figs 1 and 2). For details on the methodology, results and discussion of the study the reader is referred to the original research paper (Beckers et al., forthcoming).

5.1.2 Environmental setting

From west to east, the Petra region stretches 20 km from the low and arid plains of the Wadi Arabah, c. 300 m above sea level (asl) to the remnant oak forests of the Shara mountains, which rise up to c. 1500 m asl (Fig. 1). The bedrock of this area is composed of Precambrian granites and metamorphic rocks of the Arabian tectonic plate. The igneous basement is overlain by thick and ruptured sandstone formations of the Nubian series. The sandstone formations, in turn, are overlain by Cretaceous limestone formations which form the Shara mountains (Barjous, 1995).

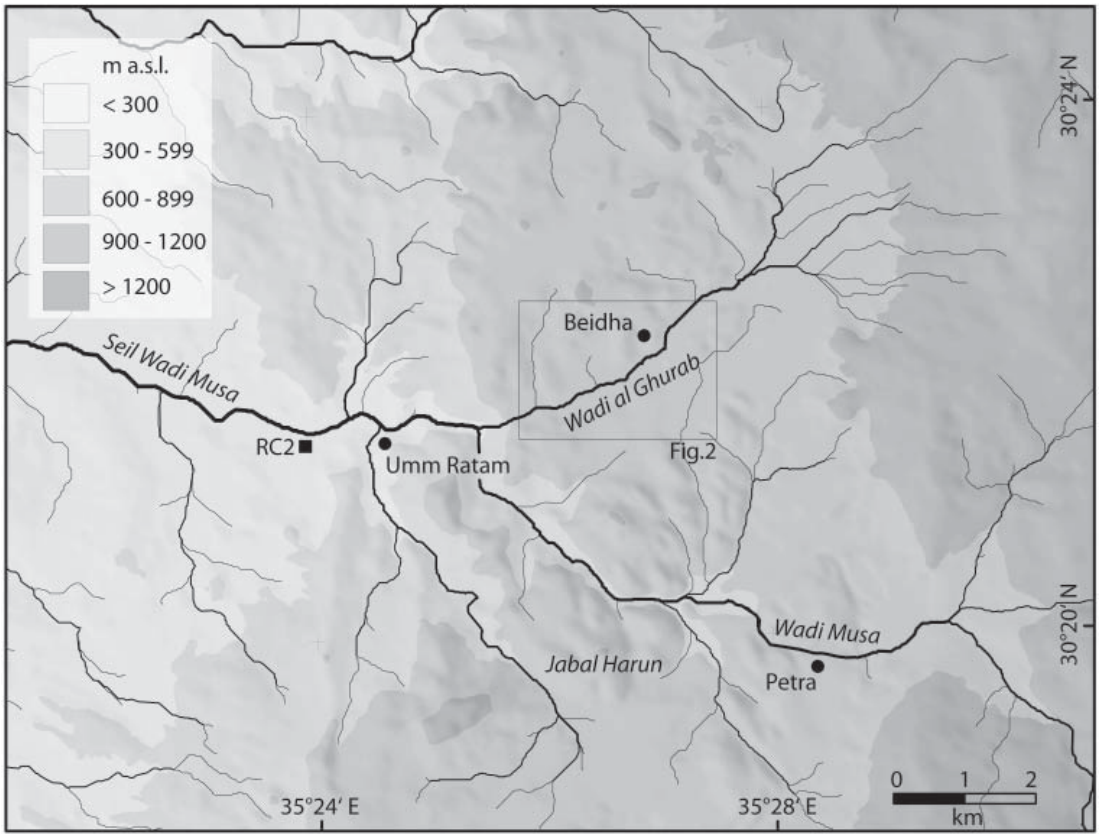

Fig. 1 Map of the greater Petra region showing sample locations, major wadis and settlements mentioned in the text. For sample locations in the Wadi al-Ghurab catchment see Fig. 2.

Since the mid-Holocene aridisation (c. 4000 BC) of the Eastern Mediterranean, the climate of the Petra region has been predominately arid to semi-arid (Robinson et al. 2006; Finné et al. 2011). Annual rainfall ranges from c. 50 to 100 mm in the Wadi Arabah to c. 150 to 200 mm in Petra and reaches up to about 250 mm in the Shara mountains. Perennially flowing watercourses are absent in the region. Only during and shortly after sufficient rainfall events do the wadis carry water (Al-Weshah & El-Khoury, 1999). A few perennial springs occur and are concentrated along the geological boundary between the limestone and sandstone units on the west-facing slopes of the Shara mountains (Al-Khashman, 2007). As is typical for mountainous areas, the region is dominated by erosion. The few remnant valley fills (e.g. the Beqah Plain) are prone to erosion and are dissected by gullies.

In the arid Wadi Arabah, vegetation is concentrated along the wadis that emerge from the highlands. Tamarix, acacias and scattered scrubs and grasses grow there. In the highlands where the rainfall is higher juniper, pines and oaks grow in favourable locations and constitute a wooded mountainous steppe. In the Shara mountains, there are only remnants of the oak forest due to century-long clearance (Al-Eisawi, 1996).

5.1.3 Study sites

The Wadi al-Ghurab catchment is located in the sandstone formations of the Petra region, approximately 3 km north of Petra (Fig. 2). The wadi is a tributary of the Wadi Musa and drains parts of the western slopes of the Shara mountains. The characteristics of the tributaries draining into the Wadi al-Ghurab's lower course are ideal for runoff farming: their areas are rather small, large parts are covered by almost impermeable bedrock and the slopes are moderate. These characteristics ensure that a high proportion of rainfall is

converted to runoff and that the occasional flash floods are usually moderate and manageable (cf. Critchley et al. 1994).

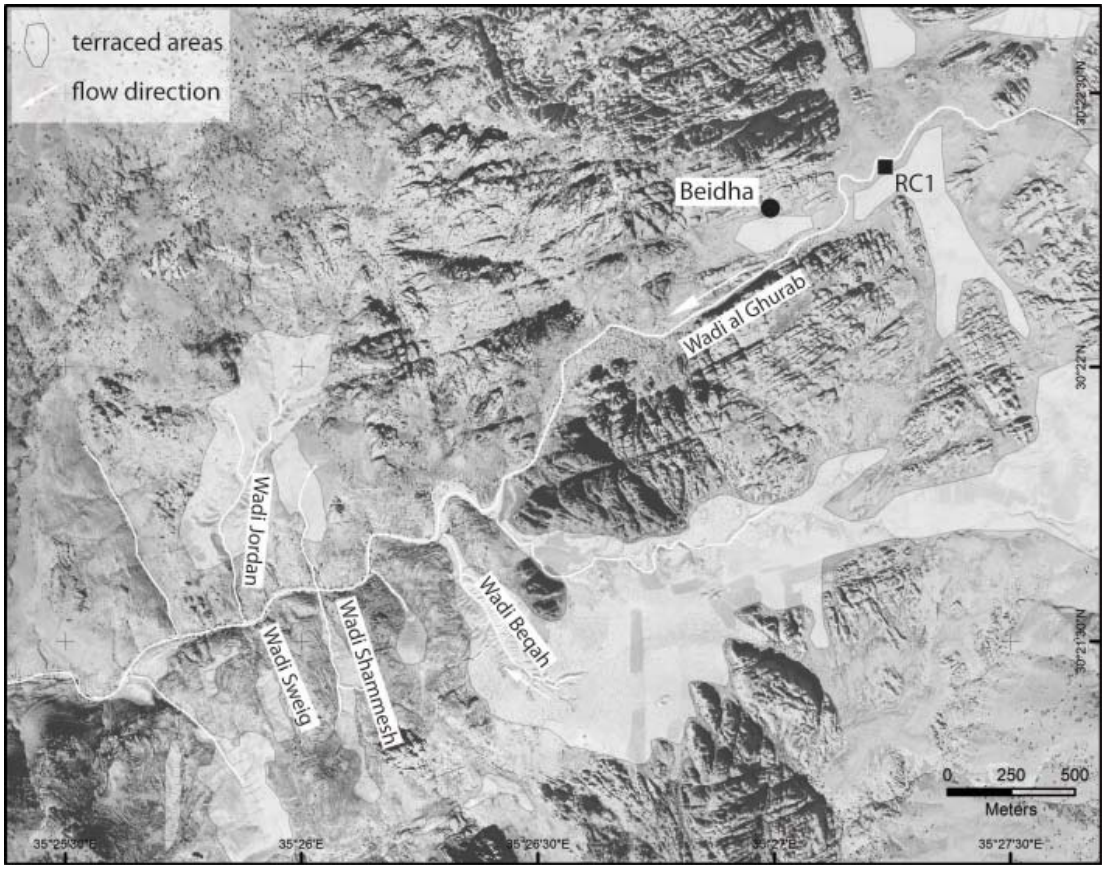

Fig. 2. Aerial photo of the lower Wadi al-Ghurab catchment showing sample locations and major wadis (photo: Institut Géographique National, France 1974).

The Wadi Shammesh and Wadi Sweig are two of these tributaries. Like the neighboring drainage basins, their catchments have been terraced from their headwaters to their outlets (Fig. 3). In general, the risers appear to be constructed in a similar manner: the walls vary in length from between 20 and 40 m and are aligned perpendicular to the direction of dominant flow; they are dry-stone walls made of interlocking, crudely cut sandstone cobbles (c.70×60×50 cm) (Fig. 3). Many walls show traces of maintenance work, such as repair of collapsed parts with gravel and smaller cobbles. The risers are about 1.50 m high, above ground level. Like almost all the fields in the region, most of the terraces nowadays are dissected by gullies and only in the headwater areas are some still cultivated (Fig. 3).

The drainage basin of Wadi Beqah differs from the other tributaries as large parts are covered by the Beqah Plain, which consists presumably of a Pleistocene valley fill (Gentelle, 2009). The plain is crossed by several hundred-metre long, partly buried dry-stone walls, which most likely enclosed ancient fields. On its northern side, the plain falls steeply towards the Wadi al-Ghurab. The Wadi Beqah is an extended gully system incised into the western edge of the plain and in the area where the wadi emerges from the plain, an elongated fan extending c. 150 m to the Wadi al-Ghurab has been deposited. The sample sites are located in this area, between the northern escarpment of the plain and the

Wadi al-Ghurab. Here several terraces have been built across the fan and a huge riser was built at the foot of the escarpment.

Sample location RC1 is c. 600 m upstream of the Neolithic settlement of Beidha. In this area the left bank of the Wadi al-Ghurab is made up of a small elevated plain crossed by several partly buried terrace walls. The plain drops up to 5 m to the gravel bed of Wadi al-Ghurab (Fig. 6). Remnants of dry-stone walls can be found along this escarpment and it is likely that they were once part of a continuous wall that retained the water and sediments originating from the southern part of the catchment and protected the plain from the floods of the Wadi al-Ghurab.

Fig. 3. Remains of runoff terraces in the Wadi Shammesh, looking south. Note the gully that dissects the valley.

In the Roman Gardens, the terraces were built on top of presumably Pleistocene fluvial terraces of Seil Wadi Musa (Fig. 7). Sample location RC2 is c. 500 m downstream of the Roman fort of Umm Rattam, on the left bank of Seil Wadi Musa (Fig. 1). The plain is crossed by terrace walls and the tributary that crosses the plain is scattered with remains of check dams. Remnants of walls along the escarpment of the plain facing the wadi, like those of RC1, could not be found. However, it is likely that they existed and were eroded since remains of such walls are present in similar locations both up and downstream of RC2.

5.1.4 Results and Discussion

The results of the radiocarbon and OSL dating are summarised in Table 1 and Fig. 8. All dates are reported in calendar ages with a 2-σ error. OSL was measured at the Leibniz Institute for Applied Geophysics (LIAG). Radiocarbon dates were determined at the Poznan Radiocarbon Laboratory (for details see Beckers et al., forthcoming).

In Wadi Shammesh, the outcrop investigated is located along the mid-course of the wadi between two risers and comparison with other outcrops along the wadi banks confirms that the stratigraphy is representative for the whole catchment. The sandstone be-

drock is overlain by up to 1.50 m of cemented silty sand, which presumably corresponds to the weathering mantle of the sandstone. This layer is overlain by approximately 50 cm of sub-rounded pebbles aligned in the direction of flow. The risers were built on top of this layer. Behind the risers and on top of the pebble layer, c. 1.50 m of silty sand with occasional stones and interbedded layers of very fine pebbles have accumulated and represent the terrace fills (Fig. 4).

Table 1 Summary of the radiocarbon and OSL dates. Dates are reported in calendar years with a 2-σ error. OSL was measured at the LIAG. Radiocarbon dates were determined at the Poznan Radiocarbon Laboratory. For details see (Beckers et al., forthcoming).

Location	Depth	Coordinates[€]		Sample Context	Calender Age
Sample ID	(cm)	North	East		(years ± 2σ)
Wadi Shammesh					
LUM2349	150	30.359	35.434	Terrace fill	440±300 AD[☼]
LUM2350	100	30.359	35.434	Underneath riser	330±420 BC[☼]
LUM2351	65	30.359	35.431	Terrace fill	730±180 AD[☼]
Wadi Sweig					
LUM2365	120	30.359	35.431	Underneath riser	1270±320 AD[☼]
LUM2366	70	30.361	35.439	Terrace fill	840±140 AD[☼]
Wadi Beqah					
LUM2352	90	30.361	35.439	Terrace fill	1000±100 AD[☼]
LUM2354	70	30.361	35.439	Terrace fill	1120±140 AD[☼]
LUM2356	70	30.362	35.438	Terrace fill	1000±200 AD[☼]
LUM2357	100	30.375	35.456	Underneath riser	1060±140 AD[☼]
Wadi al Ghurab RC1					
Pet20_1	25	30.375	35.456	Terrace fill	870±100 cal AD[†]
Pet20_2	110	30.375	35.456	Terrace fill	240±100 cal AD[†]
Pet20_3	155	30.366	35.366	Terrace fill	150±80 cal AD[†]
Seil Wadi Musa RC2					
Pet25_1	35	30.366	35.366	Terrace fill	200±110 cal AD[†]
Pet25_2	75	30.366	35.366	Terrace fill	120±110 cal AD[†]
Pet25_3	145	30.366	35.366	Terrace fill	100±90 cal AD[†]
LUM2359	220	30.366	35.366	Gravel Layer	510±130 AD[☼]

[€] Coordinates in decimal degrees

[†] radiocarbon age

[☼] OSL age

The OSL sample taken from underneath the riser gave a date of 330±420 BC (LUM2350). Another sample (LUM2349) was taken c. 2 m downstream of LUM2350 and c. 20 cm above the pebble layer. This sample is assumed to represent the initial filling of the terraces. LUM2349 dated to 440±300 AD. Considering the error ranges there might be a large time gap between the construction of the terraces and the initial filling. However, it is likely that the filling of the terrace started shortly after the construction of the riser. Hence we assume that the actual age of sample LUM2350 is around the beginning of the 1st century AD. The uppermost sample taken from the terrace fill (LUM2351) suggests that the terraces were maintained and used at least until the 6th century AD (Fig. 8).

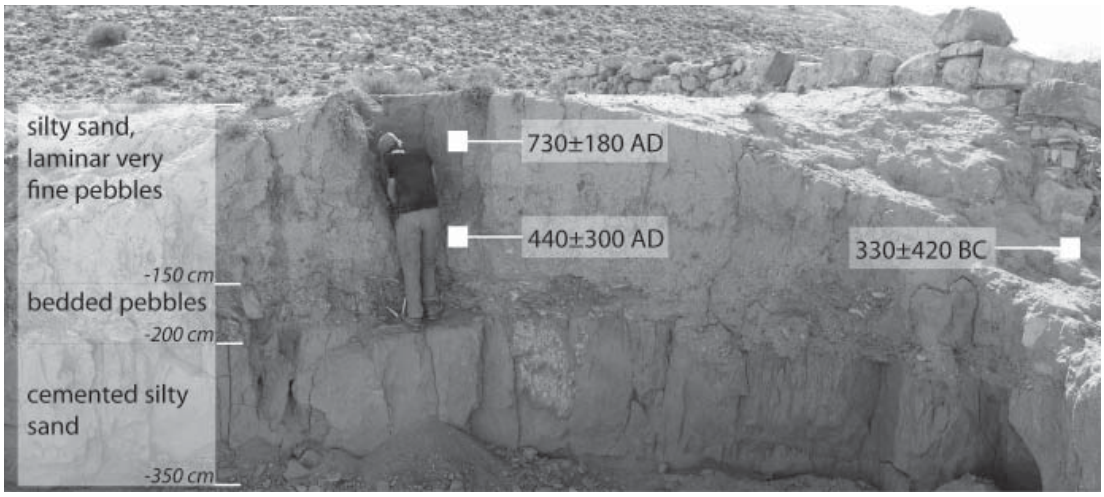

Fig. 4. Exposure investigated in Wadi Shammesh and OSL dates of samples LUM2349 to 2351, looking east. Note the terrace wall on the right side.

The terrace investigated in Wadi Sweig is the farthest downstream of a series of about 20 terraces built in the valley and is located c. 20 m upstream of the confluence of Wadi Sweig. Here we took an OSL sample c. 70 cm below the surface of the terrace fill (LUM2366). It gave a date of 840±140 AD and fits chronologically with the sample we took in Wadi Shammesh at about the same depth (see above). In order to date the

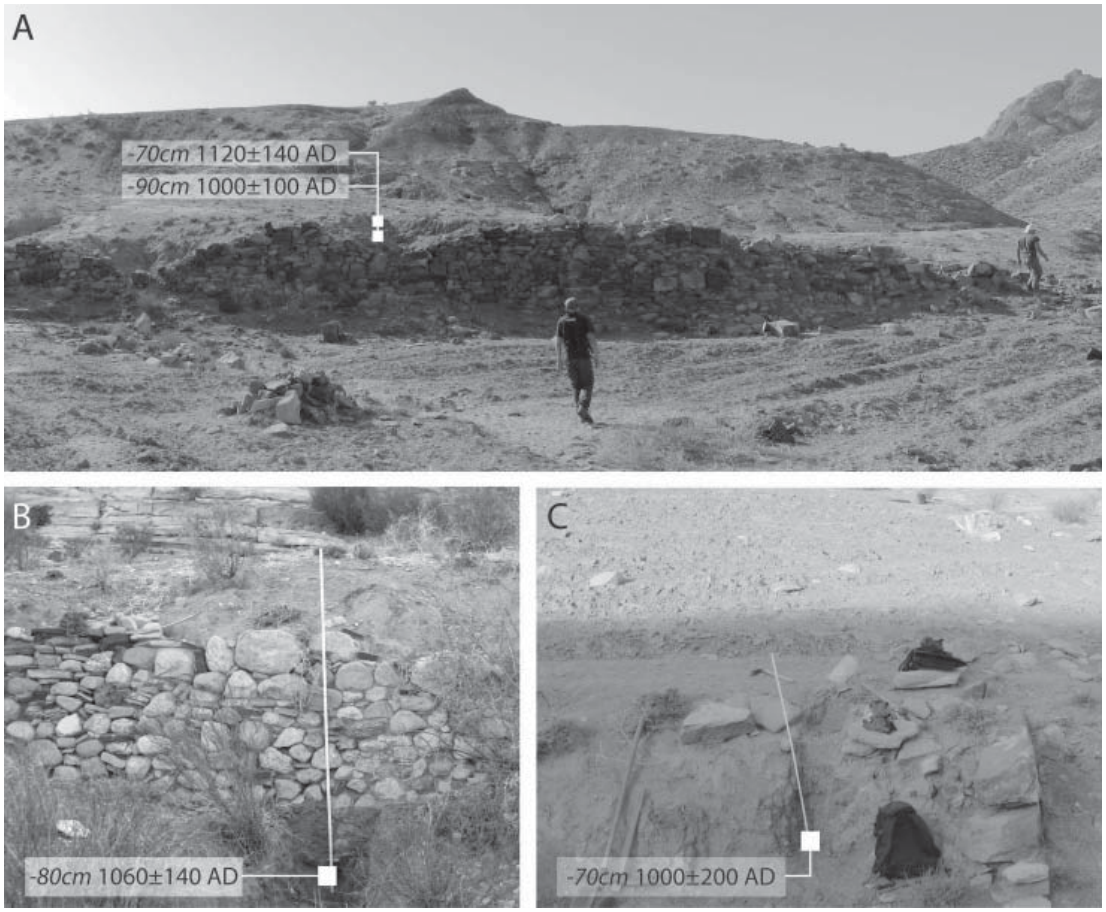

Fig. 5. A: Agricultural terrace at the foot of the escarpment where the Beqah plain descends towards Wadi al-Ghurab and OSL sample locations of LUM 2352/54, looking south. B: Riser and sample location of LUM2357, looking west. C: Riser crossing the fan of Wadi Beqah and sample location of LUM2356, looking east (Photos by Daniel Knitter).

Fig. 6. A: Landscape at sample location RC1, looking northeast. The elevated agricultural plain is in the foreground, the Shara mountains in the background. B: Exposure investigated at RC1 with radiocarbon dates of sample Pet 20_1 to 20_3, looking southeast.

base of the riser we dug a small trench to reach its sediment base. The sample dated to 1270±320 (LUM2365) and post-dates the sample taken from the terrace fill. We assume this age inversion to be caused by undercutting of the riser and subsequent deposition of fine sediments.

Three terraces were investigated in Wadi Beqah. The largest of them is about 20 m wide and 3 m high and was built at the foot of the northern escarpment of the Beqah Plain (Fig. 5 A). We took two samples from the upper part of the fill of the large terrace. They gave dates of 1000±100 AD (LUM2352) and 1220±140 AD (LUM2354).

Four hundred metres downstream we took a sample upstream of a riser built across the fan of Wadi Beqah. This sample gave a date of 100±100 AD (LUM2356, see Fig. 5 C). A further 500 m downstream we took a sample below a riser of masonry that appeared to be different compared to the ones previously described (Fig. 5 B). It was built with much smaller and crude pebbles, probably originating from the nearby Wadi al-Ghurab. This sample gave a date of 1060±140 AD (LUM2357). These dates imply that this area was used for farming and additional structures were constructed at least until the 9th

century AD. However, the time when the reclamation of this area started could not be determined.

Sample location RC1 is on the escarpment where the plain descends to the Wadi al-Ghurab (Fig. 6 A). A few metres downstream are the remains of a dry-stone wall that stabilised the escarpment. Here, on top of the gravels of Wadi al-Ghurab, about 2 m of sandy silt have accumulated (Fig. 6 B). The radiocarbon dates (Pet 20_1 - 20_3) imply that sedimentation of the fine sediments started in the 1st century AD and lasted until at least the 9th century AD.

A similar picture appears at the sample location in the Roman Gardens (RC2). According to the radiocarbon dates (Pet_25_1 to 25_3) the sedimentation of the fine sediments started here in the 1st century AD and lasted at least until the 2nd century AD (Fig. 7). These dates are in accordance with the archaeological record (Lindner et al. 2000). The OSL sample that was extracted from a sand lens in a fine pebble layer underneath a small overhang gave a date of 510±130 AD (LUM2359) and post-dates the radiocarbon age. As in Wadi Sweig, we assume that this inversion of dates is caused by undercutting of the terrace fill by floods of the Seil Wadi Musa and a subsequent (re-) deposition of the sediments.

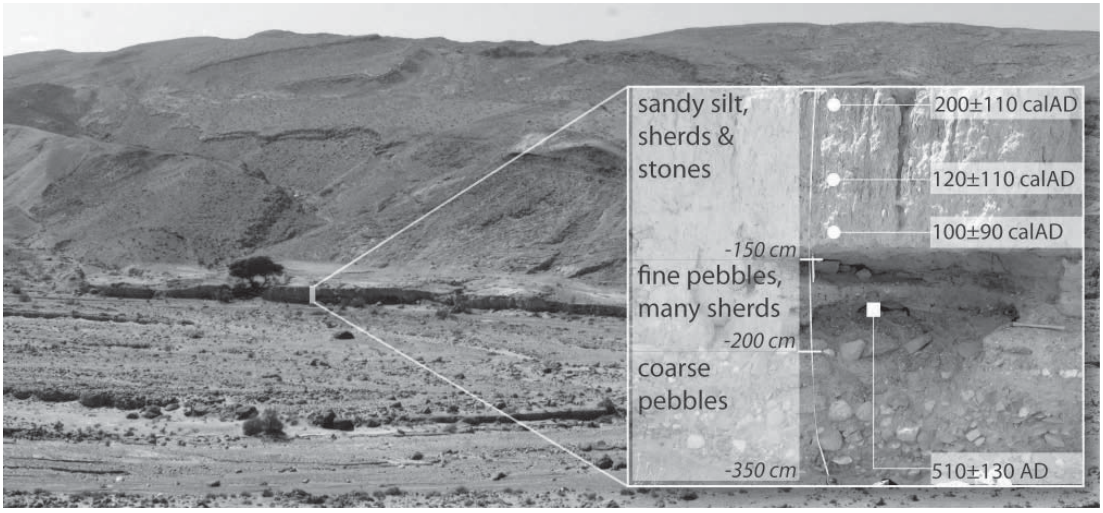

Fig. 7. Landscape at sample location RC2, looking south. The inset photo shows the exposure with radiocarbon dates of sample Pet 25_1 – 25_3 and OSL sample LUM2359.

5.1.5 Conclusion

This chapter summarises the results of a study to determine the ages of agricultural terraces by OSL and radiocarbon dating in the Petra region. The OSL and radiocarbon dates are in general agreement and so one can conclude that the construction of the agricultural terraces started in the 1st century AD (Fig. 8). The terraces were most likely constructed, used, maintained and expanded at least until the 8th century AD. This fits with a study made by Kouki (2009) who concluded, based on the archaeological record that in the Petra region agriculture expanded in the 1st century AD and was part of the local economy even after Petra lost its regional importance in the 4th century AD. However, exactly when the terraces and fields were eventually abandoned and started to degrade could not be determined. The construction of the terraces had a major impact on the landscape of the Petra region as formerly gravel-bedded wadis and floodplains were converted to arable land. However, once the terraces were abandoned most of the fields degraded

and large parts of the once arable land has been eroded (Fig. 8). If this unique cultural landscape is to be conserved, countermeasures have to be taken, such as reactivating and maintaining agriculture on the terraces.

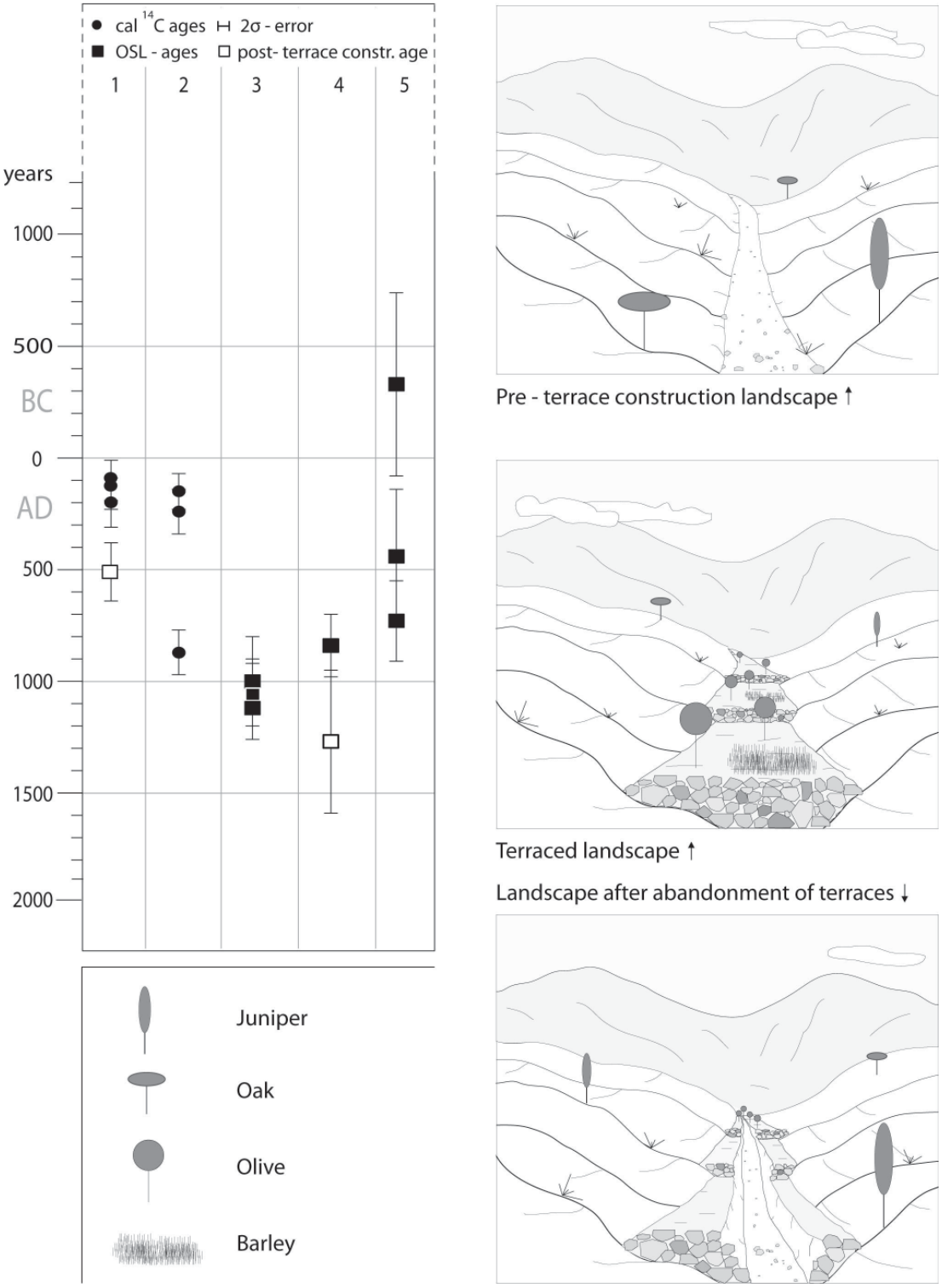

Fig. 8. Left side: Summary of the OSL and radiocarbon dates by sample location: 1. RC2, Seil Wadi Musa 2. RC1, Wadi al-Ghurab 3. Wadi Beqah 4. Wadi Sweig 5. Wadi Shammesh. Post-terrace construction date refers to dates which are thought not to be directlyrelated to the construction of the terraces.

Acknowledgments

This study was supported by the Cluster of Excellence TOPOI Exc 264. Thanks to Manfred Frechen (LIAG) and Sumiko Tsukamoto (LIAG) for granting access to the OSL-laboratory and for supporting the laboratory work and analysis. We would also like to thank the Department of Antiquities of Jordan for granting the survey permit. Special thanks to Stephan G. Schmid and Michel Mouton, without whom field work would not have been possible.

References

Al-Eisawi, D., 1996. Vegetation of Jordan. UNESCO Regional Office for Science and Technology for the Arab States, Cairo.

Al-Khashman, O.A., 2007. Study of water quality of springs in Petra region, Jordan: A three-year follow-up. Water Resources Management 21, 1145–1163.

Al-Weshah, R.A., El-Khoury, F., 1999. Flood analysis and mitigation for the Petra area in Jordan. Journal of water resources planning and management 125, 170–177.

Barjous, M.O., 1995. Supplement text to the geological map Petra & Wadi Al-Lahyana, Sheet: 3050I/3050IV, 1:50000, Natural Resources Authority, Jordan.

Beckers, B., Schütt, B., Tsukamoto, S., Frechen, M., forthcoming. Age determination of Petra´s engineered landscape. OSL and radiocarbon ages of runoff terrace systems in the Eastern Highlands of Jordan. Journal of Archaeological Science.

Critchley, W.R.S., Reij, C., Willcocks, T.J., 1994. Indigenous soil and water conservation: A review of the state of knowledge and prospects for building on traditions. Land Degradation & Development 5, 293–314.

Finné, M., Holmgren, K., Sundqvist, H.S., Weiberg, E., Lindblom, M., 2011. Climate in the eastern Mediterranean, and adjacent regions, during the past 6000 years – A review. Journal of Archaeological Science 38, 3153–3173.

Gentelle, P., 2009. Aménagement du territoire agricole de la ville de Pétra : la terre et l'eau, in Stratégies d'acquisition de l'eau et société au Moyen-Orient depuis l'Antiquité. Institut français du Proche-Orient, pp. 133–148.

Kouki, P., 2006. Environmental change and human history in the Jebel Harun area, Jordan Dissertation for the degree of Licentiate of Philosophy. University of Helsinki.

Kouki, P., 2009. Archaeological evidence of land tenure in the Petra region, Jordan: Nabataean-Early Roman to Late Byzantine. Journal of Mediterranean Archaeology 22, 29–56.

Lavento, M., 2010. Archaeological investigations of ancient water systems in Jordan, in Ostreng, W. (Ed.), Transference. Interdisciplinary Communications 2008/2009, CAS, Oslo.

Lindner, M., Hübner, U., Hübl, J., 2000. Nabataean and Roman presence between Patra and Wadi Arabah survey expedition 1997/98: Umm Ratam. Annual of the Department of Antiquities of Jordan.

Mayerson, P., Evenari, M., Aharoni, Y., Shanan, L., Tadmor, N., 1961. Ancient agriculture in the Negev. Science 134, 1751–1754.

Robinson, S.A., Black, S., Sellwood, B.W., Valdes, P.J., 2006. A review of palaeoclimates and palaeoenvironments in the Levant and Eastern Mediterranean from 25,000 to 5000 years BP: setting the environmental background for the evolution of human civilisation. Quaternary Science Reviews 25, 1517–1541.

Tholbecq, L., 2001. The hinterland of Petra from Edomite to the Islamic periods: The Jabal ash-Sharah Survey (1996-1997). Studies in the history and archaeology of Jordan, 399–405.

5.2 Age determination of Petra´s engineered landscape – optically stimulated luminescence (OSL) and radiocarbon ages of runoff terrace systems in the Eastern Highlands of Jordan

Brian Beckers, Brigitta Schütt, Sumiko Tsukamoto, Manfred Frechen, 2013. Journal of Archaeological Science 40, 333-348. DOI: http://dx.doi.org/10.1016/j.jas.2012.06.041

5.2.1 Introduction

The diverse agricultural and hydraulic systems in the Petra region in Jordan are an impressive example of ancient dryland farming and water harvesting techniques. Archaeological evidence suggests that permanent and semi-permanent settlements have been present in the region since the Epipalaeolithic, c. 8300 - 7000 BC (Byrd, 1989). Petra is by far the largest and best preserved of the ancient settlements in the region. Petra was the capital of the Nabataean Kingdom and was a regional administrative and economic centre in the southern Levant from the 3rd century BC until the 4th century AD (e.g. Schmid, 2008). The city is located in the arid and rugged Eastern Highlands of Jordan, and its unfavourable environmental conditions made elaborate landscape modifications necessary to supply permanent settlements with local food and water (Ortloff, 2005).

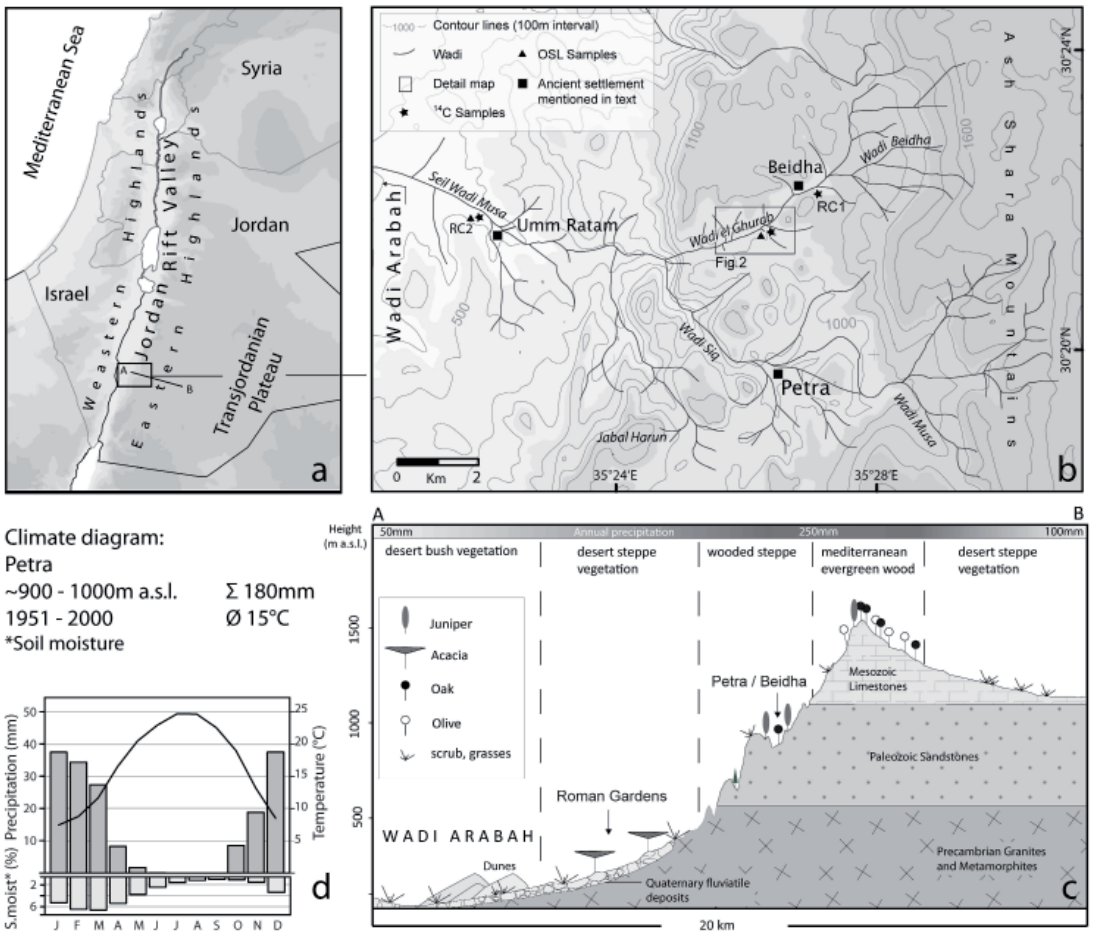

Fig. 1 1a: Location of the research area in the southern Levant, A-B indicates the approx. extent of the profile in Fig. 1c (Database: GTOPO30); 1b: Detail map of the topography, major drainage systems and sample locations in the Petra region (Database: AsterDEM); 1c: Schematic profile of the major ecoregions, annual precipitation and major geological units, from the Wadi Arabah and the Eastern Highlands to the Transjordanian Plateau adapted from Hunt et al., 2007; and Cordova, 2007) 1d: Climate diagram and soil moisture of the Petra region (data sources and methods see section 3.2.3).

The agricultural techniques applied in the area include runoff terrace systems (Lavento and Huotari, 2002; Gentelle, 2009; Kouki, 2009, and references cited). These systems are one of the various implementations of the agricultural terrace (reviewed in e.g.: Spencer and Hale, 1961; Treacy and Denevan, 1994; Frederick and Krahtopoulou, 2000). As described by Evenari and Tadmor (1982), Nabataean runoff terrace systems in the Negev consisted of a series of stone walls and were built, for example, across channel beds and floodplains of periodically discharging rivers (wadis) and on slopes. These walls (commonly called risers) retain and collect water and sediments of episodic flash floods and runoff events. Initially, the upslope area of each of the retaining walls gradually silted up (the filling technique is called self-filling), and terraces developed. When sufficiently large, the terraces were used for cultivation (the cultivated area is commonly called tread and the sediment body is called terrace fill or tread fill). Occasionally, and in the case of a positive sediment budget, the farmers added a new row of stones on top of the walls in order to heighten the terraces and thus enlarge the water storage bodies and the cultivation area. This ancient technique has been reported from many archaeological sites in the arid areas of the southern Levant and especially for the Negev (e.g.: Mayerson et al., 1961; Rosen, 2000; Avni et al., 2006; Hunt et al., 2007; Haiman and Fabian, 2009).

The Petra region is scattered with remains of such runoff terrace systems. Some of them are preserved and still cultivated by the local Bedouins, but most are abandoned and the walls and terrace fills are dissected by gullies. Most scholars attribute the initial construction of these systems roughly to the Nabataean/Roman time of occupation, mainly based on surface pottery and other relative dating techniques (e.g. Byrd, 1989; Lindner et al., 2000; Tholbecq, 2001; Lavento and Huotari, 2002; Gentelle, 2009; Kouki, 2009; Lavento, 2010). However, dating agricultural terraces using only these relative dating methods can be problematic because the pottery could indicate peak occupational phases rather than the initial time of construction. Moreover, sequent usage and maintenance work of the terraces could lead to an age underestimation (Treacy and Denevan, 1994; Frederick and Krahtopoulou, 2000; Krahtopoulou and Frederick, 2008 and references cited).

In this paper we present the results of a study to determine the chronology of selected runoff terrace systems and associated stone wall structures of the northern and western Petra region using optically stimulated luminescence (OSL) dating and radiocarbon dating.

The main goals of the study are to test the applicability of OSL dating in the Petra region and to gain first indications of the timing for the initial construction of the runoff terrace systems and phases of their usage. We therefore took OSL samples from profiles of the terrace fills and, if possible, from the sediments directly underneath the riser, assuming that (i) the tread stratigraphy generally corresponds to periods of filling by fluvial processes and (ii) the sediments underneath the walls had been reworked and exposed to sunlight during the wall construction (cf. Porat et al., 2006).

Two formerly intensively cultivated areas are investigated: the agricultural fields in the catchment of the Wadi al Ghurab, approximately 6 km north of Petra, and the cultivated fluvial terraces of the Seil Wadi Musa, the Roman Gardens, approximately 7 km downstream of Petra and next to the Roman fort of Um Rattam (see Figs. 1 and 2).

5.2.2 Study site

5.2.2.1 Occupational history

The main settlement phases before the Nabataean period have been related to the Natufian period, approximately between 10800 to 8300 BC (e.g. Byrd, 1989), the Pre-Pottery Neolithic, from about 8500 to 5500 BC, e.g. at Beidha (e.g. Byrd, 1989), and the Iron Age, at the time of the Edomite Reign, ca. 1200 to 540 BC (e.g. Bienkowski, 2001). Settlements during these phases were primarily isolated agricultural settlements, located at environmentally or strategically favourable spots such as springs or hilltops (e.g. Tholbecq, 2001). After the Iron Age the archaeological record lacks indications of permanent occupation in the study region for almost 300 years (Schmid, 2008).

Most of the archaeological remains of the area were dated to the Nabataean/Roman period of occupation (313 BC to 363 AD, see Taylor, 2002, for a general introduction to Petra). The Nabataeans were a nomadic tribe who became powerful by controlling an area of intersecting trade route networks (e.g. the incense road) in the southern Levant. Petra was built at such an intersection and soon became a regional central place and the capital of the Nabataean Kingdom, with monumental administrative and religious buildings. In 106 AD, after the Roman influence in the region grew stronger, Petra was annexed by the Romans (Graf, 1992). Petra remained an urban central place until the major trade routes shifted to the east and south in the 4th century AD. The city finally lost its significance as a functional entity after the high magnitude earthquake of 363 AD (Schmid, 2008). During the Byzantine period (324 to 630 AD), the Petra region reverted to a rural landscape with scattered villages and seasonal Bedouin camps (Lindner, 1999; Tholbecq, 2001; Schmid, 2008). After the Islamic conquest (634 - 635 AD), the former settlement characteristics of the Petra region are likely to have continued until after the Umayyad period (661 – 750 AD), when a decline of settlements is visible in the archaeological record. In the early 12th century AD, the region became strategically important for the crusaders until they were defeated by the Ayyubid in the late 12th century (´Amr and Al-Momani, 2001). Again, few changes in the general settlement pattern of the region are postulated for the Ayyubid/Mamluk period (12th - 16th century AD) and for the Ottoman period (16th - 19th century AD). Throughout the aforementioned periods, archaeological evidence and written sources suggest that agriculture was intensively practised and constituted an important part of the rural economy (Kouki, 2009 and references cited).

5.2.2.2 Geology and geomorphology

The Petra region is located in the Eastern Highlands of the Jordan Rift Valley, which rise up almost 2000 m a.s.l. from the arid plains of Wadi Arabah to the desert steppes of the Transjordanian Plateau (see Fig. 1a-c). The region is part of the Arabian plate and composed of Precambrian granites and volcanoclastics, covered by a thick sandstone section (Nubian type) and a thick sequence of marine carbonates (Fig. 1c) (Bender, 1974). Between ~ 600 and 1000 m a.s.l., corresponding to the altitudinal belt where Petra and the Wadi al Ghurab are located, deeply weathered Cambrian-Ordovician sandstones overlie the Precambrian igneous basement. The main sandstone formations are the Umm Ishrin Formation of Cambrian age and the Ordovician Disi Formation (Barjous, 1995). The sandstone formations are dissected by deep gorges and canyons which run along various faults and fissures. Sandstone cliffs, buttes and mesas, almost barren of vegeta-

tion and sediment cover, are characteristic of this area (Bender, 1974). Above ~ 1000 m a.s.l., the highlands are composed of Cretaceous limestones and are called the Ash-Shara Mountains. The moderately inclined slopes are covered with a thin layer of the weathering residues of the limestones (Barjous, 1995). The footslopes of the Eastern Highlands partly consist of massive tilted blocks of the limestone formation which were tectonised during the rift process. These blocks form the bordering hills of Seil Wadi Musa.

The sedimentary environment of the Petra region is dominated by high energy fluvial processes with localised episodic gains and losses in the sediment budget (cf. Baird, 1989; Tooth, 2000). Fluvial aggradation and incision are mainly controlled by tectonically induced base level changes, climate fluctuations and human impact. However, since the Mid-Holocene at the latest, the major wadis of the region are likely to have been mainly in an incision stage (Raikes, 1966; Field, 1989; Kouki, 2006; Rambeau et al., 2011). Fragmented alluvial terraces can be found along the major wadis, and some of the gorges are intermittently filled with gravel and sand, especially in the rocky upland of the sandstone formations. The most extensive fluvial terraces in the region are the Pleistocene terraces along the braided channel system of Seil Wadi Musa. They consist of poorly sorted gravels and sands (Bender, 1974; Barjous, 1995; Horowitz, 2001). The Roman Gardens were built on top of these terraces. Remnants of extensive valley fills are present in the few wider valleys and basins of the region, most significantly in the valley where Petra was built, the area south of Jabal Harun and the Wadi al Ghurab (Bender, 1974). In the Wadi al Ghurab catchment, the valley fills are dissected by gully systems and only a few smaller ridges and plains have remained (e.g. the Beqah Plain, Fig. 2). Some gullies expose up to 15 m thick sediment sequences, e.g. along Wadi al Beqah and Wadi al Jordan (Fig. 2). The fills are composed of unconsolidated fluvial silts and sands and occasional embedded gravel layers. The dominant source rock of the unconsolidated sediments in this area is the sandstone bedrock (Bender, 1974; Gentelle, 2009). Ongoing incision of the gullies most likely followed the entrenchment of the Wadi al Ghurab, which occurred before the Mid-Holocene (Raikes, 1966; Field, 1989; Rambeau et al., 2011).

5.2.2.3 Climate, hydrology and vegetation

The Petra region is located in the semi-arid to arid transition zone of the southern Levant. In general, these climatic conditions have prevailed since the Mid-Holocene aridisation of the southern Levant at the latest (Robinson et al., 2006; Finné et al., 2011; Rambeau et al., 2011; Roberts et al., 2011)

The region is characterised by a steep environmental gradient due to the orographic effect of the Eastern Highlands (see Fig. 1c; Cordova, 2007 and references cited). The predominant sources of moisture are Eastern Mediterranean cyclones tracking east (Harding et al., 2009). The region has a winter rain regime, and torrential rainfall events are common in the mountains (Al-Weshah and El-Khoury, 1999).

In the lowlands of the Wadi Arabah, the erratic rainfall averages about 50 mm per year, and the mean annual temperature is 25°C. The region is classified as an extension of the Sudanian and Saharo-Arabian vegetation provinces with desert bush vegetation and scattered acacias and tamarix (Al-Eisawi, 1996).

Between 900 and 1000 m a.s.l., annual rainfall increases to 180–200 mm, and the mean annual temperature is about 15°C (Al-Weshah and El-Khoury, 1999, see Fig. 1d for a climate diagram). Junipers and oaks grow in favourable spots along the shady gorges of the sandstone formations and constitute a wooded steppe ecoregion.

In the Ash–Shara Mountains annual rainfall is 300 mm, potentially allowing the growth of Mediterranean-type dry woodland (Al-Eisawi, 1996). Further east, in the rain shadow of the highlands, annual rainfall drops again below 100 mm, and the Mediterranean woodland is succeeded by the monotonous desert steppe of the Transjordanian Plateau (Al-Eisawi, 1996).

Abundant bedrock exposures, steep slopes and strong relief constitute mainly quickly responding sub-catchments with a high runoff coefficient and a short time of runoff concentration (cf. Baird, 1989; Tooth, 2000). Flash floods, either channelled in the wadis and gullies or laminar as sheet flows, are a common phenomenon in this area, occurring during and shortly after heavy rainfall events, mostly in the winter months (Al-Weshah and El-Khoury, 1999). Perennial water flow in the wadis only occurs near the few springs of the region (Al-Khashman, 2007).

5.2.3 Sample locations

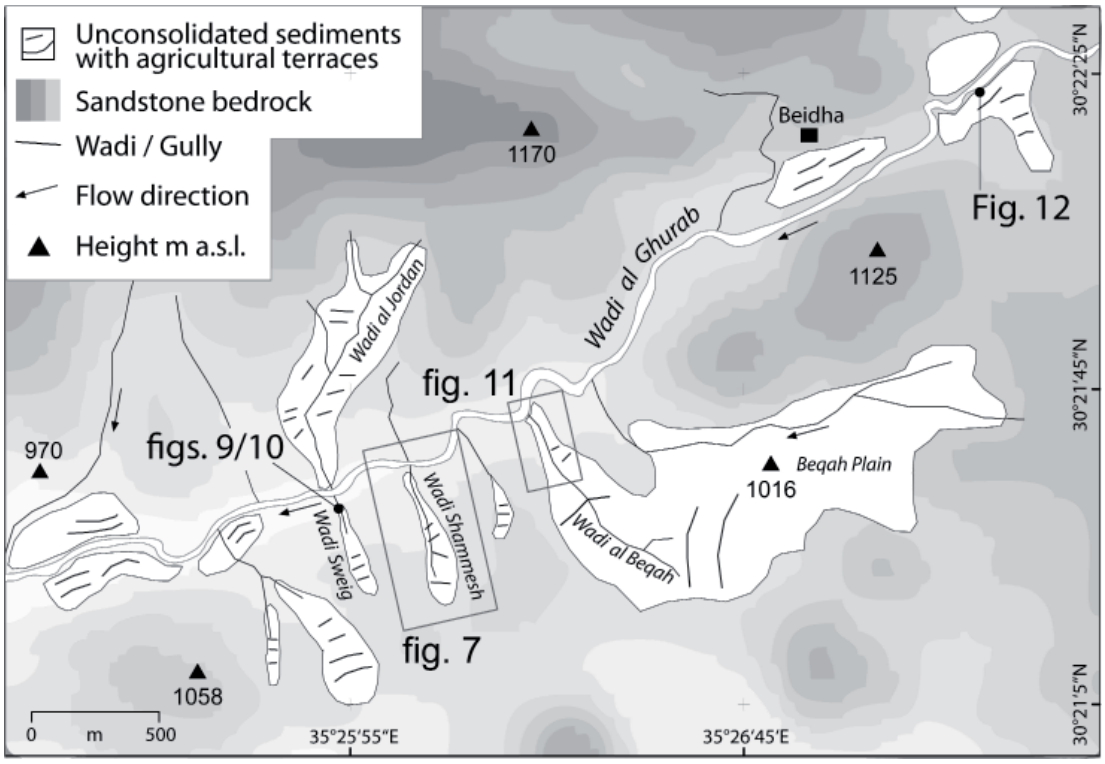

Fig. 2 Detail map of the catchment of Wadi al Ghurab with sampling areas (Database: AsterDEM and aerial photos taken by the Institut Géographique National (IGN) in France).

The following description of the study sites starts at the sample locations in the Wadi al Ghurab catchment and then continues to the site in Seil Wadi Musa. This order will be kept throughout the paper.

The Wadi Shammesh and Wadi Sweig are part of a series of tributaries of the Wadi al Ghurab that drain the northern and southern slopes of its lower catchment (Fig. 2). These tributaries have similar catchment characteristics and have been modified in a similar manner by the ancient engineers. The catchments of these tributaries have varying sizes of less than 1 km in length and up to 200 m in width, and the slopes are moderately inclined and vary between ~ 1° and 10°. The divides and backslope areas are sandstone-dominated and are covered by a thin layer of sandstone clasts and sandy weathering re-

sidues. The valley bottoms are covered with up to 3 metres of unconsolidated sediments (see section 5.1 for exemplary stratigraphy). The wide occurrence (up to 70 % of the drainage basin area) of almost impermeable bedrock creates a high runoff coefficient for the catchments. Owing to the small size of the catchments, they have a relatively short time of runoff concentration, which is attenuated by the moderately inclined slopes and the elongated catchment shape. These catchment physical characteristics in conjunction with the prevailing rainfall character (see section 2) are near to optimal for the application of water harvesting techniques (Bruins et al., 1986; Critchley et al., 1994).

The wadis were terraced by building a series of rock embanked barrage terraces, arranged ~ 20 to 40 m apart from each other, which constitute step-like, consecutive fields (Fig. 3). The similarities in masonry and general appearance of the risers suggest that the barrage terraces were constructed as one unit, as was the usual construction of these systems (cf. Evenari and Tadmor, 1982; Critchley et al., 1994; Waltham, 1994).

The risers have varying widths of 20 – 40 m, are up to 3 m high (measured from the base) and are aligned perpendicular to the dominant flow direction. The risers of the major terraces are dry-stone walls, made up of interlocking, crudely carved sandstone cobbles, with mean dimensions of ~70×60×50 cm, and the gaps are filled with gravel (Fig. 3/9). The walls show signs of maintenance work such as filling of collapsed parts

Fig. 3 Photo of the agricultural terrace system in Wadi Shammesh, looking south. Note the gully extending from the lower right corner of the picture.

with gravel and smaller cobbles. In some of the catchments, smaller check dams were built across tributary gullies in the headwater areas, which document attempts to mitigate erosion (cf. Sandor et al., 1990).

In the middle and lower course of the valleys, fine and unconsolidated sediment aggradations are almost always associated with agricultural terrace walls. Nowadays the terrace walls and fields are dissected by gullies and rills. In consequence, some of the fields give the impression of small-scaled badlands.

The Beqah Plain (see section 2 and Fig. 2) extends over large parts of the Wadi Beqah drainage basin. At the western side of the plain, a deep gully with a well-developed dendritic drainage network dissects the plain. It is assumed that the general drainage system developed prior to the construction of the agricultural terraces and retaining walls because presumably ancient retaining walls are adjusted to it. The Beqah Plain is crossed by several ancient and partly buried stone walls, running from north to south, whose purpose was most likely to intercept sheet flows and to control erosion (Gentelle, 2009). The sample site in this catchment is located where the Wadi Beqah emerges from the plain and has deposited an elongated fan, indicated by the shape of the length profile (Fig. 11a and b). The fan is composed of unconsolidated silty sand and confined by sandstone ridges along the eastern and western side. The southern side is bordered by an escarpment which descends from the Beqah Plain. The northern part of the fan is truncated, most likely by the episodic floods of the Wadi al Ghurab. This area has been reclaimed by building barrage terraces across the fan and by building retaining walls that stabilise and level the erodible slopes descending from the Beqah Plain.

Sampling site RC1 is located approximately 300 m west of the Neolithic settlement of Beidha and next to the confluence of Wadi Beidha and Wadi al Ghurab (Fig. 2). The Wadi al Ghurab conveys periodically high energy floods through its well-defined bedrock and pebble-bedded channel (Byrd, 1989). Along the southern bank of the wadi, fine sediments have accumulated on top of coarse pebbles of the Wadi al Ghurab and constitute an approximately 100 m wide and 400 m long, moderately inclined and elevated plain. To the south, the plain is bordered by sandstone mesas. At the eastern part, a small terraced wadi, originating from the Ash-Shara Mountains, emerges on the plain. The plain is crossed by several, east-west oriented, partly buried agricultural terrace walls. To the north, the plain drops – with a step of about 2 to 4 m – to the Wadi al Ghurab. The escarpment has been stabilised by retaining walls, remains of which can be found along the escarpment (see Byrd, 1989; Rambeau et al., 2011 for a comprehensive introduction to the proximate environmental setting).

RC2 is located at the southern bank of the Seil Wadi Musa, ~ 500 m downstream of the Roman fort of Umm Ratam, and is part of the Roman Gardens (Fig. 1b, cf. Lindner et al., 2000). Terrace agriculture was practised here on a small elevated plain of ~ 80 × 30 m, which is enclosed on three sides by the limestone hills of the Wadi Arabah (see section 2.1). The plain is composed of sandy silt, accumulated on top of the coarse gravels of the Seil Wadi Musa. The fine sediments presumably derive from the weathering residues of the limestone hills, rather than being floodplain sediments of the Seil Wadi Musa. To the north the plain drops about 3 m to the gravel-bedded Seil Wadi Musa. The plain is divided by a tributary wadi that drains the southern hills. Along its course, the wadi is intermittently retained by several small check dams, and the plain is crossed by rock-embanked agricultural terrace walls (see Lindner et al., 2000 for a general introduction to the Roman Gardens).

5.2.4. Methods and materials

We focused our investigations on runoff terraces that employ stone walls with a minimum height of 1 m and those which showed indications of antiquity, such as weathering marks, stone patina or lichen on the exposed terrace walls. This minimises the risk of dating modern terraces. We further concentrated on terraces where erosion exposed a readily available profile of the terrace wall and the terrace fill, as our survey permit allowed us to dig only small test trenches. Two types of runoff terraces were investigated: (i)

barrage terrace systems built in wadi channels and (ii) retention terraces constructed on slopes and floodplains.

Sediments from agricultural terrace fills with a high proportion of sand were selected for OSL dating in order to obtain sufficient amounts of medium to coarse-grained sand (see section 3.3.1). For radiocarbon dating, charcoals embedded within silt-dominated tread fills were also included in this study.

The tread fills of runoff terraces are predominantly fluvial deposits, either transported by sheet flows or channelled floods (Evenari and Tadmor, 1982; Critchley et al., 1994). OSL dating of such deposits can be challenging because of the problem of incomplete bleaching (Rittenour, 2008). However, numerous studies on fluvial deposits in drylands show OSL ages consistent with independent age control (e.g. Feathers, 2003; DeLong and Arnold, 2007; Porat et al., 2010; Guralnik et al., 2011). Of particular relevance for this study are the results of Avni et al. (2006) who used OSL to date alluvial terraces of wadi systems and agricultural terrace fills of Nabataean floodwater farms in the Negev. The OSL ages fall in the expected archaeological time frame and are stratigraphically consistent (Avni et al., 2006). By contrast, Kouki (2006) reports problems when she estimated burial ages of fluvial and agricultural terraces in the Petra region (around Jabal Harun, Fig. 1b) using OSL. The results are said to be stratigraphically inconsistent and do not match the archaeological record. She attributed this to incomplete bleaching of the sediments and the application of large aliquots for OSL measurements (cf. section 3.3.2).

Age determination of fluvial deposits, applying radiocarbon dating of embedded organic material, might also be problematic owing to reworking and redeposition processes (Schiffer, 1986; Gillespie et al., 1992). However, the sample locations are in the vicinity of ancient settlements or along ancient paths and roads (cf. Lindner et al., 2000; Tholbecq, 2001), where hearths are the likely source of charcoal. Moreover, the sediments deposited behind terrace walls are commonly only locally reworked (Frederick and Krahtopoulou, 2000). Thus, a single and short erosion-transportation-deposition cycle for the sampled charcoal is assumed.

The field survey included a preliminary documentation of the catchment characteristics with a focus on the runoff terrace structures. The results of these investigations are presented in detail for Wadi Shammesh. For the other sample locations, a brief description of the environmental and archaeological context of the OSL and radiocarbon samples is given (see sections 2.4 and 5).

5.2.4.1 Mapping and sediment analysis

Geomorphological mapping was based on aerial photos and ground surveys during two field campaigns in 2009 and 2010. Detailed cross and length profiles of valleys and slopes were measured using a measuring tape and an inclinometer. Grain size distribution of selected terrace fills, were measured using laser diffractometry (Beckman Coulter LS 13320 PIDS) for grain sizes < 2 mm, after sample partition by sieving. Statistical analysis of the grain size results was made using GRADISTAT, and grain size description in the text is based on the terminology and its associated size scale used in the program (Blott and Pye, 2001). The carbon content of one terrace fill (Wadi Shammesh) was determined using dry combustion in a Woesthoff Carmhograph 16 (e.g. Dean, 1974; Schütt et al., 2010). Loss on ignition was measured according to DIN 19684 (1977) to estimate the soil organic content (SOC) of terrace fills RC 2 and RC 3. Following Hesse et al. (2009), it is assumed that the LOI values at 550°C roughly represent the SOC and that loss from structural water in clay minerals is negligible in this study (Ball, 1964).

5.2.4.2 Radiocarbon dating

Charcoal fragments were sampled from sediment exposures after the profiles had been cleaned (Table 1 for sample laboratory numbers and locations). The samples were analysed at the Poznań Radiocarbon Laboratory in Poland, which uses accelerator mass spectrometry (AMS). The δ13C values determined by the Poznań Laboratory cannot be used for palaeoecological reconstruction because the applied graphitisation process and the AMS spectrometer introduce significant isotopic fractionation (Thomasz Goslar, Head of the Poznań Radiocarbon Lab., personal communication, March 2011).

All radiocarbon ages presented in this study were calibrated using the OxCal v.4.1 software (Bronk Ramsey, 2009) and the IntCal04 calibration curve (Reimer et al., 2009).

5.2.4.3 OSL dating

Sampling, laboratory treatment and measurement protocols

Thirteen sediment samples were taken with metal tubes from cleaned profiles under daylight (see Table 1 for sample laboratory numbers and locations of the samples). The tubes were stuffed with aluminium foil to avoid disaggregation and mixture of the sediment and sealed afterwards. For transportation to Germany the samples were repacked into opaque plastic bags in darkness, after the upper and lower ~ 4 cm of the sediment core had been removed. A few hundred grams of additional material were sampled for gamma spectrometry.

All subsequent laboratory treatment and analysis was made under subdued red light at the Leibniz Institute for Applied Geophysics in Hannover. The samples were dried at 50°C for at least one day and then sieved. The coarse-grained quartz fraction of 150 - 200 µm was chosen for further analysis, as suggested by Rittenour (2008) for fluvial sediments. For samples yielding only a low amount of material (<1 g) in the aforementioned grain size group, the 100 - 200 µm fraction was taken (two samples, Table 2).

After treatment with hydrochloric acid, sodium oxalate and hydrogen peroxide, quartz-dominated grains were separated using heavy liquid (sodium polytangstate). The quartz grains were etched for one hour in concentrated hydrofluoric acid (HF), and the acid-soluble fluorides were removed in 20 % hydrochloric acid.

Luminescence signals were measured using an automated Risø TL/OSL-DA-15 reader (Bøtter-Jensen et al., 2003), equipped with blue LEDs (wavelength 470 nm). The OSL signals were detected through a 7.5 mm Hoya U-340 filter. The quartz grains were irradiated using a calibrated 90Sr/90Y beta source within the reader. The single-aliquot regenerative-dose (SAR) protocol was used for the performance tests and the equivalent dose (De) measurements (Murray and Wintle, 2000, 2003). The SAR protocol requires performance tests for the samples to be measured in order to evaluate the applicability of the protocol and to determine the preheat temperature (Murray and Wintle, 2000, 2003). A dose recovery test at different preheat temperatures between 160 and 260 °C was made for a representative sample (LUM2349). Dose recovery tests using the selected temperature (180°C) were made on almost all analysed samples. The recuperation ratio was calculated for sample LUM2349. For De measurements 96 aliquots were measured for each sample except LUM2349, for which 69 aliquots were measured.

Aliquot size

Most of the fluvial sediments are likely to be incompletely bleached (Rodnight et al., 2006; Arnold et al., 2007). The most reliable method to determine the De for such deposits is the measurement of single grains (Duller, 2008). On a multi-grain aliquot, mineral grains

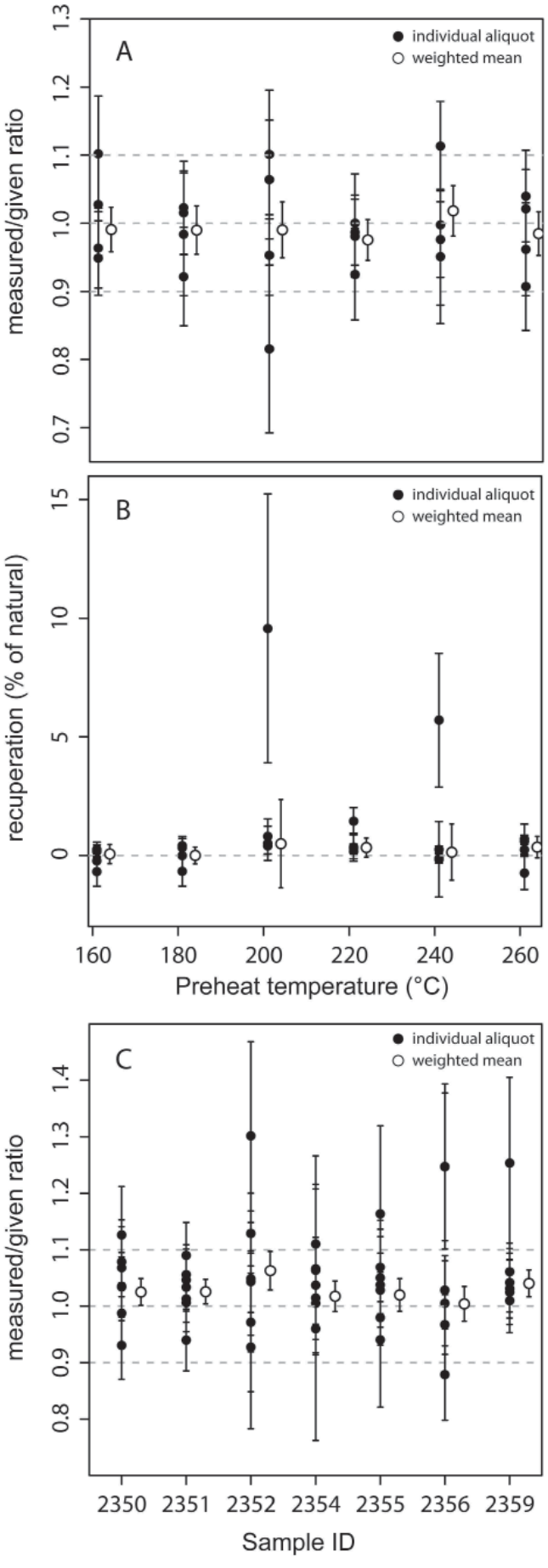

Fig. 4 Dose recovery test (4a) and recuperation ratio (4b) at different preheat temperatures for sample LUM2349. 4c: Result of the dose recovery test for selected OSL samples. Individual aliquots are shown with error bars and the respective weighted mean.

with different degrees of bleaching could contribute to the measured luminescence signal. An averaged signal might be recorded, masking the sample´s luminescence variance, and this potentially leads to an age overestimation of the burial event in question (Rittenour, 2008). Alternatively, studies show that small aliquots can yield results which represent the samples per-grain De variance, due to the low percentage of quartz grains emitting a detectable luminescence signal (Duller, 2008).

In order to find an adequate aliquot size which can avoid problems encountered with multi-grain aliquots, we made pre-tests using aliquots loaded with different mask sizes of Ø 1 mm, Ø 2.5 mm and Ø 6mm, respectively. We counted an average number of grains for each aliquot size of about 20, 100 (150 - 200 μm), 140 (100 - 200 μm) and 1200 grains, respectively.

A large scatter of De values by applying the 6-mm aliquots on LUM2349 confirmed the expected partial bleaching of the samples, and their use was rejected. Measurement of 60 1-mm aliquots showed that only ~ 5 % of the aliquots emitted a measurable signal, whereas ~ 50 % of the 2.5-mm aliquots could be measured. We therefore assume that the averaging effect is negligible for 2.5-mm aliquots and applied the 2.5-mm aliquots for all De measurements. Dose recovery tests were conducted using 6-mm aliquots.

Dose rate estimation

The dose rate was estimated by measuring the activities of 238U, 232Th series radionuclides and 40K from 50 g of the sediment using a High-Purity Germanium N-type coaxial detector. The β- and γ-dose rates were calculated using standard conversion factors (Meijdahl, 1979; Adamiec and Aitken, 1998). Owing to the HF-etching of the quartz grains the α-irradiation contribution to the dose rate is negligible (Aitken, 1998). The cosmic dose rate was estimated using the sample´s burial depth and the approach described by Prescott and Hutton (1994) and Prescott and Stephan (1982).

The water content of the sediment was estimated using the Thornthwaite Monthly Water Balance Model (Markstrom and McCabe, 2007), and the pedotransfer functions implemented in the SPAW Model (Saxton and Willey, 2006). In the absence of available data from a representative meteorological station, the climate data were estimated based on the gridded DEKLIM VASClimO data set for monthly precipitation (Beck et al., 2005) and the gridded NOAA NCEP CPC CAMS data set for monthly temperature (Fan and van den Dool, 2008). The statistical parameters of the climate data correspond to those reported for the Petra region (Al-Weshah and El-Khoury, 1999; Touchan et al., 1999). The soil input parameters (i.e. grain size distribution and organic content) for the SPAW model were measured in the laboratory (section 3.1). The modelled period was from 1950 to 2000 and an average soil moisture of 3% was calculated. The averaged monthly soil moisture variations are shown in Fig. 1d. To account for potential climate variations during the past, an error of 100% was added to the calculations and the water content was set to 3% ± 3%.

Data analysis

The OSL data were analysed using Analyst v. 3.24. We followed the suggestions of Cunningham and Wallinga (2010) to use the fast component of the OSL signal and to subtract the Early Background (EBG). Representative OSL-decay curves showed that by integrating the OSL signal from the first 5 channels (< 0.8s) and subtracting the EBG (0.8 – 1.6 s) we mainly use the fast component and minimise the influence of the medium component. These integration limits were applied to all the samples.

The rejection criteria for aliquots are as follows: (i) recycling ratio > 10 % of unity (Duller, 2003), (ii) a test dose error > 15 %, and (iii) if the luminescence signal of the test dose was within 3σ of the background signal (Alexanderson and Murray, 2009). The dose response curve was constructed by fitting an exponential function through the sensitivity-corrected OSL responses, including the recycling points and forcing the curve through the origin. An instrumental measurement error of 3 % was added to the curve fitting.

Statistical analysis

The Kolmogorov-Smirnov method was used to test normality of the dose distributions as done by e.g. Reimann et al. (2010) after removing extreme outliers (> 4σ). The burial ages of those samples determined to be normally distributed were calculated using the central age model (CAM) (Galbraith et al., 1999). This model was also used to calculate the over-dispersion (σb) for all the other samples. Samples which were considered to be non-Gaussian and had a high over-dispersion and significant skewness (according to Bailey and Arnold, 2006) were considered to be incompletely bleached. The most common age models applied for incompletely bleached fluvial deposits is the minimum age model (MAM) (Galbraith et al., 1999) and the finite mixture model (FMM) (Galbraith and Green, 1990; Roberts et al., 2000). However, both models have their drawbacks. The most significant ones for this study are (i) the potentially strong influence of outlying low De values on the MAM calculations (Rodnight et al., 2006), and (ii) the potential inability of the FMM to identify the correct number of burial dose populations in multi-grain aliquot derived De estimates (Arnold and Roberts, 2009). As suggested by Rodnight et al. (2006), we therefore applied the FMM only to identify outlying low De values and, if present, removed them for subsequent modelling with the MAM. FMM components comprising < 10% of aliquots were disregarded as suggested by Rodnight et al. (2006). For comparison and further discussion, we present the results of both models (Table 2). Depending on the statistical properties of the samples De distribution, either the MAM-3 or the MAM-4 has to be chosen (Galbraith et al., 1999); we based our choice on the criteria suggested by Bailey and Arnold (2006).

The MAM and the FMM require an estimation of the samples' σb (Galbraith et al., 1999). The σb might be estimated using well-bleached samples representative for the research area (Duller, 2008). Two samples (LUM- 2352, -2354) are normally distributed and thus considered to be well bleached (see section 4.2 for geomorphological reasoning). The CAM calculated a σb of 8% for sample LUM2352 and 18% for sample LUM2354, and the average of 13% was used for running the models. The values are consistent with values reported for well bleached and undisturbed samples (Galbraith et al., 2005; Arnold and Roberts, 2009). The models were run in R, using scripts written by Rex Galbraith in 2006 (FMM-script) and modified in 2010 (MAM- and CAM-script).

5.2.5. OSL and radiocarbon ages

5.2.5.1. OSL performance tests

The dose recovery test of sample LUM2349 shows no significant dependency of the De weighted mean (n = 4) on preheat temperatures between 180 °C and 260 °C and is consistent within the unity at 1σ. The recuperation ratio is consistent with 0 % at 1σ for both the individual aliquots and the weighted mean up to a temperature of 180 °C. However, the individual aliquots show a scatter of above 2σ from unity for the dose recovery test and 2σ above 0 % of the recuperation ratio at 200 °C (Fig. 4a/b). To avoid these (minor) thermal effects, a preheat temperature of 180 °C was chosen.

The weighted mean of the dose recovery ratio for individual samples (n=7 per sample) is consistent with unity at 1σ for all samples (Fig. 4c). Scatter is present in the results of individual aliquots, but their errors lie within the 1σ bound in more than 95 % of the cases. The SAR protocol was therefore accepted as being suitable for determining the De of the investigated samples using the selected run conditions.

5.2.5.2 Equivalent doses and ages

Thirteen OSL samples were measured to determine their burial ages. Three samples from different sub-catchments of the Wadi al Ghurab were rejected for further analysis because none of the respective aliquots emitted a measurable natural luminescence signal above background noise. There are also large differences in the rejection ratio between the remaining samples (Table 2). Eighty-seven percent of the measured aliquots of sample LUM2366 were rejected (most of the aliquots due to very low signal to noise ratios), whereas only 34 % of sample LUM2350 were rejected. In this study, we could not finally evaluate which factors are responsible for the differences in luminescence sensitivity, but they may be caused by different source rocks of the quartz grains (cf. Tokuyasu et

Table 1. List of OSL and radiocarbon samples, with location, sedimentary context and final calendar ages with 2σ-errors.

Location Sample ID	Depth (cm)	Coord. UTM 36N Easting	Northing	Material	Sample Context	Calendar Age (years ± 2σ)
Wadi Shammesh						
LUM2349	150	733975	3361037	Sand	Terrace fill	440±300 AD†
LUM2350	100	733975	3361037	Sand	Underneath riser	330±420 BC†
LUM2351	65	733975	3361037	Sand	Terrace fill	730±180 AD†
Wadi Sweig						
LUM2365	120	733687	3361024	Sand	Underneath riser#	1270±320 AD☼
LUM2366	70	733687	3361024	Sand	Terrace fill	840±140 AD☼
Wadi Beqah						
LUM2352	90	734432	3361273	Sand	Terrace fill	1000±100 AD☼
LUM2354	70	734432	3361273	Sand	Terrace fill	1120±140 AD☼
LUM2356	70	734404	3361292	Sand	Terrace fill	1000±200 AD☼
LUM2357	100	734347	3361401	Sand	Underneath riser	1060±140 AD☼
Pet13_1	140	736022	3362858	Charcoal	Fan deposits*	3320±200 cal BC†
Pet13_2	190	736022	3362858	Charcoal	Fan deposits*	4320±100 cal BC†
Wadi al Ghurab RC1						
Pet20_1	25	736022	3362858	Charcoal	Terrace fill	870±100 cal AD†
Pet20_2	110	736022	3362858	Charcoal	Terrace fill	240±100 cal AD†
Pet20_3	155	736022	3362858	Charcoal	Terrace fill	150±80 cal AD†
Seil Wadi Musa RC2						
Pet25_1	35	727419	3361704	Charcoal	Terrace fill	200±110 cal AD†
Pet25_2	75	727419	3361704	Charcoal	Terrace fill	120±110 cal AD†
Pet25_3	145	727355	3361742	Charcoal	Terrace fill	100±90 cal AD†
LUM2359	220	727419	3361704	Sand	Gravel Layer#	510±130 AD☼

* most likely pre-dates terrace construction, see section 5.3

most likely post-dates terrace construction, see section 5.2 and 5.5

† radiocarbon age

☼ OSL age

Table 2. Summary of the OSL results. Frames highlight the results chosen for age determination of the agricultural terraces (see Table 1 for final calendar ages).

Location	Dose rate					CAM		FMM[f]				MAM[f]	
Sample ID	Cosmic (Gy/ka)	Sediment (Gy/ka)	Total (Gy/ka)	n[a]	σ_{OD}[b] (%)	D_e (Gy)	Age[c] (a)	D_e (Gy)	Age[c] (a)	k[d]	Prop.[g] (%)	D_e (Gy)	Age[c] (a)
Wadi Shammesh													
LUM2349*	0.20±0.02	1.38±0.08	1.58±0.08	69/31	33.7	3.65±0.34	2310±110	2.47±0.10	1560±60	3	31±0.1	2.49±0.21	1570±150
LUM2350*	0.20±0.02	2.00±0.12	2.20±0.12	96/64	33.3	6.76±0.33	3070±70	6.00±0.27	2730±70	4	58±0.1	5.15±0.38	2340±210
LUM2351*	0.22±0.02	2.24±0.12	2.46±0.12	96/60	45.5	4.48±0.45	1820±110	3.25±0.09	1320±60	3	62±0.1	3.14±0.14	1280±90
Wadi Sweig													
LUM2365*	0.20±0.02	2.70±0.13	2.89±0.14	96/25	53.5	3.71±0.54	1280±150	2.10±0.29	730±150	4	21±0.2	2.14±0.33	740±160
LUM2366*	0.22±0.02	2.94±0.14	3.15±0.14	96/13	66.5	4.85±0.67	1540±140	3.51±0.22	1110±80	3	74±0.2	3.68±0.19	1170±70
Wadi Beqah													
LUM2352*	0.21±0.02	2.84±0.13	3.06±0.13	96/25	8.02	3.08±0.08	1010±50	Na	Na			3.08±0.12	1010±100
LUM2354[$]	0.22±0.02	2.84±0.13	3.05±0.13	96/40	18.4	2.71±0.18	890±60	Na	Na			2.56±0.19	840±120
LUM2356[$]	0.22±0.02	3.17±0.14	3.38±0.14	96/52	44.6	5.08±0.45	1500±100	3.57±0.26	1050±80	4	39±0.2	3.41±0.31	1010±100
LUM2357*	0.21±0.02	2.64±0.13	2.85±0.13	96/41	51.9	3.52±0.52	1240±160	2.66±0.14	930±70	4	63±0.2	2.70±0.14	950±70
Seil Wadi Musa													
LUM2359*	0.19±0.02	1.50±0.11	1.67±0.11	96/52	57.4	4.10±0.57	2460±150	2.51±0.10	1510±80	3	43±0.1	2.50±0.14	1500±90

CAM - Central Age Model / FMM - Finite Mixture Model / MAM - Minimum Age Model

a - number of aliquots, measured/accepted

b - overdispersion value (Galbraith et al., 1999)

c - Age calculated by dividing the D_e by the total dose rate, in years ago (before 2010)

d - number of components

f - σ_{OD} value to run the models was set to 13%, which is the σ_{OD} average of the well bleached equivalents LUM2354 and LUM2352

g - Proportion of the (lowest) population

* 150 - 200 µm, [$] 100 - 200 µm, grain size fraction

al., 2010). In the Wadi al Ghurab catchment two major sandstone units are exposed: the fine to medium grained, micaceous sand- and siltstones of the Disi formation, considered to be sediments of a transitional, marine to fluvial facies, and the quartzose, medium to coarse grained Umm Ishrin sandstones, whose environment of origin is assumed to be an extensive braided river system (Barjous, 1995). Unfortunately, the scale of the geological map (1:50,000) is too small to reliably attribute a geological unit to an individual sub-catchment. Porat et al (2009), facing similar problems in their study, used the very fine sand fraction to determine the age of alluvial deposits in the southern Negev and the Judean desert. Some of these sediments are fluvially reworked aeolian deposits which originated in North Africa. They showed excellent OSL characteristics in comparison to the quartz, which was recently eroded from the local granites and sandstones. However, the sediments of the OSL-dated terrace fills in this study are dominated by locally eroded quartz (see section 2.2), and an aeolian component could not be clearly identified (cf. Rambeau et al., 2011).

The location, environmental context and final calendar ages of the remaining 10 samples are summarised in Table 1. The final calendar ages are additionally plotted in Fig. 6.

The results of the statistical analysis and the dose rates for each sample are summarised in Table 2. Ages in Table 2 are reported in years ago (before 2010, ± 1σ errors). In the site-specific discussion and Table 1, ages are reported in calendar years (BC, AD, ± 2σ errors) for better comparison with the 14C ages and the archaeological record. Histograms and radial plots of one well-bleached and one partially bleached sample are shown in Fig. 5a and Fig. 5b respectively.

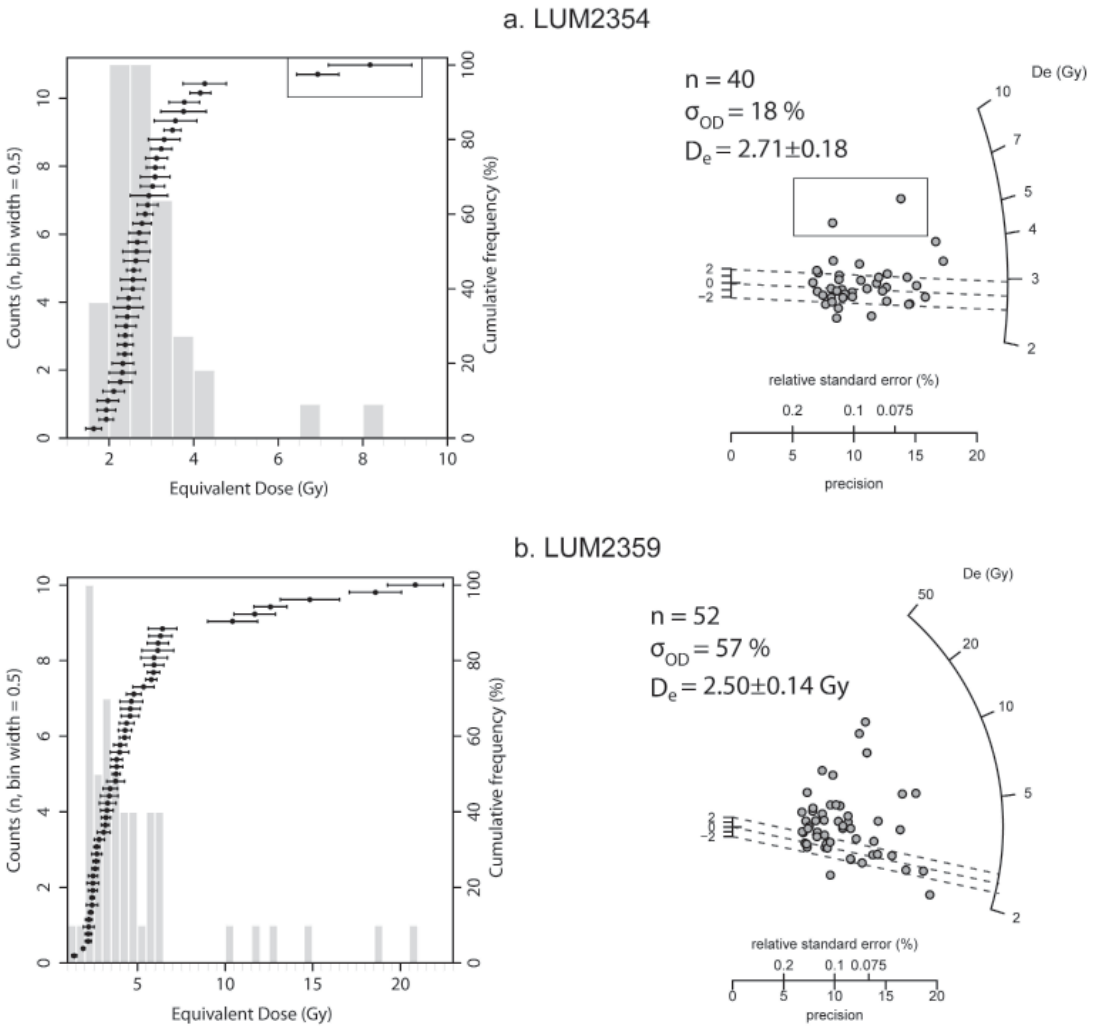

Fig. 5 Histogram and cumulative frequency plots (left side) and radial plots (Galbraith, 1988) of De distributions for selected samples. The dotted lines show the De values with 1σ errors, calculated with the respective age model; the boxes highlight the De values which were removed before further analysis (see section 3.2.5.).

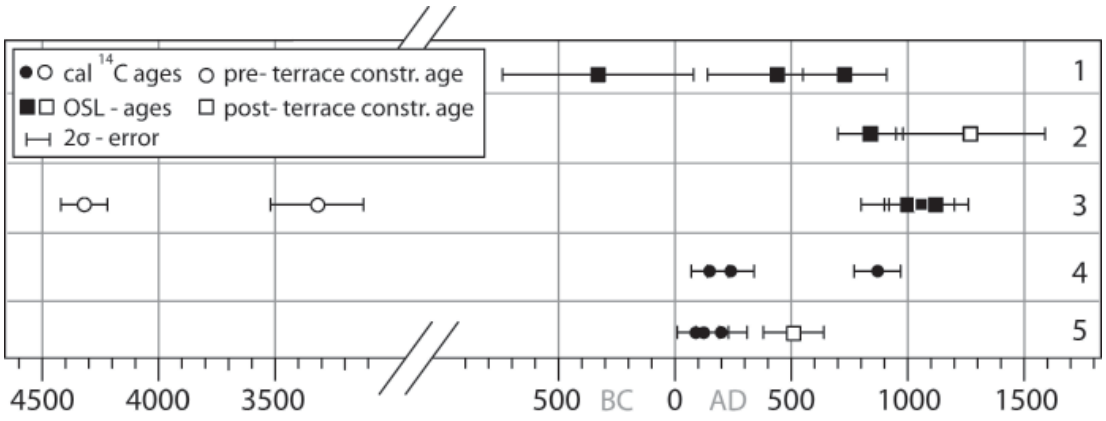

Fig. 6 Summary plot of the OSL and radiocarbon ages at the respective sample sites, with 2σ-errors (see also Table 1, listed from top to bottom according to order in study site section). 1. Wadi Shammesh, 2. Wadi Sweig, 3. Wadi Beqah, 4. Wadi al Ghurab RC1, 5. Seil Wadi Musa RC2. Pre-/post-terrace construction age refers to samples which are assumed to be not directly associated with the construction of the agricultural terraces.

Two samples (LUM2352, -2354) were determined to be normally distributed and therefore considered to be well bleached after extreme outliers had been removed (Fig. 5a). Both samples originate in the same tread fill of a terrace, which stabilises a short slope in the Wadi Beqah area (Fig. 11). Shallow sheet flows are presumed to be the dominant transport process, which makes homogeneous bleaching of the sediments more likely than, for example, in sediments transported by channelled flash floods (Rittenour, 2008).

All the other OSL samples show a positive skewness and a high over-dispersion (~ 30 - 70 %, Table 2 and Fig. 5b), indicative of poorly bleached sediments, as is often the case in fluvial and archaeological environments (Jacobs and Roberts, 2007; Rittenour, 2008). The respective FMM and the MAM results for all the samples are consistent within 2σ errors. Only for sample LUM2350 the FMM identify outlying low values (n =3, Proportion = ~ 4 %), which were removed for subsequent analysis. Possible causes of outlying low luminescence signals are argued by Rittenour (2008). For the samples taken from presumably cultivated terrace fills, the effect of ploughing has to be considered. Avni et al. (2006) compare the accumulation rates behind Nabataean agricultural terraces in the Negev to the penetration depth of traditional ploughs. They conclude that owing to turbation by tillage the OSL ages of the terrace fills might be 15 - 40 years younger than their deposition age. In this study, however, only a maximum of two OSL samples are in stratigraphic order from a single site, thus reliable sedimentation rates could not be calculated. Nonetheless, the effect of ploughing has to be accounted for.

All except two OSL ages at the studied sites are in stratigraphic order. All of the OSL ages fall within the time frame of the archaeological record and the radiocarbon ages (see section 2 and Fig. 6). A possible age inversion of the samples LUM2365 and LUM2359 (see sections 5.2 and 5.5) is likely to be caused by fluvial entrainment and subsequent sediment deposition. We therefore consider the OSL ages to be reliable.

5.2.5.3. Radiocarbon ages

Radiocarbon ages, summarised in Table 3, are shown in uncalibrated years BP and calibrated years BP (years before 1950, ± 1σ errors) respectively, and for the discussion in calibrated calendar years (cal BC/AD, ± 2σ errors) and summarised in Table 1 and Fig. 6.

Table 3. Summary of the radiocarbon results (for additional information see section 3.2.).

Sample Location	Sample ID	Depth (cm)	BP (a)	cal BP (a)
RC1	Pet20_1	25	1155±30	1080±100
	Pet20_2	110	1780±30	1720±100
	Pet20_3	155	1875±35	1800±80
RC2	Pet25_1	35	1820±30	1750±110
	Pet25_2	75	1905±30	1830±90
	Pet25_3	145	1920±30	1850±100
RC3	Pet13_1	140	4600±40	5270±200
	Pet13_2	190	5470±40	6290±100

Only at site RC2 did we find datable organic material in a stratigraphic context with OSL samples. Other comparisons of OSL and radiocarbon results are conducted across the sample sites. The sampled charcoal fragments are likely to be detrital, as they do not occur in large concentrations (cf. DeLong and Arnold, 2007). However, the radiocarbon dates are in stratigraphic order. Moreover, the charcoal samples (with the exception of RC2) are found in context with sharp-edged pottery fragments, an indication of short transport distances (see assumptions made in section 3.2) and fit into the expected archaeological time frame. It is therefore assumed that the radiocarbon ages are a reasonable estimate of the deposition age.

5.2.6. Site-specific results and discussion

5.2.6.1. Wadi Shammesh

An up to 3 m deep, gravel-bedded gully, reaching from the mid-course of the valley to its outlet, exposes the stratigraphy of the runoff terraces and their underlying sediments in the catchment of Wadi Shammesh (Fig. 7a). The exposure described in the following is located in the lower mid-course of the valley, between two consecutive barrage terrace walls, and is typical of the stratigraphy of the valley fill (see section 2.4 and Fig. 7b). The base of the profile is made up of an approximately 1.50 m high, carbonate-cemented, massive, reddish-brown silty sand layer with scattered sandstone clasts, overlying the sandstone bedrock. Outcrops of this unit can be found all over the catchment of Wadi al Ghurab.

The cemented layer is overlain by ~ 50 cm of bedded, sub-rounded medium to fine pebbles aligned in flow direction, indicating deposition in a high-energy fluvial regime.

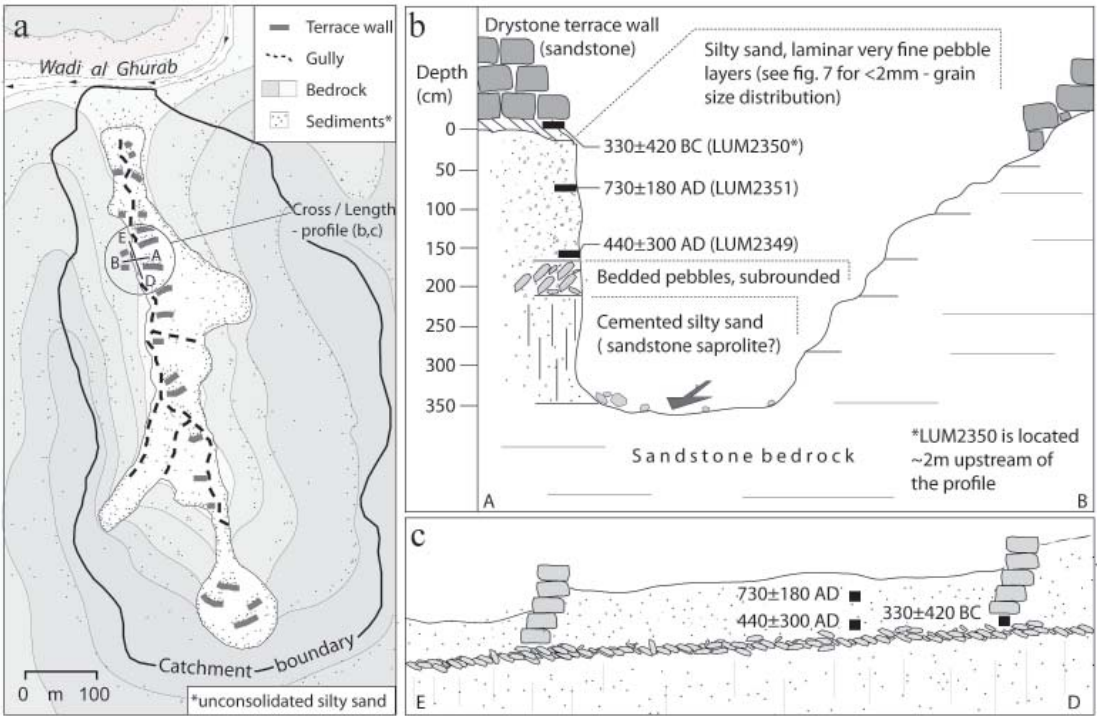

Fig 7a: Sketch of the catchment of Wadi Shammesh (Database: aerial photos of the IGN and ground surveys), with OSL results (2σ-errors); A-B, C-D indicates the approx. location and extent of Figs 7b and 7c respectively; 7b: Sketch of the investigated profile with major stratigraphic units and OSL results; 7c: Idealised length profile along the investigated exposure for additional orientation of the OSL sample locations (see Fig. 7b for sample IDs).

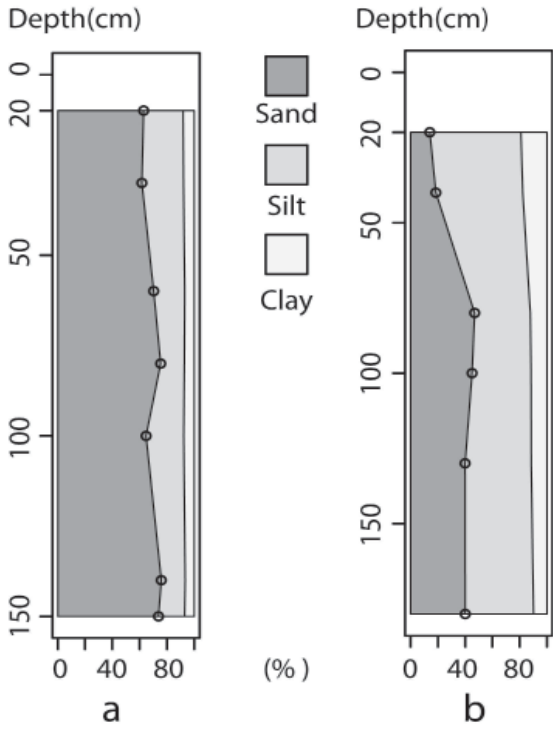

Fig. 8 Cumulative percentage plot of grain size classes of the investigated tread fills at Wadi Shammesh (a) and RC1 (b). The dots indicate the sample depth.

The layer is graded at the upper part, where fine pebbles with interbedded sand layers and sand lenses dominate. The terrace walls were built on top of this layer and on the western side of the valley, on top of the bedrock.

OSL sample LUM2350 was taken directly below the lowermost stone of the riser (Fig. 7b and c). An OSL sample taken from the subsequent riser downstream emitted no measurable luminescence signals (see section 4.2.) However it is assumed that the major barrage terraces were built simultaneously. The age of 330±410 BC (LUM2350) should therefore be representative for the construction of all major terraces.

The pebble layer is overlain by ~ 160 cm of a reddish brown silty sand with scattered and laminar layers of sub-rounded fine gravels (see Fig. 8a for < 2mm grain size distribution), which were deposited upstream of the terrace walls, thus representing the terrace fill. The bedding of the fine gravel layers and the poor sorting of the fine sediment matrix imply a medium-energy fluvial transport and deposition regime and support the assumption that the agricultural terraces were self-filling (cf. Smith and Price, 1994; Treacy and Denevan, 1994). Moreover, the lack of significant variations in the grain size distribution (with the exception of the thin gravel layers) indicates that the depositional and erosional conditions were more or less constant. Dry combustion of 15 samples in stratigraphic order revealed a mean total organic carbon content (TOC) of less than 0.2 mass-% and a mean total inorganic carbon content (TIC) of less than 2 mass-%, with slight variations (σ – TOC = 0.05, σ – TIC = 0.23). The low TOC is typical of arid soils (Hill and Schütt, 2000; Dixon, 2009). Sediment layers enriched in soil organic matter, often found in tread fills of ancient agricultural terraces (Frederick and Krahtopoulou, 2000; Schütt, 2006), cannot be identified. However, this does not exclude the possibility that the terraces have been cultivated. TOC is prone to decay processes even when buried (Schütt, 1998; Retallack, 2001), and the crop residues might have been fed to the livestock rather than being accumulated. Moreover, a study by Sandor et al. (1990) shows that the TOC of terrace fills of cultivated ancient agricultural terraces in the semi-arid region of New Mexico had lower TOC values than sediments from the uncultivated neighbouring areas.

Two OSL samples were taken from the tread fill, 20 and 60 cm above the pebble layer (Fig. 7b and c). LUM2349, approximately representing the initial sediment fill, gave an age of 440±300 AD and LUM2351 yielded an age of 730±180 AD. Considering the 2σ error limits, there is a max. age difference of ~ 1500 years and a min. of ~ 50 years between the construction and the initial filling of the terraces (LUM2350 vs. LUM2349). However, the terrace fills at RC1 and RC2 (see sections 5.4 and 5.5) most likely started to accumulate in the 1st century AD, which is in accordance with the archaeological record (Kouki, 2009; see also section 6). Moreover, self-filling terraces commonly start to accumulate sediments shortly after the construction of the risers (Critchley et al., 1994). We therefore suggest that the actual age of the riser construction is at the younger end of the error range (1st century AD) and that filling started at the older end of the age constraint of LUM2349. LUM2351 indicates that the terraces had been maintained at least until 550 AD (see also Fig. 6).

5.2.6.2 Wadi Sweig

The runoff terraces of Wadi Sweig are dissected by a gully from the mid-course of the valley to its outlet. The investigated agricultural terrace is located ~ 20 m upstream of the confluence of Wadi Sweig and Wadi al Ghurab and is the lowermost terrace of the runoff terrace system in Wadi Sweig. The gully has incised ~ 1 m deep into the terrace fill and the riser. The sediment properties of the fill are similar to those described for Wadi Shammesh (cf. section 5.1). The riser is about 2.50 m high (from base) and 8 m long and

Fig. 9 Photo of the investigated agricultural terrace in Wadi Sweig, looking south-east. Arrows point to the approx. sample locations and their final calendar ages. Note the different masonry of the riser in the left part compared to the riser section where the samples were taken.

partly collapsed. The eastern part of the riser appears to have been completely rebuilt with a different masonry technique and smaller cobbles, compared to the western part of the riser and the majority of the major terraces in the catchment (Fig. 9).

Sample LUM2366 was taken from the terrace fill at the profile created by the gully, ~ 70 cm underneath the surface (Fig. 10). LUM2366 dates to 840±140 AD and is similar

in age to LUM2350 (730±180 AD) in Wadi Shammesh, which was taken from ~ 60 cm underneath the surface of a terrace fill.

The base of the riser is covered by silty to sandy sediments and the stones of the collapsed wall. An 80 cm deep trench was dug to expose the sediment base of the ri-

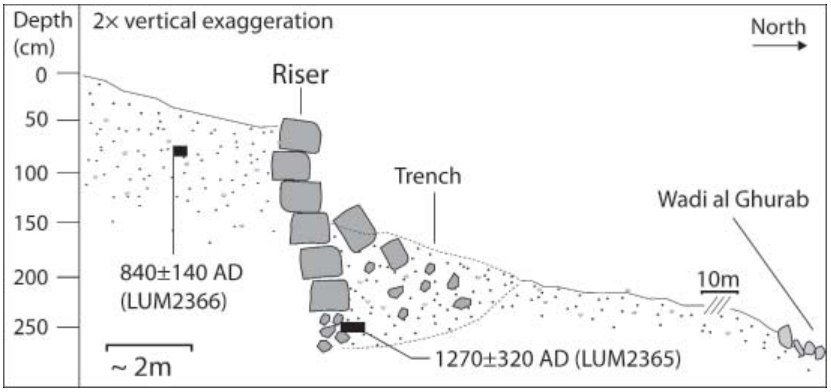

Fig. 10 Sketch of the section and sample location at Wadi Sweig (see Fig. 2 for orientation), with OSL results (2σ-errors). The dotted lines indicate the outlines of the trench that was dug to excavate the base of the riser. For the stratigraphic units refer to legend of Fig. 7.

ser. OSL sample LUM2365 was taken from a sand lens embedded in the gravel layer on which the riser was built. The penetration depth of the sample tube was limited to about 15cm, as stones blocked a further penetration. This sample gave an age of 1270±320 AD. Considering the errors, sample LUM2365 might be of the same age as LUM2366 or younger. However, we expected this sample to be older than the terrace fill. The almost contemporaneous concurrence of riser construction and sedimentation of more than 2 m of tread fill seems unlikely in comparison to the results in Wadi Shammesh and at RC1. Considering the limited penetration depth of the sample tube, it is assumed that the age of LUM2366 is not representative for the construction of the riser and might correspond to sediments that were accumulated after the construction of the riser. As the terrace is the lowermost of the runoff terrace system in the valley, the lower parts of the riser are not covered by the terrace fill of a subjacent terrace. Flash floods overflowing the riser could have undercut the sediment base, similar to a plunge pool of a waterfall, and could have eroded a cavity which was subsequently filled with sediments.

5.2.6.3 Wadi Beqah

OSL samples were extracted from the silty sand fill of a large retaining wall which stabilises the slope of an escarpment descending from the Beqah Plain (Fig. 11). The tread of the agricultural terrace is ~ 20 m long and 10 m wide and moderately inclined. The riser is ~ 2.50 m high, measured from the ground surface, and ~ 20 m long. Like the walls in the Wadi Shammesh catchment, the riser is built with crudely carved sandstone cobbles. The upper part of the wall has collapsed, and the partly buried residues are deposited at the foot of the wall. LUM2352 was sampled on the level of the uppermost remaining stone row of the wall, 90 cm beneath the surface. LUM2354 was sampled 20 cm above LUM2352 (Fig. 11b). Both samples gave an age of around 1000 to 1100 AD.

A trench that was dug to take an OSL sample at the base of this terrace had to be stopped at a depth of 1.50 m, because the trench was at risk of collapsing, and the base of the

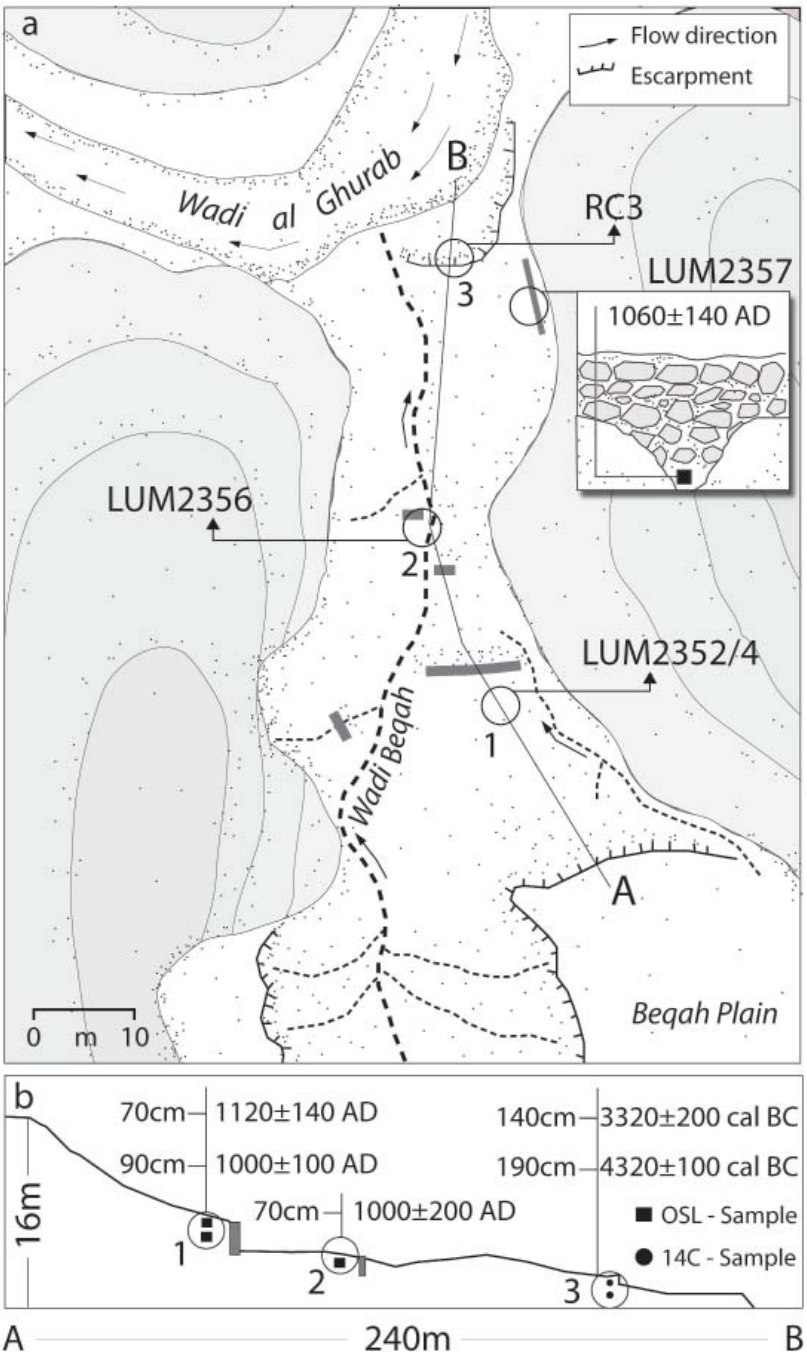

Fig. 11a: Map of the sample site at Wadi Beqah (see Fig. 2 for orientation and for the legend cf. Fig. 7a, Database: aerial photos of the IGN and ground surveys). The inset section at LUM2357 displays the riser under which the sample was taken; 11b: Length profile (two times vertical exaggeration) between A and B in Fig. 11a, with OSL and radiocarbon results (2σ-errors).

riser could not be reached. Given the extraordinary height of the terrace (> 4m) compared to the other terraces we found in the study area (up to ~ 2 m), the initial construction of the terrace might be expected to be older than at the neighbouring sites RC1 and in Wadi Shammesh, for example. At these sites the 1.50 to 1.80 m of dated terrace fill accumulated roughly from the 1st century AD to the 8th century AD. However, as the catchment of the terrace at LUM2352/54 is mostly covered by a thick valley fill of unconsolidated fine sediments, we assume the sediment delivery rate of the catchment and in consequence the accumulation rate behind the terrace to be relatively high. Moreover, the masonry of the terrace is similar to that in Wadi Shammesh. Hence, we assume the initial

construction of the terrace to be similar in age to that in RC1, RC2 and Wadi Shammesh, i.e. the ~ 1st century AD.

LUM2356 was sampled from a terrace fill of a barrage terrace that crosses the fan, about 30 m downstream of LUM2352/4. The masonry of the riser is similar to that described in section 2.4. This wall is partly buried under fan deposits and dissected by the Wadi Beqah. The sample was taken from 70 cm underneath the surface and dated to 1000±200 AD.

At the north-eastern margin of the study site, OSL sample LUM2357 was taken directly underneath the base of a stone wall that is partly buried under poorly sorted gravelly sands, presumably colluvial deposits from the upper eastern slopes. The wall is ~ 20 m long and was built along the sandstone ridge that borders the eastern side of the study site. The function of this wall was most likely to stabilise the sediments that covered the sandstone ridge. The sample gave an age of 1060±140 AD (LUM2357).

Charcoal samples Pet13-1 and Pet13-2 were taken at a trench we dug at the foot of the entrenchment, from about 140 cm and 190 cm below the surface. These samples yielded ages of about 3000-4000 BC. These ages imply that the charcoal was deposited by the Wadi Beqah before the construction of the water harvesting measures in the area.

It is concluded that either the runoff terraces and retaining walls at this site were maintained or new ones were built at least until around 1000 AD. However, it was not possible to establish when the terraces at sample sites LUM2356 and LUM2352/4 were initially built (see also discussion of LUM2352/4).

5.2.6.4 Wadi al Ghurab - RC1

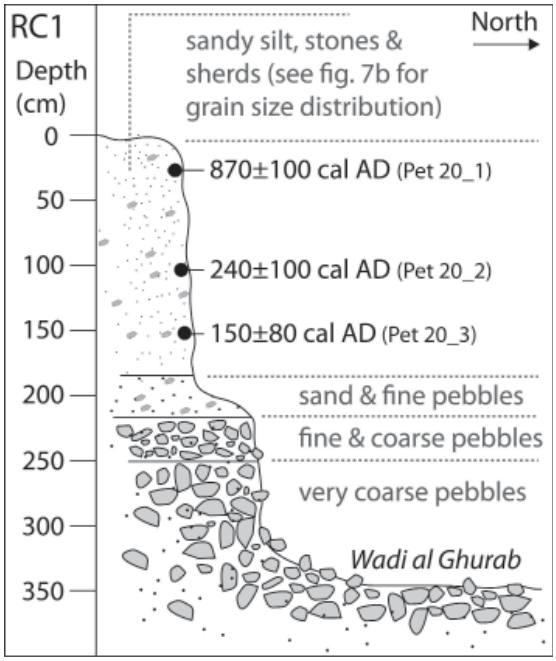

Fig. 12 Sketch of the exposed section at RC 1 with radiocarbon ages (for location see Fig. 1b and 2).

The investigated sediment sequence at RC1 is exposed along the southern bank of Wadi al Ghurab. It is situated at the steep escarpment, where the cultivated plain (section 2.4) descends to Wadi al Ghurab (Fig. 2 and Fig. 12). The lowermost section of this exposure is made up of graded, coarse to fine pebbles of Wadi al Ghurab. On top of the pebble layers, a sediment sequence of about 2 m of yellowish white, sandy silt, with fine gravels and

sharp-edged potsherds has been accumulated (Fig. 8b for grain size distribution). LOI measurements of this unit at 550° show a mean of < 0.3 mass-%, with sligth variations (σ – LOI550 = 0.05, n=10, see section 5.1 for discussion of the low organic carbon content of the sediments). This stratigraphic sequence is present along the escarpment of the plain.

Remains of drystone retaining walls can be found intermittently alongside the silty sediment unit. The walls were built on top of the gravel layers, and it is likely that they were part of a continuous wall along the escarpment of the plain. Its purpose was presumably twofold: (i) to retain fine sediments and runoff originating from the south of the plain and (ii) to protect the agricultural fields of the plain from the floods of Wadi al Ghurab (cf. Evenari and Tadmor, 1982). The radiocarbon ages indicate that fine sediments accumulated at this site, at least from around the beginning of the Common Era, and lasted until 1000 AD. These ages agree with those of Wadi Shammesh as well as with the archaeological record and suggest that the accumulation of fine sediments at this site is linked to the construction of the retaining walls. Rambeau et al. (2011) postulate a wider channel and floodplain of the Wadi al Ghurab during the Early Holocene compared to present-day conditions. The results presented here support this assumption and suggest that in general these conditions prevailed until the Nabataeans began to reclaim the area.

5.2.6.5 Seil Wadi Musa - RC2

Profile RC2 (Fig. 1 and Fig. 13) is situated at the escarpment where the plain (section 2.4) descends to the channel bed of Seil Wadi Musa. The stratigraphy of this exposure is similar to the one found at RC1 (Fig. 12). Almost 2 m of yellowish white, sandy silts, with few scattered fine pebbles and sharp-edged pottery fragments have been accumulated on top of pebble layers deposited by Seil Wadi Musa. The uppermost section of the pebble layers is made up of fine pebbles with many rounded potsherds. The similarities in grain size distribution and colour of the silty sediments with the weathering residues of the limestone hills support the assumption that the sediments originate from sheet flows of the

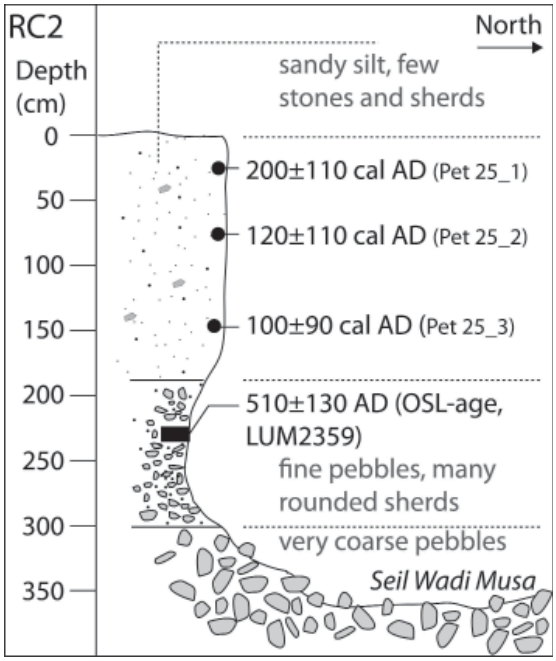

Fig. 13 Sketch of the exposed section at RC 2 with OSL and radiocarbon ages (for location see Fig. 1b).

surrounding limestone hills (see section 2.4). The presence of fine gravels within the silty sand matrix makes a fluvial deposition likely. LOI measurements of this sediment unit at

550° show a mean of < 0.25 mass-%, with slight variations (σ – LOI550 = 0.03, n=8, see section 5.1 for a discussion of the low organic carbon content).

The charcoal samples dated from 100±90 cal AD, at the bottom of the silty sediment unit, to 200±110 cal AD at its top and therefore lack a statistically significant age difference (Fig. 13). It is concluded that sedimentation of fine sediments started at the earliest around the beginning of the Common Era and lasted until at least ~100 cal AD. The radiocarbon ages are in general agreement with the pottery-based dating of the Roman Gardens (Lindner et al., 2000). Remains of retaining walls could not be found along the escarpment. However, cultivated alluvial terraces of the Roman Gardens in the south show remains of such retaining walls alongside Seil Wadi Ghurab, and it is likely that this was also the case at this site (cf. section 5.4).

The OSL sample LUM2359, taken from the pottery-rich, fine pebble layer underneath the silty sediment unit, dated to 510±180 AD and is either of the same age as the lowermost charcoal sample (Pet 25_3) or younger. We assume that this probable age inversion is caused by undercutting of the fine sediment layer during flood events of the Seil Wadi Musa and subsequent deposition of the fine pebble layer. This is also indicated by the overhanging topography of the fine sediment layer, which might have been caused by fluvial undercutting. The embedded sherds in this layer may originate from the Roman fort at Umm Ratam and the upstream agricultural terraces and settlements of the Roman Gardens.

5.2.7. Conclusion

The overall agreement of OSL and radiocarbon ages and the archaeological record of the study area suggests the general applicability of OSL dating in the Petra region. However, incomplete bleaching is present in almost all samples. Moreover, some samples showed a weak OSL signal, probably owing to the dominant source rock of the quartz and the limited cycles of irradiation and bleaching (Pietsch et al. 2008).

The majority of the investigated exposures have a similar stratigraphic sequence: a sudden shift from the underlying pebble layers, indicating high energy fluvial environments, to fine sediments reflecting low energy fluvial deposition regimes. This sedimentological shift is almost always associated with the construction of agricultural terraces, which caused retention of surface runoff in the upslope areas and forced infiltration and storage of the water in the terrace fills. Hence, the construction of the terraces had a major impact on the landscape of the Petra region and temporarily converted large parts of it from erosion-dominated, unfavourable areas to cultivable land. The OSL and radiocarbon ages indicate that the construction of these terraces and the accumulation of fine sediments started around the beginning of the Common Era and that terrace agriculture was practised at least until around 800 AD (Fig. 6). This confirms the assumptions made by Kouki (2009), based on the archaeological record, that agriculture in the Petra region was rapidly expanding in the first century AD and that agriculture was an important part of the regional economy, even after the decline of Petra as an urban central place.

Acknowledgements

This study was supported by the Cluster of Excellence TOPOI Exc 264. We would like to thank the Departement of Antiquities in Jordan for granting survey permission. Special thanks to Stephan G. Schmid and Michel Mouton without whom field work would not have been possible. We also thank Sabine Mogwitz , Astrid Techmer and Sonja

Riemenschneider of the LIAG for the support in the laboratory. The comments of Naomi Porat and an anonymous reviewer have greatly improved the manuscript.

References

Amr, K., Al-Momani, A., 2001. Preliminary Report on the Archaeological Component of the Wadi Musa Water Supply and Wastewater Project (1998-2000). ADAJ.

Adamiec, G., Aitken, M.J., 1998. Dose-rate conversion factors: update. Ancient TL 37–50.

Aitken, M.J., 1998. An Introduction to Optical Dating: The Dating of Quaternary Sediments by the Use of Photon-Stimulated Luminescence. Oxford University Press, Oxford.

Al-Eisawi, D., 1996. Vegetation of Jordan. UNESCO Regional Office for Science and Technology for the Arab States, Cairo.

Alexanderson, H., Murray, A.S., 2009. Problems and potential of OSL dating Weichselian and Holocene sediments in Sweden. Quaternary Science Reviews.

Al-Khashman, O.A., 2007. Study of water quality of springs in Petra region, Jordan: A three-year follow-up. Water Resources Management 21, 1145-1163.

Al-Weshah, R.A., El-Khoury, F., 1999. Flood analysis and mitigation for Petra area in Jordan. Journal of water resources planning and management 125, 170–177.

Arnold, L.J., Bailey, R.M., Tucker, G.E., 2007. Statistical treatment of fluvial dose distributions from southern Colorado arroyo deposits. Quaternary Geochronology 2, 162-167.

Arnold, L.J., Roberts, R.G., 2009. Stochastic modelling of multi-grain equivalent dose (De) distributions: Implications for OSL dating of sediment mixtures. Quaternary Geochronology 4, 204-230.

Avni, Y., Porat, N., Plakht, J., Avni, G., 2006. Geomorphic changes leading to natural desertification versus anthropogenic land conservation in an arid environment, the Negev Highlands, Israel. Geomorphology 82, 177-200.

Bailey, R.M., Arnold, L.J., 2006. Statistical modelling of single grain quartz De distributions and an assessment of procedures for estimating burial dose. Quaternary Science Reviews 25, 2475-2502.

Baird, A.J., 1989. Overland flow generation and sediment mobilisation by water, in: Thomas, D.S.G. (Ed.), Arid Zone Geomorphology. Belhaven Press ; Halsted Press, London : New York.

Ball, D.F., 1964. Loss-on-ignition as an Estimate of Organic Matter and Organic Carbon in Non-calcareous Soils. Journal of Soil Science 15, 84-92.

Barjous, M.O., 1995. Supplement text to the geological map Petra & Wadi Al-Lahyana, Sheet: 3050I/3050IV, 1:50000, Natural Resources Authority, Jordan.

Beck, C., Grieser, J., Rudolf, B., 2005. A New Monthly Precipitation Climatology for the Global Land Areas for the Period 1951 to 2000. DWD, Klimastatusbericht KSB.

Bender, F., 1974. Geology of Jordan, Contributions to the regional geology of the earth = Beiträge zur regionalen Geologie der Erde. Gebrüder Borntraeger, Berlin.

Bienkowski, P., 2001. The Iron Age and Persian Periods in Jordan. SHAJ 7, 265-274.

Blott, S.J., Pye, K., 2001. GRADISTAT: a grain size distribution and statistics package for the analysis of unconsolidated sediments. Earth Surface Processes and Landforms 26, 1237-1248.

Bøtter-Jensen, L., Andersen, C.E., Duller, G.A.T., Murray, A.S., 2003. Developments in radiation, stimulation and observation facilities in luminescence measurements. Radiation Measurements 37, 535-541.

Bronk Ramsey, C., 2009. Bayesian analysis of radiocarbon dates. Radiocarbon 51, 337-360.

Bruins, H.J., Evenari, M., Nessler, U., 1986. Rainwater-harvesting agriculture for food production in arid zones: the challenge of the African famine. Applied Geography 6, 13-32.

Byrd, B.F., 1989. The Natufian Encampment at Beidha: Late Pleistocene Adaptation in the Southern Levant, Excavations at Beidha. Jysk arkæologisk selskab, Højbjerg.

Cordova, C.E., 2007. Millennial Landscape Change in Jordan: Geoarchaeology and Cultural Ecology. University of Arizona Press, Tucson, Ariz.

Critchley, W.R.S., Reij, C., Willcocks, T.J., 1994. Indigenous soil and water conservation: A review of the state of knowledge and prospects for building on traditions. Land Degradation & Development 5, 293-314.

Cunningham, A.C., Wallinga, J., 2010. Selection of integration time intervals for quartz OSL decay curves. Quaternary Geochronology 5, 657-666.

Dean, W.E., 1974. Determination of carbonate and organic matter in calcareous sediments and sedimentary rocks by loss on ignition; comparison with other methods. Journal of Sedimentary Research 44, 242 -248.

DeLong, S.B., Arnold, L.J., 2007. Dating alluvial deposits with optically stimulated luminescence, AMS 14C and cosmogenic techniques, western Transverse Ranges, California, USA. Quaternary Geochronology 2, 129-136.

DIN19684, 1977. Bodenuntersuchungensverfahren im landwirtschaftlichen Wasserbau. Chemische Laboruntersuchungen. DIN 19684, Teil 3: Bestimmung des Glühverlustes und des Glührückstandes. Deutsches Institut für Normung, Berlin.

Dixon, J.C., 2009. Aridic Soils, Patterned Ground, and Desert Pavements, in: Abrahams, A.D., Parsons, A.J. (Eds.), Geomorphology of Desert Environments. Springer, New York.

Duller, G.A.T., 2003. Distinguishing quartz and feldspar in single grain luminescence measurements. Radiation Measurements 37, 161-165.

Duller, G.A.T., 2008. Single-grain optical dating of Quaternary sediments: why aliquot size matters in luminescence dating. Boreas 37, 589-612.

Evenari, M., Tadmor, N., 1982. The Negev: The Challenge of a Desert, 2nd Ed, New. ed. Harvard Univ Pr.

Fan, Y., van den Dool, H., 2008. A global monthly land surface air temperature analysis for 1948–present. J. Geophys. Res. 113.

Feathers, J.K., 2003. Single-grain OSL dating of sediments from the Southern High Plains, USA. Quaternary Science Reviews 22, 1035-1042.

Field, J., 1989. Appendix A. Geological Setting at Beidha, in: The Natufian Encampment at Beidha: Late Pleistocene Adaptation in the Southern Levant, Excavations at Beidha. Jysk arkæologisk selskab, Højbjerg, pp. 86 - 90.

Finné, M., Holmgren, K., Sundqvist, H.S., Weiberg, E., Lindblom, M., 2011. Climate in the eastern Mediterranean, and adjacent regions, during the past 6000 years – A review. Journal of Archaeological Science 38, 3153-3173.

Frederick, C., Krahtopoulou, A., 2000. Deconstructing Agricultural Terraces: Examining the influence of Construction Method on Stratigraphy, Dating and Archaeological Visibility, in: Frederick, C., Halstead, P. (Eds.), Landscape and Land Use in Postglacial Greece. Continuum International Publishing Group, pp. 79 - 93.

Galbraith, R.F., 1988. Graphical Display of Estimates Having Differing Standard Errors. Technometrics 30, 271-281.

Galbraith, R.F., Green, P.F., 1990. Estimating the component ages in a finite mixture. International Journal of Radiation Applications and Instrumentation. Part D. Nuclear Tracks and Radiation Measurements 17, 197-206.

Galbraith, R.F., Roberts, R.G., Laslett, G.M., Yoshida, H., Olley, J.M., 1999. Optical Dating of Single and Multiple Grains of Quartz from Jinmium Rock Shelter, Northern Australia: Part I, Experimental Design and Statistical Models. Archaeometry 41, 339–364.

Galbraith, R.F., Roberts, R.G., Yoshida, H., 2005. Error variation in OSL palaeodose estimates from single aliquots of quartz: a factorial experiment. Radiation Measurements 39, 289-307.

Gentelle, P., 2009. Aménagement du territoire agricole de la ville de Pétra : la terre et l'eau, in: Stratégies D'acquisition De L'eau Et Société Au Moyen-Orient Depuis l'Antiquité. Institut français du Proche-Orient, pp. 133-148.

Gillespie, R., Prosser, I.P., Dlugokencky, E., Sparks, R.J., Wallace, G., Chappell, J.A., 1992. AMS dating of alluvial sediments on the southern Tablelands of New South Wales, Australia. Radiocarbon 34, 29-36.

Graf, D.F., 1992. Nabataean settlements and Roman occupation in Arabia Petraea. SHAJ 253-260.

Guralnik, B., Matmon, A., Avni, Y., Porat, N., Fink, D., 2011. Constraining the evolution of river terraces with integrated OSL and cosmogenic nuclide data. Quaternary Geochronology 6, 22-32.

Haiman, M., Fabian, P., 2009. Desertification And Ancient Desert Farming Systems. Encyclopedia of Life Support Systems (EOLSS), Land Use, Land Cover And Soil Science.

Harding, A., Palutikof, J., Holt, T., 2009. The Climate System, in: Woodward, J.C. (Ed.), The Physical Geography of the Mediterranean, The Oxford Regional Environments Series. Oxford University Press, Oxford ; New York.

Hesse, R., Baade, J., 2009. Irrigation agriculture and the sedimentary record in the Palpa Valley, southern Peru. CATENA 77, 119-129.

Hill, J., Schütt, B., 2000. Mapping Complex Patterns of Erosion and Stability in Dry Mediterranean Ecosystems. Remote Sensing of Environment 74, 557-569.

Horowitz, A., 2001. The Jordan Rift Valley. Taylor & Francis.

Hunt, C.O., Gilbertson, D.D., El-Rishi, H.A., 2007. An 8000-year history of landscape, climate, and copper exploitation in the Middle East: the Wadi Faynan and the Wadi Dana National Reserve in southern Jordan. Journal of Archaeological Science 34, 1306-1338.

Jacobs, Z., Roberts, R.G., 2007. Advances in optically stimulated luminescence dating of individual grains of quartz from archeological deposits. Evolutionary Anthropology: Issues, News, and Reviews 16, 210-223.

Kouki, P., 2006. Environmental Change and human history in the Jebel Harun area, Jordan.

Kouki, P., 2009. Archaeological Evidence of Land Tenure in the Petra Region, Jordan: Nabataean-Early Roman to Late Byzantine. Journal of Mediterranean Archaeology 22, 29-56.

Krahtopoulou, A., Frederick, C., 2008. The stratigraphic implications of long-term terrace agriculture in dynamic landscapes: Polycyclic terracing from Kythera Island, Greece. Geoarchaeology 23, 550-585.

Lavento, M., 2010. Archaeological Investigations of Ancient Water Systems in Jordan, in: Ostreng, W. (Ed.), Transference. Interdisciplinary Communications 2008/2009, CAS, Oslo.

Lavento, M., Huotari, M., 2002. A water management system around Jabal Harun, Petra - its design and significance, in: Tsuk, T., Ohlig, C., Peleg, Y. (Eds.), Cura Aquarum in Israel. Books on Demand Gmbh, pp. 93 - 106.

Lindner, M., 1999. Late Islamic Villages in the Greater Petra Region and Medieval

"Hormuz". ADAJ 479-500.
Lindner, M., Hübner, U., Hübl, J., 2000. Nabataean and Roman presence between Patra and Wadi Arabah survey expedition 1997/98: Umm Ratam. ADAJ.
Markstrom, S.L., McCabe, G.J., 2007. A monthly water-balance model driven by a graphical user interface.
Mayerson, P., Evenari, M., Aharoni, Y., Shanan, L., Tadmor, N., 1961. Ancient Agriculture in the Negev. Science 134, 1751 -1754.
Murray, A.S., Wintle, A.G., 2000. Luminescence dating of quartz using an improved single-aliquot regenerative-dose protocol. Radiation Measurements 32, 57-73.
Murray, A.S., Wintle, A.G., 2003. The single aliquot regenerative dose protocol: potential for improvements in reliability. Radiation Measurements 37, 377-381.
Ortloff, C.R., 2005. The Water Supply and Distribution System of the Nabataean City of Petra (Jordan), 300 BC– AD 300. Cambridge Archaeological Journal 15, 93-109.
Pietsch, T.J., Olley, J.M., Nanson, G.C., 2008. Fluvial transport as a natural luminescence sensitiser of quartz. Quaternary Geochronology 3, 365–376.
Porat, N., Amit, R., Enzel, Y., Zilberman, E., Avni, Y., Ginat, H., Gluck, D., 2010. Abandonment ages of alluvial landforms in the hyperarid Negev determined by luminescence dating. Journal of Arid Environments 74, 861-869.
Porat, N., Rosen, S.A., Boaretto, E., Avni, Y., 2006. Dating the Ramat Saharonim Late Neolithic desert cult site. Journal of Archaeological Science 33, 1341-1355.
Prescott, J.R., Hutton, J.T., 1994. Cosmic ray distributions to dose rates for luminescenceand ESR dating: large depths and long-term variations. Radiation Measurements 497–500.
Prescott, J.R., Stephan, L.G., 1982. The contribution of cosmic radiation to the environmental dose for thermoluminescent dating — Latitude, altitude and depth dependences. PACT 17-25.
Raikes, R., 1966. Appendix C - Beidha: prehistoric climate and water supply. Palestine Exploration Quarterly 68-72.
Rambeau, C., Finlayson, B., Smith, S., Black, S., Inglis, R., Robinson, S., 2011. Palaeoenvironmental reconstruction at Beidha, southern Jordan (c. 18,00-8500 BP): Implications for human occupation during the Natufian and Pre-Pottery Neolothic, in: Mithen, S.J., Black, E. (Eds.), Water, Life & Civilisation: Climate, Environment, and Society in the Jordan Valley, International Hydrology Series. Cambridge University Press, Cambridge ; New York.
Reimann, T., Naumann, M., Tsukamoto, S., Frechen, M., 2010. Luminescence dating of coastal sediments from the Baltic Sea coastal barrier-spit Darss–Zingst, NE Germany. Geomorphology 122, 264-273.
Reimer, P.J., Baillie, M.G.L., Bard, E., Bayliss, A., Beck, J.W., Blackwell, P.G., Ramsey, C.B., Buck, C.E., Burr, G.S., Edwards, R.L., others, 2009. IntCal09 and Marine09 radiocarbon age calibration curves, 0–50,000 years cal BP.
Retallack, G.J., 2001. Soils of the Past: An Introduction to Paleopedology, 2nd ed. Blackwell Science, Oxford ; Malden, MA.
Rittenour, T.M., 2008. Luminescence dating of fluvial deposits: applications to geomorphic, palaeoseismic and archaeological research. Boreas 37, 613-635.
Roberts, N., Brayshaw, D., Kuzucuoğlu, C., Perez, R., Sadori, L., 2011. The mid-Holocene climatic transition in the Mediterranean: Causes and consequences. The Holocene 21, 3 -13.

Roberts, R.G., Galbraith, R.F., Yoshida, H., Laslett, G.M., Olley, J.M., 2000. Distinguishing dose populations in sediment mixtures: a test of single-grain optical dating procedures using mixtures of laboratory-dosed quartz. Radiation Measurements 32, 459-465.

Robinson, S.A., Black, S., Sellwood, B.W., Valdes, P.J., 2006. A review of palaeoclimates and palaeoenvironments in the Levant and Eastern Mediterranean from 25,000 to 5000 years BP: setting the environmental background for the evolution of human civilisation. Quaternary Science Reviews 25, 1517-1541.

Rodnight, H., Duller, G.A.T., Wintle, A.G., Tooth, S., 2006. Assessing the reproducibility and accuracy of optical dating of fluvial deposits. Quaternary Geochronology 1, 109-120.

Rosen, S.A., 2000. The decline of desert agriculture: a view from the classical period Negev, in: Barker, G., Gilbertson, D.D. (Eds.), The Archaeology of Drylands: Living at the Margin, One World Archaeology. Routledge, London ; New York.

Sandor, J.A., Gersper, P.L., Hawley, J.W., 1990. Prehistoric Agricultural Terraces and Soils in the Mimbres Area, New Mexico. World Archaeology 22, 70-86.

Saxton, K.E., Willey, P.H., 2006. The SPAW Model for Agricultural Field and Pond Hydrologic Simulation, in: Singh, V.P., Woolhiser (Eds.), Mathematical Modeling of Watershed Hydrology, Transactions of American Society of Agricultural Engineers. pp. 673-677.

Schiffer, M., 1986. Radiocarbon dating and the "old wood" problem: The case of the Hohokam chronology. Journal of Archaeological Science 13, 13-30.

Schmid, S.G., 2008. The Hellenistic Period and the Nabataeans, in: Adams, R. (Ed.), Jordan: An Archaeological Reader. Equinox Pub, Oakville, CT.

Schütt, B., 1998. Reconstruction of palaeoenvironmental conditions by investigation of Holocene playa-sediments in the Ebro Basin, Spain: Preliminary results. Geomorphology 273-283.

Schütt, B., 2006. Rekonstruktion, Abbildung und Modellierung der holozänen Reliefentwicklung der Canada Hermosa, Einzugsgebiet des Rio Guadalentin (SE Iberische Halbinsel). Nova Acta Leopoldina NF 94 346, 83-111.

Schütt, B., Berking, J., Frechen, M., Frenzel, P., Schwalb, A., Wrozyna, C., 2010. Late Quaternary transition from lacustrine to a fluvio-lacustrine environment in the northwestern Nam Co, Tibetan Plateau, China. Quaternary International 218, 104-117.

Smith, M., Price, T., 1994. Aztec-period agricultural terraces in Morelos, Mexico: evidence for houshold-level agricultural intensification. Journal of Field Archaeology.

Spencer, J.E., Hale, G.A., 1961. Origin, Nature and Distribution of Agricultural Terracing. Pacific Viewpoint 1-40.

Taylor, J., 2002. Petra and the Lost Kingdom of the Nabataeans. Harvard University Press.

Tholbecq, L., 2001. The hinterland of Petra from Edomite to the Islamic periods: The Jabal ash-Sharah Survey (1996 - 1997). SHAJ 399-405.

Tokuyasu, K., Tanaka, K., Tsukamoto, S., Murray, A., 2010. The Characteristics of OSL Signal from Quartz Grains Extracted from Modern Sediments in Japan. Geochronometria 37, 13-19.

Tooth, S., 2000. Process, form and change in dryland rivers: a review of recent research. Earth-Science Reviews 51, 67-107.

Touchan, R., Meko, D., Hughes, M.K., 1999. A 396 Year Reconstruction of Precipitation in Southern Jordan. JAWRA Journal of the American Water Resources Association 35, 49-59.

Treacy, J., Denevan, W., 1994. The Creation of Cultivated Land through Terracing, in: Miller, N.F., Gleason, K.L. (Eds.), The Archaeology of Garden and Field. University of

Pennsylvania Press, Philadelphia.
Waltham, T., 1994. The sandstone fantasy of Petra. Geology Today 10, 105-111.

6. Major conclusions and synthesis

6.1. Major conclusions of the case studies

6.1.1 Resafa

The ancient city of Resafa, located in the Syrian desert steppe was supplied with drinking water by a floodwater harvesting system. Periodical floods of a nearby wadi were collected and stored in large cisterns. The major research questions are how reliable the floodwater harvesting system was and if the ancient engineers built an extended embankment system along the floodplain of the Wadi es Sélé to channel periodical floods to the city cisterns.

The major conclusions of the study are:

The analysis of aerial photographs, excavations and flood pattern analysis revealed additional constructional details of the floodwater harvesting system. In addition to the dam and cisterns which were documented in previous studies it was shown that the system consisted most probably of a several hundred meter long embankment system which channeled the periodical floods to the retaining dam. The embankment system most likely enhanced the viability of the floodwater system and protected settled areas from flooding. The radiocarbon ages which were taken at selected structures associated to this system confirmed previous studies which state that the floodwater system was maintained and extensively developed during the Early Islamic settlement period of the city in the 8th century AD.

The investigated sediments in the alluvial plain which adjoins Resafa shows no evidence of a significant change in the depositional environment since the Antiquity. The sediments of the eastern wadi bank consist of up to six meters of silty sand with little variations in the grain size distribution. Neither significant accumulation nor erosion phases were present in this sediment archives. The depositional environment has been dominated by sheet floods superimposed by aeolian processes. It is assumed that in general the environmental conditions during Antiquity were similar to today. This assumption is confirmed by palaeoclimatic proxy records from the Eastern Mediterranean and climate modeling results which agree that climate during the past 2000 years was similar to today.

The modeled runoff time series reveal that the environmental conditions were favorable for floodwater harvesting in terms of water availability. Flood volumes regularly surpassed the storage capacity of the cisterns. Only in one of 29 modeled years sufficient flood events were absent. Apart from this exceptional dry year the cisterns of the city could have been filled at least every 13 to 14 months. The floodwater harvesting system is therefore considered reliable. The present climate is somewhat dryer compared to various periods since the Antiquity and it is conceivable that the floodwater harvesting system was even more productive during the heydays of Resafa.

From a management and engineering point of view the operation and maintenance of the system has most likely been challenging. The major runoff contributing catchment of the floodwater harvesting system can be considered large (> 30 km^2) for a water harvesting systems (chapter 3). Typical for a dryland catchment of this dimension the sizes of floods are highly variable and range from small ones to large floods which inundated large parts of the wide alluvial plain of the Wadi es Sélé. As shown by the rainfall runoff

modeling the exact timing of the floods during the rainy season is unpredictable and the floods are short lasting and occasionally of high magnitude. Moreover, floods flowing in wadis usually carry a high sediment load. Thus, sluice gates had to be closed at the right time to avoid overtopping of the channels and cisterns, the system had regularly to be cleaned from sediments and it is likely that the earthen dam and embankments necessitated regular maintenance. Moreover, the water distribution among the population is likely to have been restricted and managed so as to avoid water shortage.

6.1.2 Petra

Large parts of the rugged and arid environs of Petra were cultivated by installing water harvesting systems. The chronology of these systems is still debated and the major aim of this case study is to establish a chronology of these systems by applying OSL and radiocarbon dating.

The major conclusions are:

OSL dating of the agricultural terraces proved to be successful and applicable. Almost all ages were in stratigraphic order and were consistent with the radiocarbon ages. However, in general the OSL samples were incompletely bleached and some samples had a weak luminescence signal.

The major water harvesting techniques applied to enable agricultural activity in the study area are terraced wadi systems. The systems were installed in small tributary wadis with a limited catchment area. No evidence for the usage of the higher order wadis for water harvesting were found in the study area. According to scholars and practitioners concerned with water harvesting systems these systems have been implemented and maintained by individual non-expert households (chapter 3).

The OSL and radiocarbon ages revealed that these terraced wadi systems were initially built around the beginning of the Common Era. This coincides with the first archaeologically attested major building phase in the city center of Petra. The terraces were used, maintained and extended at least until the 8th century AD.

6.2 Synthesis and future perspectives

The question was raised whether the complexity of the water supply systems of Resafa and Petra accelerated the decline of the cities after the fundamental source of income and importance ceased. While this question cannot be answered with the presented case studies alone their results built an important basis to approach this question and point to future research perspectives. With this focus the results will briefly be synthesized in the following.

A modern analogue might illustrate the problems ancient, declining cities might have faced concerning their infrastructure. One of the major management problems of modern shrinking cities is the operation and maintenance of their central infrastructure facilities which is often owed to their lack of adaptive capacity (Oswalt and Rieniets, 2006; Hummel, 2008). The maintenance and operation costs of e.g. sewage and water supply structures of cities often increase when population and industrial user numbers decrease. Strategies to mitigate these problems are often expensive beyond feasibility (Schiller, 2007). Where adaptions of the infrastructure to the demographic and economical changes are not feasible, beyond political will or cannot be conducted by individuals, the infrastructure is often decommissioned or left abandoned (Hummel, 2008). This has direct

consequences to the inhabitants of the affected areas which are either forced to move or to adapt by applying autonomous systems (Hummel, 2008).

In the case study of Resafa it is shown that the environmental conditions were favorable for floodwater harvesting. However, the maintenance and the operation of the main water supply system was most likely labor intensive and necessitated expert knowledge. As the system was designed to harvest water from a large catchment it can be assumed that the system could not easily be downsized and controlled by non-experts and there is no evidence that attempts were made to scale down the system. Hence, when the experts migrate or the labor force is not sufficient to control and maintain the floodwater system it soon will ultimately collapse and the remaining population is subsequently forced to leave.

In Petra previous studies show that the drinking water supply of the farmsteads and farming villages was predominantly conducted with small runoff harvesting systems that collected and stored runoff from bedrock outcrops (Tholbecq, 2001; Kouki, 2006). These water supply systems as well as the terraced wadi systems can be installed and maintained by non-experts and small organizational units (chapter 3). According to Ortloff (2005) the complex water supply system of Petra´s city center necessitated expert knowledge and constant labor-intensive maintenance. A reuse or reimplementation after the 4th century AD is not evident in the archaeological record (Ortloff, 2005). In contrast, the agricultural terraces where constantly used and extended from the 1st century to at least the 8th century AD and most likely along them the small scale runoff harvesting systems that supplied the associated farmsteads and villages with drinking water (see also Kouki, 2009).

In conclusion it can be stated that both case studies support the assumption that the lack of adaptive capacity of the complex water supply systems either accelerated or contributed to the ultimate abandonment of the cities of Resafa and Petra. However, many questions remain: Is it rather insufficient labor force or the lack of expert knowledge that prevented a continuation of usage or reimplementation of the systems? How was the water supply organized and were complex water supply systems an instrument of power with the knowledge reserved for a selected few?

Research on the sustainability of ancient settlements and the mutual dependencies between settlement dynamics and water supply strategies are an important and promising research field. Remains of ancient water supply systems are abundant in the drylands of West Asia and offer the possibility for further research on the topic. The archaeological record as well as information on their environmental conditions during their usage is limited. Moreover, the temporal evolution and diffusion of many water supply systems is still unclear. Geoarchaeological research concerned with the water and food supply of ancient settlements and settlement dynamics in general should therefore concentrate on the establishment of a comprehensive chronology of these systems and an evaluation of their functioning and reliability.

Given the current trend to establish large settlements in unfavorable environments, most prominently on the Arabian Peninsula and given the fact that those settlements are built and supplied with enormous organizational and financial efforts, their fate depending on a fragile economical and political framework, this research could contribute to the challenges and problems to come.

References

Genequand, D., 2006. Some Thoughts on Qasr al-Hayr al-Gharbi, its Dam, its Monastery and the Ghassanids. Levant 38, 63–84.

Hummel, D., 2008. Supporting the Population: Interactions of Demographic Changes and Supply Systems for Water and Food. Campus Verlag.

Kouki, P., 2006. Environmental Change and human history in the Jebel Harun area, Jordan.

Kouki, P., 2009. Archaeological Evidence of Land Tenure in the Petra Region, Jordan: Nabataean-Early Roman to Late Byzantine. Journal of Mediterranean Archaeology 22, 29–56.

Ortloff, C.R., 2005. The Water Supply and Distribution System of the Nabataean City of Petra (Jordan), 300 BC– AD 300. Cambridge Archaeological Journal 15, 93–109.

Oswalt, P., Rieniets, T., 2006. Atlas of Shrinking Cities: Atlas Der Schrumpfenden Städte. Hatje Cantz Verlag GmbH & Company KG.

Schiller, G., 2007. Demographic Change and Infrastructural Cost – A Calculation Tool for Regional Planning. Paper proposed for SUE-MoT Conference"Economics of Urban Sustainability", Glasgow.

Tholbecq, L., 2001. The hinterland of Petra from Edomite to the Islamic periods: The Jabal ash-Sharah Survey (1996 - 1997). SHAJ 399–405.

Curriculum Vitae

For reasons of data protection,
the curriculum vitae is not included in the online version